FINAL REPORT

INVESTIGATION OF THE REINFORCEMENT OF DUCTILE METALS WITH STRONG, HIGH MODULUS DISCONTINUOUS, BRITTLE FIBERS

prepared for

NATIONAL AERONAUTICS AND SPACE ADMINISTRATION

by

A. Gatti, J.M. Berry, J.J. Gebhardt, J. Mullin, E. Feingold

DECEMBER 1968

CONTRACT NASw-1543

Space Sciences Laboratory
Missile and Space Division
GENERAL ELECTRIC COMPANY
Philadelphia, Pa.

2410–2E2 (Final Report)

Final Report

INVESTIGATION OF THE REINFORCEMENT OF DUCTILE METALS WITH STRONG, HIGH MODULUS, DISCONTINUOUS, BRITTLE FIBERS

by

A. Gatti, J. M. Berry, J. V. Mullin, J. J. Gebhardt

Prepared for

NATIONAL AERONAUTICS AND SPACE ADMINISTRATION

December 1968

Contract NASw-1543

Space Sciences Laboratory
GENERAL ELECTRIC COMPANY
Missile & Space Division

TABLE OF CONTENTS

ILLUSTRATIONS

LIST OF TABLES

SUMMARY

This final report covers the period from 1 November 1967 to 31 October 1968. The work was performed under Contract NASw-1543, with Mr. James J. Gangler of NASA Headquarters serving as Program Monitor.

The purpose of this program was to define and investigate the critical factors affecting the reinforcement of ductile metals with short, brittle fibers. The materials selected for study were aluminum (or its alloys) and "ductile" epoxies reinforced with B_4C whiskers or with high modulus filaments, such as B_4C/B/W*, SiC/W, B/W, etc. Related tasks in the program included the development of a more economical process for growing B_4C whiskers, the investigation of deposition parameters, the production of continuous B_4C filaments, and the characterization of the individual constituents in the final composites. The latter task involved a study of the structural and chemical interactions of the combined elements (fibers, matrix, coatings, etc.).

The results obtained during this period are summarized as follows:

(1) Process studies were carried out which led to conditions permitting the coating of boron/W substrate filaments with boron carbide. Deposition conditions were as follows:

Temp.	1230 C - 1280 C		Heated Length 6 in.
Press.	1 atm.		Draw Speed 2 ft./min.
Flow:	BCl_3	29-42 s.c.c./min.	Counterflow parallel feed
	H_2	31 s.c.c./min.	
	CH_4	10 s.c.c./min.	

(2) Approximately 14,000 feet of coated boron/W filament was prepared for composite studies over a one month period. Average tensile strength of this material was 396,000 psi, modulus 52-59 million psi, diameter 0.004 in., coating thickness 0.0001 in.

(3) The weak areas in coated filament were believed to be associated with regions of weakness or latent weakness in the substrate, produced probably by overheating in the substrate deposition process. Latent weakness refers to areas of the substrate strong enough to pass specifications, but which become weak by heating to the boron carbide deposition temperature for a short time. Certain production quantities of B/W substrate appear to be latently weak throughout.

(4) Boron carbide was successfully deposited on boron/SiO_2 filaments, yielding material of higher strength than the initial substrate, using the same deposition conditions as those developed for boron/W.

* This terminology is used through the text and denotes a multiphase filament, in which B_4C is vapor deposited over a boron filament having a W-substrate core. Other filaments, such as SiC/W denote a SiC deposit on a W–substrate core.

(5) In both cases (B/W and B/SiO_2), excessive BCl_3 and H_2 flow rates produced weak filament, possibly due to deposition of free boron instead of the boron-carbon deposit.

(6) The room temperature strength properties of a group of filamentary materials, including E-glass, hydrogen-embrittled tungsten wire, etched out $B_4C/B/W$, normal B/W and a special batch of high strength B/W, were tested. The results are discussed in terms of their strength scatter and of their maximum, minimum and average strength properties.

(7) Aluminum specimens containing single, five-filament and ten-filament arrays of continuous $B_4C/B/W$ filaments were fabricated by a hot pressing technique developed earlier [1]. The series of specimens were tested at room temperature in tension both as a function of strain rate and filament-matrix bonding. The extent of matrix-fiber bonding was varied by sputtering iron on filament surfaces and using as-deposited filament surfaces and graphite-coated filament surfaces. Single filament specimens show a definite correlation between the apparent bonding efficiency and the number of pieces etched out of the specimens after tensile testing. A minimum number of pieces is counted for the graphite-coated filaments (2-3), an intermediate number is counted for the as-deposited filaments (4-6), and a larger number of pieces is counted for the iron-coated filaments (10-11).

Multi-filament specimens, however, after tensile testing and matrix desolution do not show any variation with surface treatment. It appears that filament interaction dominates during fracture and only one break per filament is observed. These experiments are described.

(8) A series of Al-$B_4C/B/W$ continuous filament composites containing 50 v/o filament were fabricated by liquid infiltration. Room temperature tensile strength values of these specimens varied considerably depending on the strength scatter of the starting filament. The highest value attained was 198,000 psi. It is hypothesized that the scatter in composite strength can be related to the position of the weak area of each filament in relation to its nearest neighbors. Thus, completely randomized defects can lead to higher than average composite strengths, while aligned defects in a given cross section can lead to lower than average strength. Examination, both microscopically and by etching of both failed and unfailed specimens showed that the fracture (failed) specimen averaged one break per filament while the unfailed (not fractured) specimens experienced a few broken filaments up to their rule-of-mixture fracture stress. However, as will be pointed out, the appearance of failed filaments in the unfractured tensile specimens can arise because of processing damage. Thus, it appears likely that composites fail at a stress which is determined by the failure stress of the first filament break. This lack of apparent cumulative damage behavior is rationalized by proposing a model based on an inhomogeneous strain criteria enabling weak fibers to be stressed above their individual test strength due to interaction with their stronger neighbors.

(9) Some elevated temperature tensile tests at 500 C were attempted using identical specimens to those described above. However, the tests were unsuccessful because the gage section would always shear out of the grips. Such tests were difficult to perform and meaningful results will not be available until larger specimens can be fabricated.

(10) A series of discontinuous aluminum-B_4C/B/W composites were also fabricated by a liquid infiltration technique. One specimen had a room temperature tensile strength of 85,000 psi which was 50% of the value predicted by the rule of mixtures.

(11) A cursory examination of the room temperature fatigue properties of 50 v/o Al-B_4C/B/W composites was made without obtaining definitive results.

(12) Studies of the tensile fracture behavior of epoxy specimens containing single filaments and multi-filament arrays were continued. Results have substantiated previous conclusions [1] that strain-rate effects are inadequately described by present theories of composite strengthening. It is also shown that when the volume fraction of strong, brittle filaments in a specimen is increased beyond a certain value, the specimen consistently fails after the first filament fails. Thus, an hypothesis is advanced which asserts that a rule-of-mixture theory cannot be used to explain the general strength level of composite materials without a more complete description of the in situ strengths of the individual composite components. Thus, results which agree with the rule-of-mixture criteria may be fortuitous.

(13) A method was developed which allows the bond strength of filamentary materials in epoxy Novalac to be varied independent of chemical and mechanical properties of the matrix. This was accomplished by applying intermittent (porous) coatings of graphite and Teflon, which are chemically inert, to the resin. A chemical approach (the addition of more plasticizer) proved impractical because of its accompanying modification of the mechanical behavior of the cured resin.

(14) A generalized model has been developed to explain and predict many effects of material properties, specimen configurations and test conditions on composite performance. The concept is advanced that mechanical compatibility as well as chemical compatibility is an important attribute of successful composites and is of comparable importance.

(15) Fifty volume percent continuous copper-tungsten composites were fabricated by liquid infiltration and tested in tension at room temperature and at various strain rates. The results closely follow the tensile behavior of annealed tungsten wire. It was concluded that tungsten wire cannot be used as a model for high-strength, brittle filaments, since it is too weak ($>$ 100,000 psi) in its most brittle state to provide valid comparisons with other brittle, high modulus filaments, viz., B_4C/B/W.

I. INTRODUCTION

From a reinforcement viewpoint, whiskers (single-crystal fibers) appear to have many desirable characteristics. A number of classes of compounds have been prepared in this form including metals, oxides, nitrides, carbides, and graphite. The strengths observed for these whiskers range from about 0.05 to 0.1 of their elastic moduli, the latter values approaching predicted theoretical strengths. Many also have relatively low densities and are stable at high temperatures. Calculations of whisker-reinforced composite properties based on whisker properties, particularly for the brittle whiskers of high modulus materials, show that they have an enormous potential compared to more conventional materials on both a strength/density and a modulus/density basis.

The incorporation of whiskers into composites requires the following series of processing steps:

(1) Whisker growth.
(2) Whisker beneficiation, to separate strong fibers from the growth debris.
(3) Whisker classification, to separate according to size.
(4) Whisker orientation, to align the whiskers and maximize reinforcement along a specific axis.
(5) Whisker coating, to promote wetting and bonding.
(6) Whisker impregnation with matrix material, to form a sound strong composite.

Because of the many processing steps, there are a large number of imposing technical problems to be solved in order to achieve the high potential strengths. Many of these problems have not yet been solved.

In a few isolated cases, involving very small and carefully prepared samples, the predicted strengths of the brittle whisker/ductile matrix composites have been achieved. However, all too frequently, attempts to scale up the composites into even modest size specimens have resulted in strengths that range from about 10 to 30 percent of the predicted values.

A list of possible reasons for the low composite strength values is given in Table I. As can be seen there are many variables to contend with, and many of these are interrelated and difficult to study experimentally.

A fundamental difficulty in evaluating the performance of whisker composites is the lack of knowledge concerning the whiskers themselves. This is understandable when one realizes that there are about 10^9 to 10^{10} of them per pound, and characterization of even a small fraction becomes a major task. These and other problems have limited the immediate use of B_4C whiskers, which had been synthesized and characterized in previous studies.[2,3,4,5]

An alternate means to gain useful, fundamental knowledge concerning whisker-reinforced composites involves the use of brittle, continuous filaments. Continuous filaments have several advantages over whiskers when investigating the reinforcement of materials; some of these advantages are listed below:

(1) It is much easier to characterize the relevent and critical parameters listed in Table I.
(2) The available continuous filaments are large relative to the whiskers and can be more readily handled and incorporated into composites.
(3) The filaments can be cut to uniform, desired lengths so that the effects of discontinuous reinforcements can be assessed.

Experimental work of this type has already been done using ductile tungsten filaments in a ductile copper matrix [6]. Although this work has provided a wealth of information regarding the reinforcement of metals, it does not uncover all of the key problems encountered with truly brittle fibers in a ductile matrix. The chief difference between the reinforcement of metals with brittle and with ductile fibers is that the ductile fibers can deform to accommodate local, high stress concentrations, whereas brittle fibers cannot do so. Thus, it is necessary to carry out further studies and to evaluate the potential and engineering limitations of metals reinforced with brittle fibers and whiskers.

TABLE I. VARIABLES AFFECTING THE TENSILE STRENGTH OF WHISKER-REINFORCED COMPOSITES

A. Whisker Variables

1. Average strength
2. Dispersion of strength values
3. Strength versus whisker diameter and length
4. Strength degradation during handling and fabrication
5. Strength versus temperature
6. Elastic Modulus

B. Matrix Variables

7. Yield strength
8. Flow properties
9. Strength versus temperature (particularly shear strength)
10. Matrix embrittlement due to mechanical constraints and new phases formed

C. Composite Variables

11. Volume fractions of components–fiber and matrix

12. Homogeneity of whisker distribution

13. Whisker aspect ratio

14. Whisker orientation

15. Interfacial bond strength

This program was therefore initiated to investigate in detail the behavior of a ductile metal (aluminum) reinforced with various brittle fibers, such as B_4C/B/W, SiC/W, B/W, etc. (in both continuous and chopped lengths) to provide data which would be pertinent to whisker-reinforced metals. Included in this investigation was a parallel study using a "ductile" epoxy Novalac, which in turn has led to the recognition and documentation of three failure modes possible in fiber-reinforced composite materials. This program is being conducted in two parts: (1) The development of a process to grow B_4C whiskers which would be amenable to eventual scale-up and (2) An investigation of the reinforcement of aluminum and "ductile" epoxies with brittle, high modulus filaments, such as B_4C which would simulate the B_4C whiskers.

A review of the results of the first year of effort [1] includes the following:

(1) Extensive studies were made of B_4C whisker growth systems which utilized chemical vapor deposition rather than direct B_4C bulk vaporization. These systems included boron tribromide + hydrogen + CCl_4 and the volatile substituted boranes, tributyl borane and ethyl decaborane. This approach appeared to lend itself most easily to whisker growth scale-up.

(2) A ready supply of B_4C/B/W filament materials was necessary to continue composite studies. A previously developed process [6] was modified so that purchased B/W filaments could be coated with a layer of B_4C while still maintaining the high strength capability of B/W filaments. B/W filaments coated in this manner were able to withstand molten aluminum for significant times without reaction, and thus allowed liquid infiltration techniques to be used in the preparation of composites.

(3) B_4C/B/W filaments were the mainstay of the filament-composite work. However, many other filamentary materials including, B/W, SiC/W, B/SiO_2 and W were also examined for potential usage and to document the mechanical behavior characteristics of composite materials as a function of individual filament characteristics. A final phase of the characterization portion of this study considered the matrix-filament stability of aluminum-filament composites of the Al-B_4C/B/W and Al-SiC/W systems.

(4) Composite studies encompassed a variety of filaments utilizing "ductile" epoxy Novalac resins and aluminum matrices using both single and multiple filament arrays. This work has established experimentally the critical fracture modes of an epoxy matrix in the vicinity of a break in a high modulus, high strength filament. Three distinct failure modes were observed to occur and the nature of these three modes was explained through an analysis of the stress state in the matrix [1].

(5) Continuous filament Al-B_4C/B/W composites were fabricated which showed full utilization of the strength potential of individually tested filaments in a number of instances. SiC/W-Al composites, however, suffered a large decrease in strength because of an unfavorable reaction between the filaments and a Ti/Ni coating which had been used to promote wetting.

(6) By being cognizant of the literature concerning composite mechanical behavior coupled with the present study, a tentative judgement of the expected mechanical behavior of all types of fiber composite materials was made through consideration of individual filament strength and modulus, bond strength between filament and matrix, matrix and filament ductility, and matrix and filament mechanical response to strain rate changes.

This final report covers the work performed for NASA under Contract NASw-1543 from 1 November 1967 to 31 October 1968 and is a summary of the second year's efforts. It is to be noted that the chronological order of the material presented here does not necessarily correspond to the order presented in former progress reports (NASw-1543 Fifth, Sixth and Seventh Quarterly Reports).

Work on this program, of necessity, proceeded along many fronts simultaneously. However, it is felt that a neater package can be made by an ordered arrangement of the results of the total year's effort. Thus, no formal eighth quarter's effort is presented, but has been integrated within this final report.

Studies during this past year included an assessment of the continuous processing of B_4C/B/W filaments with the objective of upgrading the strength of the resulting material. The processing technique used had decreased the strength of the original starting B/W filament material by about 30%. However, refinements have led to a B_4C coating process which results in B_4C/B/W filamentary material which is at least equal to the starting substrate material (B/W). Also, statistical evidence indicates that under ideal deposition conditions, substrate strength can be improved slightly.

The characterization of filamentary materials was continued. Brittle W, "E" glass, and an exceptionally strong batch of B/W filaments were tested. Also an extensive statistical study was made of B_4C/B/W filaments which had been infiltrated with aluminum and removed from the resulting aluminum matrix by etching with HCl. These filaments were samples of those which were concurrently used in composite studies presented in later sections of this report.

Aluminum matrix B_4C/B/W composite studies using continuous filaments during this reporting period dealt exclusively with two types. A group of single-layered composites were fabricated

containing arrays of one, five and ten filaments. These composites were then tested in tension at room temperature and their mechanical behavior examined. These results are described. A second group of aluminum-B_4C/B/W 50 volume percent composites were also fabricated by liquid infiltration and these specimens were tested in tension as a function of temperature and strain rate. These results are presented together with a proposed model to explain the results.

Discontinuous aluminum-B_4C/B/W composites were also fabricated from chopped filament. The strongest composite broke at 85,000 psi which was approximately 50% of its potential.

Studies using single filament-epoxy composites containing "E" glass filaments; weak, brittle W wires; normal B/W filaments; and exceptionally high strength B/W filaments were made to further illustrate the effects of various filament characteristics on the resultant mechanical behavior of composites. Multifilament composites were also prepared and studied. A most important variable, the "bond strength" was varied by coating with graphite and Teflon. These studies are described. Multifilament composites and composites containing discontinuous filament arrays were also prepared and studied.

Since a technique has been developed which can effectively vary the bonding efficiency of epoxy Novalac - B/W composites by coating the filaments with graphite, Teflon, or other organic or inorganic lubricants, it has been possible to assess more fully the variables shown in Table I. A term, "mechanical compatibility", has been coined to describe this analysis. These results are explained.

Strain-rate effects have been observed to lead to deviations from the predicted strengths of composites (when using a rule-of-mixtures analysis). Experiments were thus begun to study these effects in a classically ideal composite material: copper reinforced with W-wires [5]. Cu-W composites were fabricated by liquid infiltration [5]; however, because of the limitations imposed by the mechanical properties of tungsten wire used to fabricate these composites, the study was not definitive in its results.

A qualitative discussion of "intermittent bonding" is presented as Appendix A. The significance of a bonding system which varies only as a function of filament contact area and not a chemical "bond strength" variation is used for this discussion. It is shown by using stress trajectory analysis that the crack sensitivity of a matrix can be altered significantly when intermittent bonding is used.

A qualitative discussion of the relationship between bond strength and composite strength is included as Appendix B. This work is the rationale of the epoxy-filament studies presented in this final report and earlier work [1].

A paper, "The Role of Mechanical Compatibility in Advanced Filament Composites", was presented in Toronto, Canada during the International Conference on Macromolecular Chemistry, September 3 to 6, 1968 and is reproduced in this report as Appendix C.

II. EXPERIMENTAL PROCEDURES – RESULTS AND DISCUSSION

A. Preparation of Continuous Boron Carbide Coated Filaments

1. INTRODUCTION

Boron carbide is a promising material for use as a diffusion barrier to prevent interaction between metals and reinforcing filaments in reinforced metal-matrix composites. In previous work, [7] a process for the vapor deposition of boron carbide of very small crystallite size had been developed for use on continuous boron filament substrate prepared in situ. The purpose of the experimental work in this program was to apply the process in a continuous manner to available, strong, stiff preformed substrates and to prepare an adequate supply of filament for reinforcement studies.

The basic method used for coating continuous filaments with boron carbide consisted of passing a mixture of boron trichloride, methane and hydrogen at atmospheric pressure over a heated filament substrate. In this manner coatings of boron carbide from 0.1 to 0.3 mils thick could be deposited at reasonable rates using laboratory apparatus, although the process is diffusion controlled and deposition rates were relatively low.

In the course of the program, experimental studies were concentrated on three goals: (1) to optimize the deposition conditions in order to achieve high strength, high modulus, uniform diameter filament; (2) to explore the possibility of using substrates other than boron on tungsten (B/W); and (3) to prepare a sufficiently large quantity of high quality filament for metal matrix composite studies.

2. EXPERIMENTAL

The deposition apparatus used for all of the studies, see Figure 1, was similar to the atmospheric

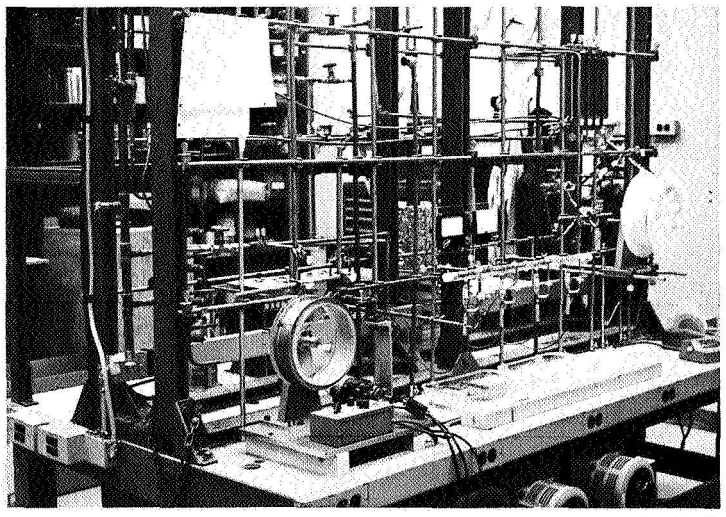

Figure 1. View of Continuous Deposition Apparatus for Boron Carbide on Boron

pressure, hot-wire, cold-wall systems described previously [7]. These systems embody the following principal concepts: a simple friction method of tensioning and taking up the filament, appropriate atmospheric pressure seals to prevent gas leakage in or out of the reactor, mercury standpipe electrical contacts within the reactor, a feed gas metering and mixing system, and cryogenic trapping of condensible exhaust gases. Compaction between stages was eliminated since a countercurrent parallel gas flow direction was used instead of cross filament gas feed. No advantage is gained in this deposition reaction by using cross feed flows since it appears to be diffusion limited rather than mass flow limited.

Although six consecutive electrical stages were built into the reactor, only one six inch stage was actually used for most of the work, together with a hydrogen cleaning stage, also heated by using mercury/filament contacts.

Feed gases were metered through flowmeters and mixed in the feed lines before entering the reactor at the downstream end; at the upstream end these gases left the reactor and entered a copper recovery trap kept at -78 C. The majority of the boron trichloride condensed while the volatiles entered a vent system. The feed and recovery cylinders were interchangeable, simplifying the gas handling. Table II lists the gases and substrate materials used in the deposition studies and filament preparation.

TABLE II. MATERIAL LIST OF GASES AND SUBSTRATES USED IN DEPOSITION STUDIES AND FILAMENT PREPARATION

A. GASES

Boron Trichloride – Commercial – Matheson Co.
Methane - Commercial - Matheson Co.
Hydrogen - Commercial - Burdette Co.

B. SUBSTRATE

Boron on Tungsten	–	Texaco Experiment Inc. Avg Tensile Str. 339 Ksi
Boron on Tungsten Reel UAL 1124	–	United Aircraft Res. Lab. Avg Tensile Str. 485 Ksi
Boron on Tungsten Reel HS2364	–	Hamilton Standard Div., UAC. Avg Tensile Str. 410 Ksi
Boron on Silica	–	General Electric Co., Space Sciences Lab. Avg. Tensile Str. 350 Ksi
Silicon Carbide on Tungsten	–	General Technologies Corp. Avg. Tensile Str. 296-387 (various lots)

3. *RESULTS AND DISCUSSION – PROCESS STUDIES*

Earlier experiments, on which the present studies were patterned, led to development of a deposition process in which a layer of boron was first deposited on the tungsten substrate before deposition of the boron carbide layer. [7] This was done to protect the substrate from premature breaking in the reactor, due to what appeared to be rapid carbide formation, and to provide a larger area for deposition and hence increase the growth rate to the desired 4 mils. However, this technique added to the complexity of the apparatus and increased the difficulty of optimizing the process with respect to filament properties. The latter were variable from run to run and often poor. In the present program, (where the eventual production of a sizable quanity of filament, from a laboratory standpoint, was desired) in situ preparation of the boron subcoat appeared to be a less efficient way than to procure good quality substrate filament and to procede from there. With the exception of a few trial runs to produce a wholly boron carbide deposit on tungsten, all of the process studies to be discussed were carried out using the substrates listed in Table II. The rationale in altering conditions was to proceed in the direction which would produce coated filament equal or superior to the virgin substrate with respect to tensile strength.

a. Tungsten Substrate

Initial efforts to produce a deposit of boron carbide directly on tungsten led to formation of extremely weak, crumbly filaments, largely incapble of being tested. Table III summarizes the

TABLE III . SUMMARY OF INITIAL DEPOSITION CONDITIONS TO FORM B_4C DIRECTLY ON W SUBSTRATE

Experiment	N_2	SCC/Min BCl_3	CN_4	Filament Speed ft/min	Initial Diam (mils)	Final Diam (mils)
21	250	200	10	2	0.5	—
25	250	128	10	2	0.5	1.25
25[a]	250	180	10	2	0.5	1.0[b]
26[a]	225	80	10	2	0.5	2.7

(a) No Hydrogen cleaning stage

(b) Strength 5140 psi Tensile Strength
25×10^6 psi Modulus

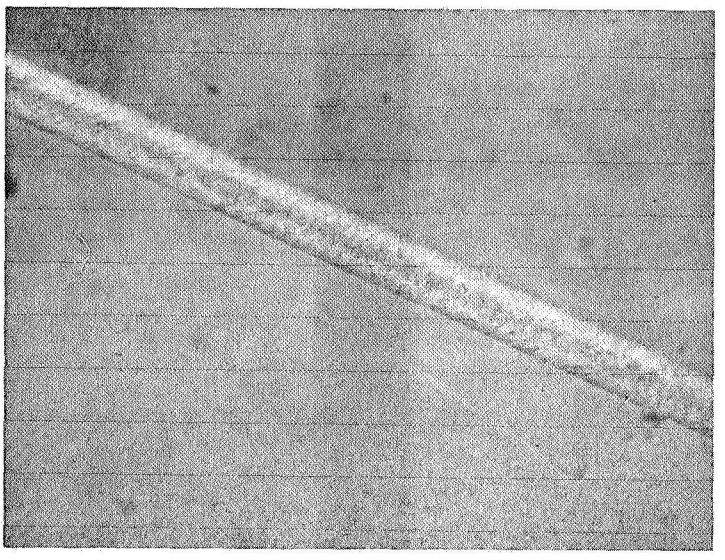

A. SURFACE VIEW (116X)

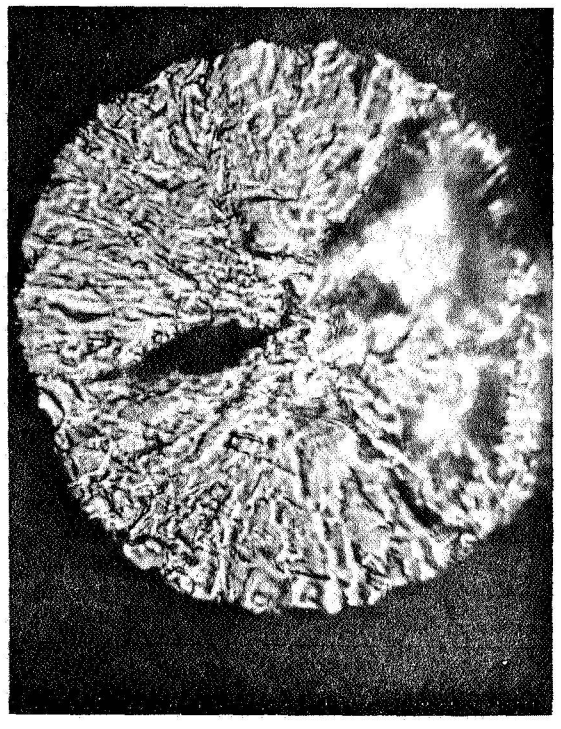

B. FRACTURE SURFACE (1210X)

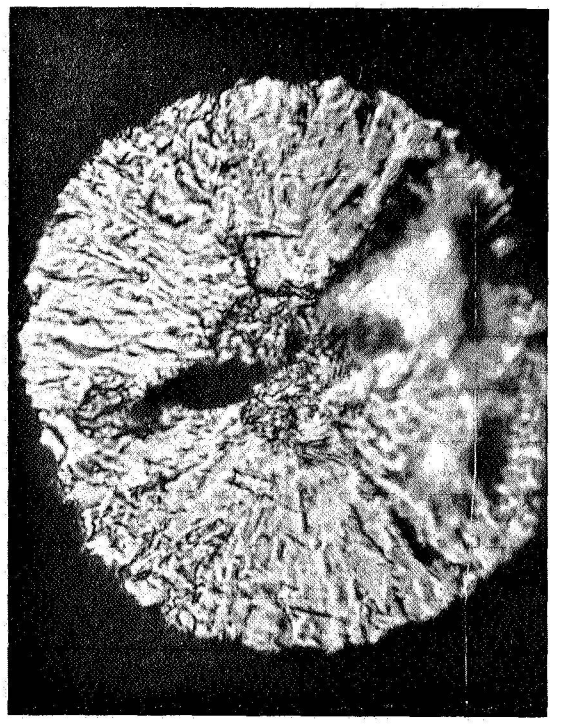

C. FRACTURE SURFACE AFTER ETCHING (HOT 50% H_2O_2) (1210X)

Figure 2. Boron Carbide on Tungsten Substrate, Dia. 2.25 mil

deposition conditions and results, while Figure 2 illustrates the cracked and grainy nature of the deposit. Unlike the simpler boron/tungsten system, the deposition of boron carbide can introduce both carbon and boron to the tungsten matrix and may thus bring about a number of rather complicated crystallographic changes as the various tungsten carbide and boride species form, interact and disappear, depending on the stoichiometry of the local volume element with respect to tungsten, boron, boron carbide and the various tungsten carbides and borides. Simple calculations of the change in volume produced by the transition of the tungsten (b.c.c.) unit cell to the WC (hex.) unit cell indicate that a large volume contraction occurs. On the other hand, the formation of the tungsten borides W_2B and WB_4, involves a volume expansion. The stress picture within the core is complicated not only by volume changes due to the reactions, but by the different coefficients of thermal expansion of the species which happen to be present as the filament cools down. Thus, a preliminary layer of boron also serves as a buffer between carbon and the tungsten/tungsten boride, preventing these solid state interactions from perturbing the structure. The experimental manifestation of carbide interactions is probably the appearance of hot spots which often burn out the filaments. For these reasons, the remainder of the work was conducted using coated substrate, as listed in Table II.

b. Filament Coating Thickness

The first set of experiments, carried out using substrate filament obtained from Texaco Experiment, Inc., involved determining the effect of filament speed on coating thickness, inasmuch as it was then thought desirable to have a group of materials with different coating thicknesses for later compatibility studies. The substrate was representative of boron filament made rather early in the history of the boron filament development program and had thus not yet achieved maximum strength. However, it was convenient for the purpose. Table IV shows the results of variations made

TABLE IV. SUMMARY OF MECHANICAL AND PHYSICAL PROPERTIES OF B_4C/B/W AS A FUNCTION OF SUBSTRATE SPEED

Speed ft/min	Tensile Strength, ksi Avg.	High	Low	Modulus 10^6 psi	Thickness (mils on radius)	Total Dia. mils
1.08	209	231	186	61	0.5	5.0
1.08	101	132	80	52	0.65	5.3
2.16	36	86	5	40	0.5	5.0
3.24	119	156	101	64	0.4	4.8
9.72	232	266	120	52	0.15	4.3

Initial B/W Strength = 241 ksi; B/W Strength after Heating = 104 ksi.

in filament speed. Two conclusions were reached: (1) that coating thickness could be varied between 0.025 mil and 0.65 mil (i.e., total thickness increases of 0.05 mil and 1.30 mils), within reasonable limits of filament speed and (2) that filament strenghts were much lower than had been expected. This led to the conclusion mentioned above regarding deposition parameters. Therefore, the next phase of the study was tto optimize conditions before attempting variations in the filament structure.

A further significant observation made in the course of efforts to obtain thick coatings of boron carbide, at increased production rates occurred in the following experiments. While one approach to thick coatings would be to increase temperature and another to draw the filament more slowly, the availability of more than one deposition stage permitted a twelve inch stretch of filament to be heated using two power supplies with a common ground, instead of the previous single six inch stage. The filament was drawn through the reactor at the usual rate of two feet per minute at optimized feed ratios. However, thicker coatings were achieved at the expense of strength. When the filament draw speed was increased so that residence time at temperature was nearly the same as it had been for the single six inch stage, stronger filament was again obtained. These results are summarized in Table V.

TABLE V. EFFECT OF TIME-AT-TEMPERATURE ON FILAMENT STRENGTH

Experiment No.		151A	151B
Flow Rates s.c.c./min.	H_2	31	31
	BCl_3	37	37
	CH_4	10	10
Draw Speed ft/min		3.25	2
Heated Length Ft		1	1
Time at Temp.[(a)] min.		0.31	0.5
Temperature ^oC		1255	1255
Tensile Str. ksi	High	603	206
	Low	538	90
	Avg.	584	162
Coating Thickness mils		0.05	0.15
Original Substrate Tensile Str.		485 ksi	

(a) Time at temp. during 'normal' runs, using 1 0.5 ft. stage = 0.25 min.

One interpretation of this effect is that the weakening of the filament was not due to the thicker coating alone, but rather that it was kept at deposition temperature (1250 C) for too long a period, permitting structural changes to occur within the boron. The deposition temperature was probably as high, if not higher than that at which the filament had originally been prepared, so that structural changes which had not reached equilibrium or which had not begun during the original substrate deposition could be initiated. The nature of such changes is not clear, although crystal growth of the 'vitreous' boron of the filament to a beta-rhombohedral form is known to be favored in this temperature range [8].

Further evidence of an incipient degree of instability is presented later in connection with production of boron carbide coated boron filament using two sources of boron filament substrate. Time did not permit more detailed structural evaluations to be made to provide a firmer explanation.

c. Process Variables

The first set of process variables to be checked for the parallel feed system comprised the feed ratio, particularly the feed volumes of boron trichloride and hydrogen. To determine if any of the individual components of the reaction system was, in itself, harmful to boron filament the uncoated substrate was heated to deposition temperature at normal residence times (i.e., filament draw speeds) and tested for tensile strength. Hydrogen, nitrogen, boron trichloride, hydrogen chloride and methane had no effect individually on filament strength. However, a mixture of boron trichloride and hydrogen of the proportions used in making the original deposits of boron carbide had a pronounced weakening effect, so that the deposition of boron on an already formed boron filament appeared to be the source of weakness. The boron trichloride volume in the boron carbide feed mixture was therefore systematically reduced, with a resulting rise in tensile strength of the coated filament over that obtained at higher BCl_3 flows, see Table VI. However, the strength of the

TABLE VI. EFFECT OF BCl_3 CONTENT ON FILAMENT STRENGTH

Expt.	Flow scc/min			Temp °C	Strength			Diam Change (mils)	Substrate
	H_2	BCl_3	CH_4		High	Low	Avg.		
65	250	200	10	1240-1260	146	22	---	0.5	B/W UAL
66	250	200	10	1240-1260	–	–	---	---	B/W UAL
67	250	200	10	1240-1260	55	7	165	0.2	B/W UAL
72	225	42	10	1240-1260	300	134	231	0.2	B/W UAL
73	225	42	10	1240-1260	261	138	198	0.2	B/W UAL
74	225	42	10	1240-1260	378	208	335	0.3	B/W UAL
75	225	42	10	1240-1260	230	138	182	0.7	B/SiO_2 GE

coated filament was still considerably below that of the uncoated substrate, particularly in the case of the United Aircraft Laboratory filament. Therefore, the quantity of hydrogen was also reduced, with the results shown in Table VII for comparison to those in Table VI. It appeared that with the

TABLE VII. EFFECT OF HYDROGEN CONTENT ON TENSILE STRENGTH

Expt. No.	Flow scc/min H_2	BCl_3	CH_4	Temp °C	Strength High	Low	Avg.	Diam Change (mils)	Substrate
146	63	35	10	1250	510	58	319	0.1	B/W UAL
146A	31	37	10	1240	605	384	527	0.2	B/W UAL
146B	0	42	10	1230	570	52	295	0.0	B/W UAL
147A*	31	37	10	1250	580	67	413	0.0	B/W UAL
147B*	31	37	10	1255	590	410	552	0.2	B/W UAL
147C	31	37	10	1275	397	206	309	0.2	B/SiO_2 GE
147D	31	29	10	1260	430	170	293	0.2	B/SiO_2 GE
148	31	37	10	1240	410	296	344	0.3	B/SiO_2 GE
150	31	37	10	1240	522	322	453	0.15	B/SiO_2 GE

*High Filament Speed.

Substrate Properties (KPSI)

UAL	High	505	GE	
B/W	Low	389	B/SiO_2	Avg. 360
	Avg.	449	(this lot)	

feed ratios of 31 s.c.c./min of hydrogen, 36 s.c.c./min boron trichloride and 10 s.c.c./min of methane, reproducibly strong boron carbide coated filament could be prepared. Throughout these studies, temperatures were maintained in the vicinity of 1230-1250 C, as estimated from a disappearing filament pyrometer. Because a marked improvement was noted in the comparison between uncoated and coated filament, deposition conditions for later production runs were kept at the ratio of 31 cc/min H_2 to 37 cc/min of BCl_s (NTP).

d. Boron Carbide Coated Boron/W Filament – Production

Having established what appeared to be satisfactory operating conditions for obtaining a coated boron filament which retained the strength of the original substrate, the remainder of the work conducted with boron filament having a tungsten core consisted of producing sufficient material for future composite studies. The deposition system was modified slightly to simplify the transfer of trapped unused boron trichloride to the feed cylinder simply by making the trap and feed vessels interchangeable with respect to valving and fittings. It was found that once the deposition had been started, few unexpected interruptions occurred. Careful bookkeeping of the amount of boron trichloride in the feed and trap cylinders prevented shut down because of insufficient feed material,

and the only incidents of unscheduled shut-down were due to flow meter plugs or the appearance of a splice in the boron filament substrate feed spool, which was the original spool on which it had been shipped. A hydrogen cleaning stage, resistively heated using the filament resistance, was used throughout the preparative sequence. As time went on, a noticeable film of condensed boric oxide built up on the inner wall of this stage, which was separated from the reactor by a mercury filled septum. A typical production run began in the morning and was terminated deliberately somewhat after the end of the normal working day, permitting about 1000 feet of filament to be made per day. Little direct attention by the operator was required, freeing him to carry out the testing associated with each day's production. This consisted of measuring 10 tensile breaks (1 in. gage) and several modulus values (15 in. gage). These values are recorded in Table VIII.

TABLE VIII. BORON CARBIDE PRODUCTION DATA

Conditions: Temperature 1215-1280 as noted (Pyrometer)
Pressure: 1 atmosphere
Speed: two feet per minute
Gas Feed Rate: BCl_3 42 cc/min
H_2 31 cc/min
CH_4 10 cc/min
Reactor: Single Stage, 6" long, Parallel Feed
Substrate: Boron on Tungsten. Source: Hamilton Standard Div., United Aircraft Corp.

Run #	Date	# of feet/run	Substrate Identity	°C	(inches) Diameter		Tensile Strength KPSI			Modulus Meg PSI	Reason for Termination and Remarks
					Orig.	Final	Hi	Lo	Avg		
1	3/8/68	29.25	1124	1250	.0038	---	---	---	---	---	splice
2	3/8/68	29.25	1124	1275	.0038	---	---	---	---	---	wavy filament
3	3/8/68	13.00	1124	1250	.0038	---	---	---	---	---	wavy filament
4	3/18/68	270	1124	1270	.0038	---	---	---	---	---	splice; wavy filament
5	3/18/68	42	1124	1270	.0038	.0039	550	420	488	58.5	
6	3/19/68	20	1124	1215	.0038	---	---	---	---	---	change traps
7	3/19/68	616	1124	1220	.0038	.004	640	500	571	54.2	
			1124	1265	.0038						
8	3/20/68	206	1124	1240	.0038	.004	580	75	403	---	splice
9	3/20/68	300	1124	1225	.0038	.004	665	460	612	58.9	
10	3/21/68	472	1124	1265	.0038	.004	590	79	429	54.0	bend in substrate
11	3/21/68	120	1124	1250	.0038	.004	611	151	488	---	
12	3/22/68	690	1124	1250	.0038	.0041	605	398	504	53	splice
13	3/22/68	210	1124	1250	.0038	.0042	612	246	466	---	
14	3/25/68	760	1124	1180	.0038	.0043	606	48	425	51.8	
			1124	1220	.0038						
			1124	1285	.0038						
15	3/26/68	650	1124	1265	.0038	---	---	---	---	---	clogged CH_4 meter
16	3/26/68	30	1124	1285	.0038	---	---	---	---	---	fresh BCl_3
17	3/26/68	120	1124	1285	.0038	---	---	---	---	---	replace BCl_3 bottle
18	3/26/68	150	1124	1285	.0038	.0042	600	36.2	249	53	
19	3/27/68	660	1124	1205	.0038	.0042	640	51	462		
			1124	1240	.0038					51.8	
			1124	1295	.0038						

TABLE VIII. BORON CARBIDE PRODUCTION DATA (Cont'd.)

Run #	Date	# of feet/run	Substrate Identity	°C	(inches) Diameter		Tensile Strength KPSI			Modulus Meg PSI	Reason for Termination and Remarks
					Orig.	Final	Hi	Lo	Avg		
20	3/28/68	610	1124	1255	.0038	---	---	---	---	---	clogged CH_4 meter
21	3/28/68	258	1124	1280	.0038	.00415	608	45	314	52.9	slight back pressure
22	3/29/68	140	1124	1275	.0038	.0043	410	59	295	54.4	splice
			HS								
23	3/29/68	780	2364	1275	.004	.00425	575	71	407	51.8	
24	4/1/68	720	2364	1255	.004	---	---	---	---	---	trap change
25	4/1/68	390	2364	1255	.004	.0043	548	48	283	55.8	
26	4/2/68	450	2364	1285	.004	---	---	---	---	---	CH_4 meter clogged
27	4/2/68	300	2364	1260	.004	---	---	---	---	---	splice
28a	4/2/68	106	2364	1285	.004	.00415	534	74	341	52.9	stop to get sample
28b	4/2/68	174	2364	1280	.004	.0042	558	25	373	51.9	slight back pressure
29	4/3/68	320	2364	1235	.004	.0042	506	116	402	51.7	weak break
30	4/3/68	240	2364	1265	.004	.0042	543	51	160	51.7	
31	4/4/68	600	2364	1260	.004	---	---	---	---	---	
32	4/4/68	24	2364	---	.004	---	---	---	---	---	reactor (weak) break
33	4/4/68	206	2364	1255	.004	.0043	427	93	301	51.7	reactor (weak) break
34	4/5/68	50	1124	1250	.0039	---	---	---	---	---	plugged CH_4 meter
35	4/5/68	578	1124	1260	.0039	---	---	---	---	---	splice and trap change
36	4/5/68	280	1124	1255	.0039	.0041	368	72	223	54.2	grey B_4C
37	4/8/68	840	1124	1225	.0039	.0041	606	140	404	53	
38	4/9/68	840	1124	1225	.0039	.004	591	420	506	52.9	last run
		13294									

Overall average tensile strength 396,000 psi

Uncoated Substrate Room Temperature Strength

UAL 1124: 515 506 485

HS 2364 410

During the course of the production runs the substrate material with which it had begun, Reel 1124 from United Aircraft Laboratories, was replaced by Reel 2364 obtained sometime later from Hamilton Standard Division of United Aircraft Co. Tensile strength values dropped off immediately, as is noted in Table VIII, while filament breakage during deposition became more frequent. Although the vendor's quoted average tensile value for this material, 410 Ksi, was substantiated by additional testing, values of coated filament frequently fell below 350 Ksi. At length, the original substrate material was again used to complete the production.

Evidently the deposition of boron carbide was carried out at a sufficiently high temperature to cause any incipient weaknesses to become pronounced, through crystal growth, or through increased interaction with the coating environment. Since filament from both sources showed variations in tensile strength, as indeed all continuous filament does, it would appear that the material made at United Aircraft Laboratory had been produced at a slightly lower temperature than that made at Hamilton Standard; therefore, temperature-dependent structural changes were not as far advanced as they were in the Hamilton Standard filament. Since the latter facility was designed for production of relatively large amounts of filament, it was not unexpected that the boron deposition process would be operated as close to its limit as possible while still meeting specifications of strength. The United Aircraft Laboratory filament had a higher average strength to begin with, therefore, higher strengths would be expected from the coated filament. Nevertheless, in

studies with TEI filament and boron/silica filament, both of lower average strength than the Hamilton Standard material, the strength of the original substrate was preserved, and in some cases improved. The conclusion seems to be that the strength of the coated filament is dependent not so much on the absolute strength of the substrate, but rather how severely it was heated in its own production facility. It is probable that a shorter time at boron carbide deposition temperature, or a slightly lower deposition temperature would have yielded strong filament in the case of the Hamilton Standard substrate as well as somewhat thinner coating. However, time did not permit the development of these conditions nor, in the light of the relatively modest production effort, did it seem to be justified at the time to seek them.

As is noted in Table VIII a total of 13.29 thousand feet of filament was produced, with a coating thickness of about 0.1 mil on the radius. The overall average tensile strength, including the lower values characteristic of coated Hamilton Standard filament,was 396,000 psi.

e. Boron Carbide Coated Boron/SiO_2 Filament

The availability of an experimental quantity of boron on silica filament, prepared by decomposition of diborane in the Space Sciences Laboratory [9], made possible a limited effort to coat it with boron carbide. In the hydride deposition process, the deposition temperature is around 750 C - 800 C, considerably below that of the halide process. One might expect that the hydride boron filament would be less stable structurally at boron carbide deposition temperatures since the (1250-1280 C) difference in temperatures is considerable. On the other hand, the changes in the boron structure between 750 and 1250 C, although they might be observable, might not begin to be catastrophic from the standpoint of strength until they could promote significant grain growth. Structural studies made in another connection [10] give rise to the conclusion that the hydride boron might indeed be inherently more stable than halide boron because of the more complex nature of the depositing species of the hydride process (hydride fragments vs. individual boron atoms). For example, a higher coordination number was observed for boron in hydride boron filament than for halide boron, indicating a more complex bonding arrangement which would restrict diffusion of individual atoms and crystal like growth, as was verified experimentally.

Initial experiments with high percentages of boron trichloride in the feed gas were just as deleterious to boron/silica filament as they were for boron/tungsten. With a reduction in both boron trichloride and hydrogen content,however, the strength of boron carbide coated boron/silica filament increased to levels somewhat above the strength of the uncoated filament (Table VII). Weak breaks were attributable to weaknesses in the substrate in the form of nodules and solid inhomogeneous inclusions originating from polymeric hydridic side reactions during formation of the substrate.

It can be concluded from these studies, therefore, that the use of boron/silica as a substrate for producing coated boron reinforcing filaments for metal matrices is quite feasible, with good material properties resulting. The lower density and potentially lower cost of the boron/silica substrate offer economic advantages to its use in metal matrix composites.

f. Boron Carbide Coated Silicon Carbide/W

A limited set of experiments was carried out to determine if silicon carbide filament could be satisfactorily coated with boron carbide. An experimental spool of substrate was obtained from General Technologies Corp. containing four or five individual runs of varying strength values. Experiments were begun using the original feed ratio of boron trichloride and hydrogen, with the same result that had been obtained with boron on tungsten and silica. However, reduction of the boron trichloride and hydrogen volumes did not produce a coated filament of any significant strength. Boron trichloride feed volumes were reduced still further with little effect on the low strength values, until no coating was produced.

It is possible that the substrate used, being still of an experimental nature, was not of uniform or proper stoichiometry. Studies with this substrate and with silicon carbide coated boron filament also gave disparate results under identical conditions, so that it should not be concluded that silicon carbide filament cannot be coated with boron carbide and still retain strength. A thin carbon coating placed on the silicon carbide surface before depositing boron carbide did enable strengths of about 187,000 psi average to be achieved compared to 30,000 psi average without a carbon precoat. The carbon may have prevented entrance of free boron into the silicon carbide coating, or it may have satisfied unbonded silicon if the silicon carbide deposit was not stoichiometric. At this point no firm reason can be given.

g. Structural Properties of $B_4C/B/W$ Filament

Figure 3 shows a longitudinal section of the matte-black boron carbide coating characteristic of the majority of the stronger deposits. Figure 4 is a view of a smoother silvery-gray area occasionally noted on the filament, for which there is no firm explanation. Figure 5 is a cross-sectional view of a fracture surface of high strength, while Figure 6 shows a low strength fracture surface. The latter two are both spiral breaks with a rather steep pitch compared to material made in the early studies where low strength was encountered. This may be a function of the substrate used, i.e., TEI vs. UAL filament. The larger fracture area and slower crack propagation which may be associated with this type of surface could explain the rather remarkably high strength of this filament. On the low strength break, a number of sharp radial steps can be seen. These were usually associated with low strength breaks; the lower the strength, the longer the steps appeared to be in the radial direction. These are judged to be fracture phenomena rather than regions of intrusion, diffusion or recrystallization due to the coating as had been thought at first. While Figures 5 and 6 do not clearly show the boron carbide coating, Figures 7 and 8 made from the same material, give an idea of the thickness of the coating, as well as an indication of its uniformity. Figure 8, in particular, shows one of the bare areas discussed above. Figure 9 shows the appearance of a boron carbide coated B/SiO_2 filament, virtually the same as that of coated B/W filaments. In the latter case, when the coating became thin enough (less than 0.05 mil on the radius), the "corn cobs" of the tungsten substrate become clearly distinguishable.

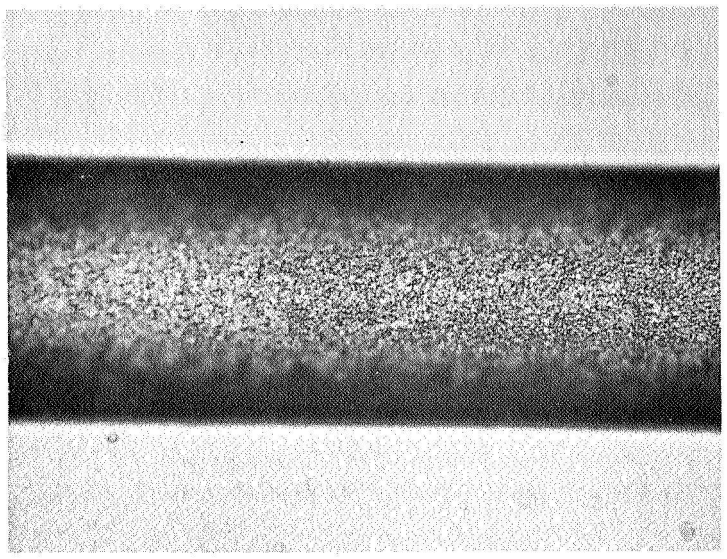

Figure 3. Lateral View of $B_4C/B/W$ Filament (400X)

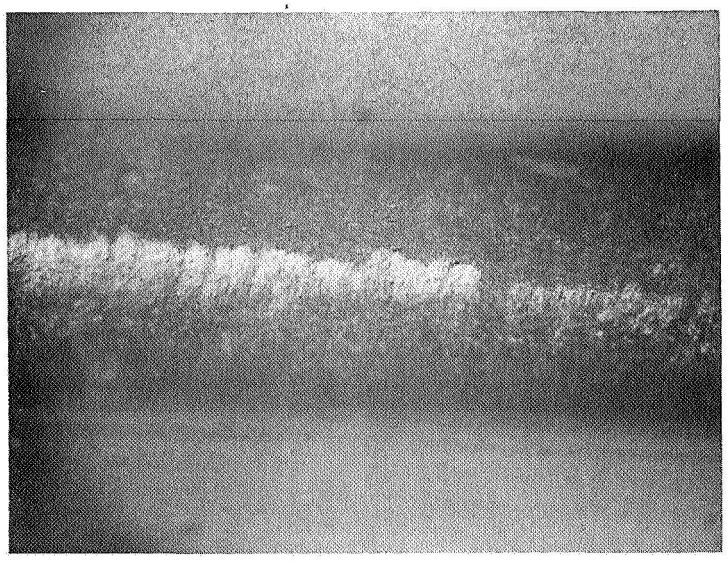

Figure 4. Uncoated Area on $B_4C/B/W$ Filament (400X)

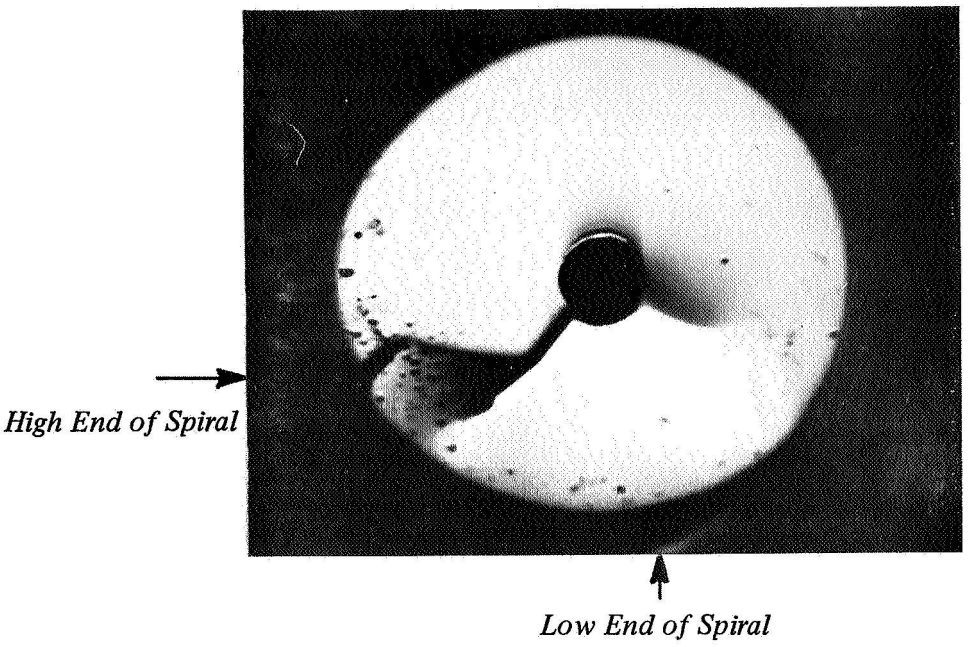

Figure 5. *Electron Microprobe Positive Specimen Current Images of Special Fracture Surfaces. High Strength Failure (600X)*

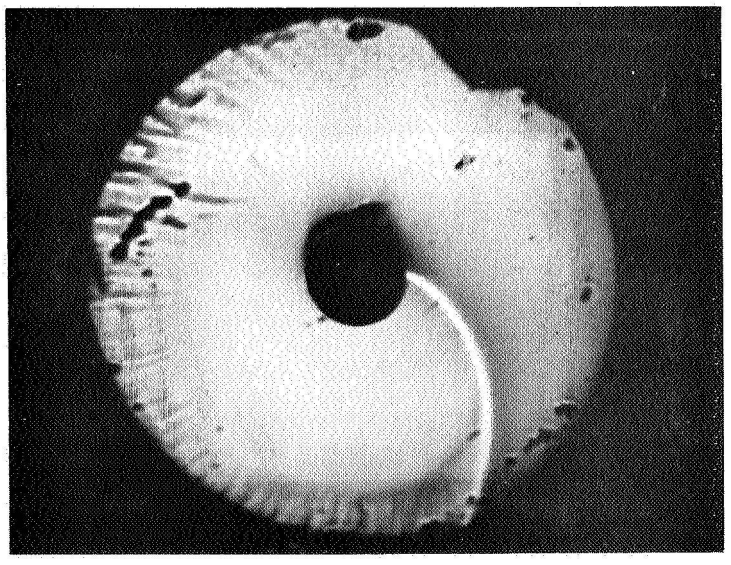

Figure 6. *Electron Microprobe Positive Specimen Current Image of Low Strength Failure Showing Radial Steps (650X)*

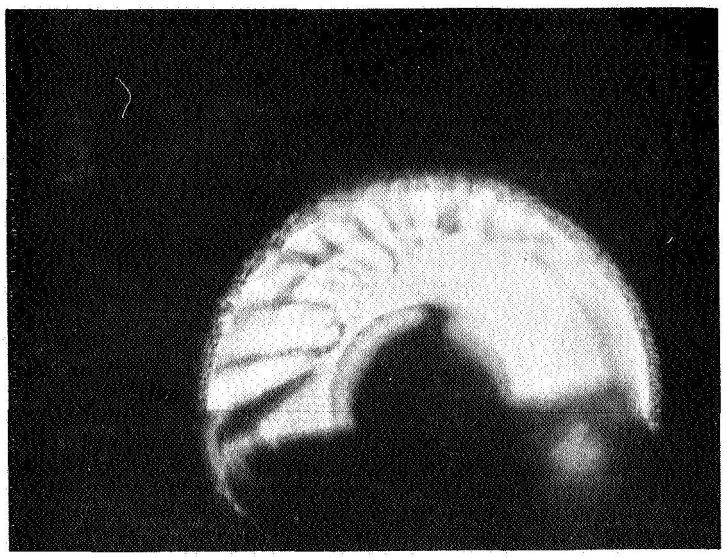

Figure 7. *Cross-Section of $B_4C/B/W$ Filament after Etching 1 Hour in H_2O_2 (Run 7). Coating Thickness Approx, 0.13 mils (593X)*

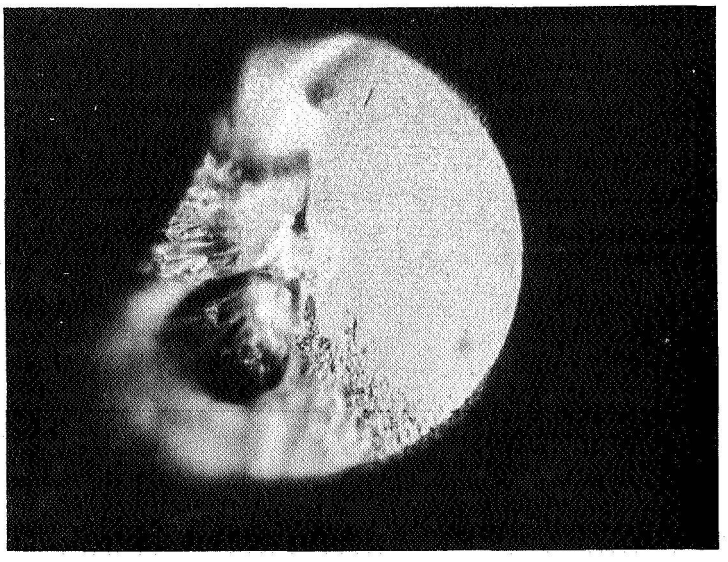

Figure 8. *Cross-Section of $B_4C/B/W$ Filament (Run 7) Unetched, Showing Base Area. Tapered Edge Indicates Uneven Deposition, Rather Than Spalling as the Cause. Coating Thickness Approx. 0.07 mils (593X)*

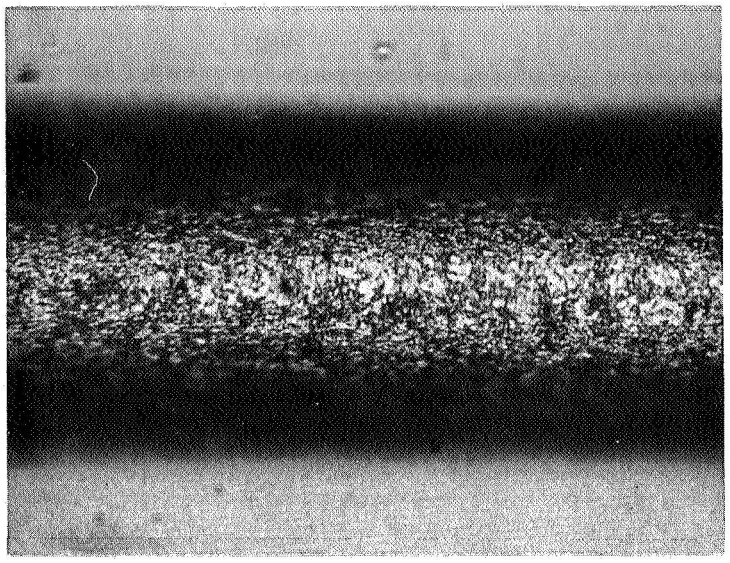

Figure 9. Boron Carbide Coated Boron on Silica (490X)

No crystallographic characterization of the coating was possible because of the diffuse nature of the X-ray diffraction patterns obtained. However, the resistance of the coating to etching by hot 50% hydrogen perioxide is indicative of a strongly oxidation resistant material, while the room temperature electrical conductivity of the coated filament was considerably lower than that of the uncoated filament. Both of these characteristics have in the past been accepted as an indication of a boron carbide, or at least a boro-carbide coating.

B. Characterization of Composite Materials

Since this program is concerned with an investigation of the factors which control the mechanics, the physical and the chemical behavior of metal-matrix composites reinforced with brittle, discontinuous fibers, it is highly important that parameters which affect this behavior be well identified and characterized. The approach used evolves simply from the concept of combining well-characterized brittle fibers with a well-characterized matrix metal and with simple composite test configurations.

The characterization of the variables includes such factors as the average strength and strength dispersion of the fibers, fiber aspect ratio (L/d), fiber strength degradation during processing, and so forth. By systematically varying composite parameters and by comparing the results with theory, either the existing theory will be verified or the theory will be modified to account for the experimental observations. Such understanding will delineate the key variables and their relative importance.

1. *FILAMENT EVALUATION*

The strength properties of composites containing high modulus, high strength, brittle fibers are primarily dependent on the fiber properties. Therefore, it is essential to measure the strength characteristics of the fibers both before and after fabrication into composites. A group of filamentary materials, including E-glass, hydrogen embrittled tungsten wire, normal boron filament $B_4C/B/W$ filaments and a special batch of high strength boron filament, were used in this evaluation. Table IX is a summary of the results of room temperature tensile tests on these additional filamentary materials. All tests were performed in an Instron tensile machine at a strain-rate of 0.02 in./in./min. on specimens of one inch gauge length.

TABLE IX. A SUMMARY OF ROOM TEMPERATURE TENSILE DATA ON VARIOUS FILAMENTARY MATERIALS

Specimen Type	Average Tensile Strength (Psi)	Highest Tensile Strength Value (psi)	Lowest Tensile Strength Value (psi)
E-glass	30,500	48,000	22,400
H_2 Embrittled WIC*	148,000	250,000	76,500
H_2 Embrittled WCA**	99,000	74,200	54,900
Normal Boron/W	200,000	350,000	62,500
H.S. Boron/W	541,000	582,000	485,000

**WCA - 0.005 in. diameter tungsten wire, capillary action

*WIC - 0.005 in. diameter tungsten wire-Infiltration cycle

} See Table X

Tungsten wire of varying mechanical properties proved invaluable. As a convenience, identification of the wire as a function of thermal history is presented in Table X.

The hydrogen embrittled tungsten (WCA) differs from the vacuum annealed "brittle" tungsten tested previously [1] (WAA), in that the wire was heated in flowing hydrogen at 1200 C for 30 minutes compared to 1600 C for 16 hours for the vacuum treated wire. The hydrogen treatment produced a very weak, completely brittle material (no measureable reduction of area at fracture). This weak, brittle condition persisted where as-received wire (WAR), as-received cleaned wire (WARC) or vacuum annealed wire (WAA) was used. The infiltration processed tungsten wire (WIC) also was weakened somewhat when compared to WAA and had a larger variability in strength. Definitive metallographic differences in the various wires were not detected. The difference between

TABLE X. TERMINOLOGY OF TUNGSTEN WIRE AS A FUNCTION OF ITS THERMAL TREATMENT

Terminology Symbol	Thermal Treatment Conditioning
WAR	As Received from Manufacturer (as drawn, straightened, electrolytically cleaned)
WAA	Vacuum Annealed 1600°C-16 hrs.
WARC	As Received plus 30 min in boiling 50-50 H_2O - NaOH
WCA	Wire which has received same thermal treatment as capillary action copper-tungsten composites
WIC	Wire which has received same thermal treatment as Infiltration cycle copper-tungsten composites

hydrogen and vacuum annealing, especially for the WCA wire, were disconcerting. Later consultations with R. Signorelli [11] of the NASA-Lewis Research Center revealed that such behavior was not uncommon. Their work indicated that the ductility of tungsten wire while fabricating Cu-W composites was a function both of the wire batch received from the supplier and of the minimizing of hydrogen flow past the wires during thermal cycling. Their observations are consistent with those observed here, in that the WCA wire was exposed to high hydrogen flow and therefore suffered severe strength losses, while the WIC wire was exposed to essentially static hydrogen flow conditions so that its strength characteristics were similar to the WAA material except for increased scatter in the individual measurements and a resulting lower average strength. Thus, the variability of tungsten wire tensile strength as a function of thermal history is apparent when the tensile data shown in Table IX is compared after various processing treatments. Figure 10 shows an example of the strength scatter of WIC wires for a given thermal treatment.

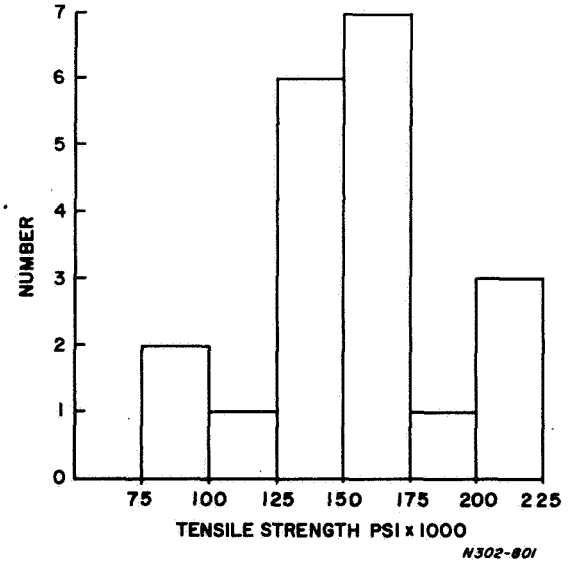

Figure 10. Distribution of Strength of 20 WIC Wires Tested at $\dot{\epsilon}$ *= .02 in./in./min.*

In summary, the above work is a further example of the precautions which must be taken to insure complete characterization of composite components before comparisons between seemingly similar composite materials can be made. The different thermal treatments were the result of attempts to make copper-tungsten composites by capillary-rise action and liquid infiltration and characterizing the wires which were to be incorporated into these composites.

B_4C/B/W filaments which had been fabricated into a composite by liquid infiltration of aluminum at 720 C for 10 minutes and then the aluminum removed by etching in HCl solution (see Figure 11)

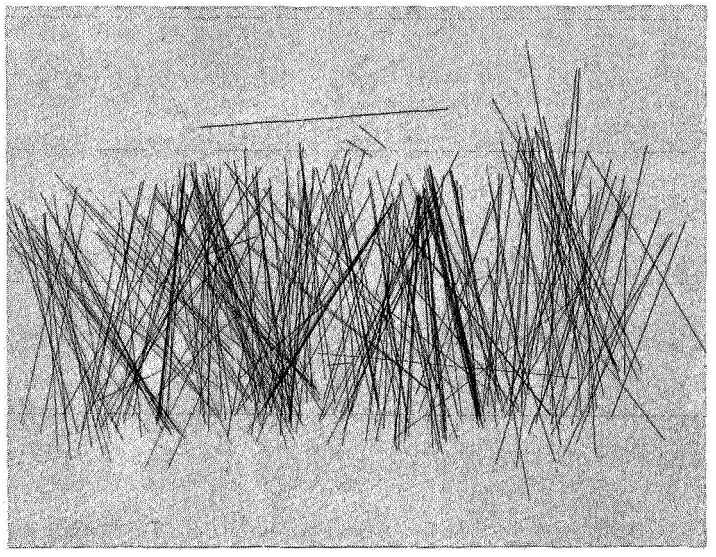

Figure 11. 300 B_4C/B/W filaments which had been etched out of an aluminum infiltrated composite by a 50% solution of HCl (1/2 size)

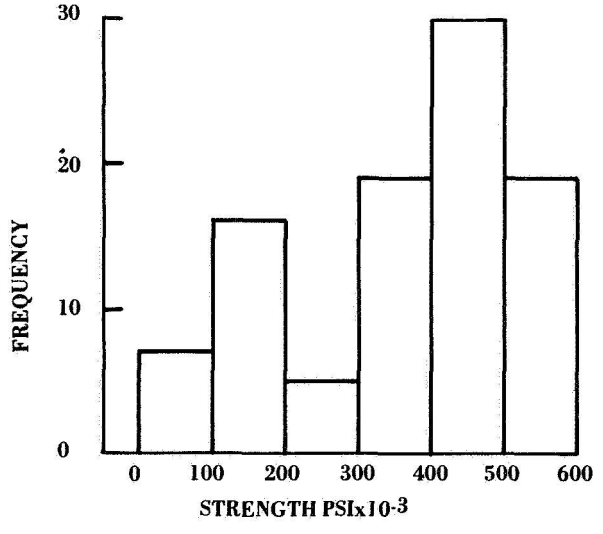

Figure 12. Frequency/strength distribution curve for 96 etched out B_4C/B/W filaments.

were tested extensively during this reporting period. Ninety-six filaments were tested on an Instron machine in tension at room temperature at a strain rate of 0.02 in/in/minute. The frequency/strength distribution curve derived from these data are shown in Figure 12. There is an

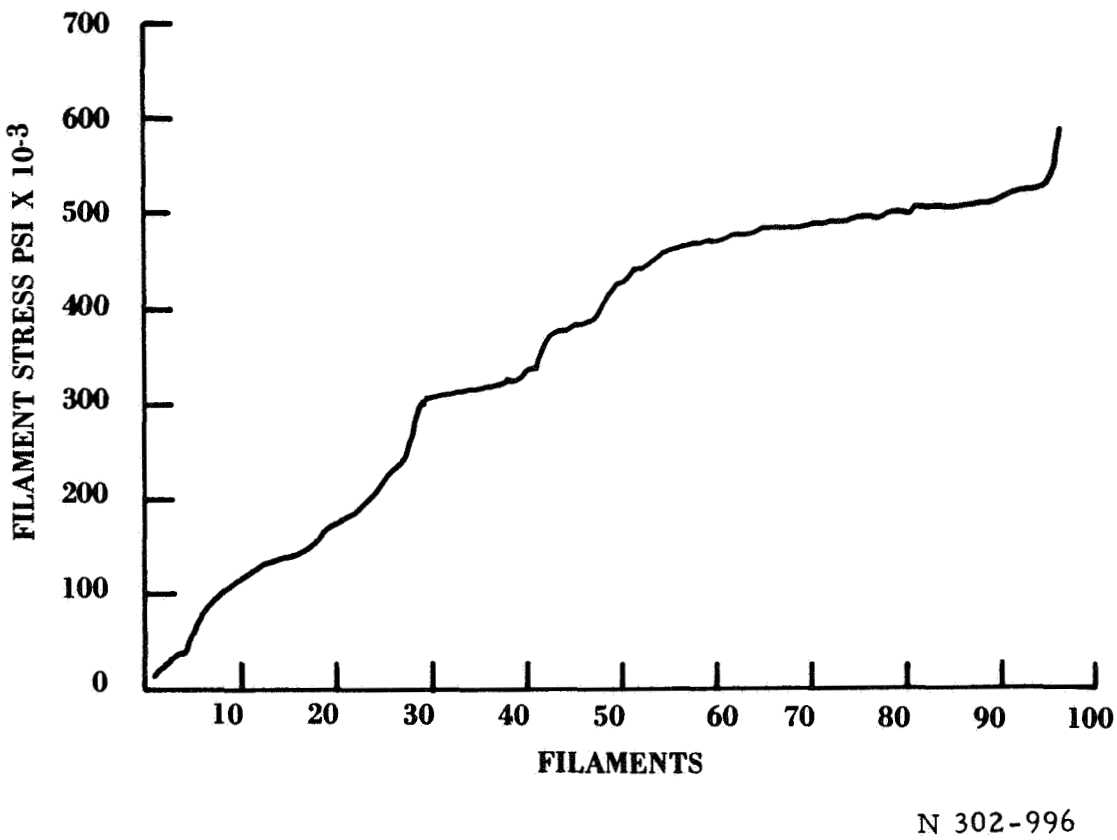

Figure 13. Failure stress of 96 filaments plotted from lowest to highest values

obvious bi-modal distribution of strength peaking in the 100,000-200,000 psi range and the 400.000-500,000 psi range.

All the tensile data is shown in Figure 13, plotted from lowest to highest value as a convenience. This plotting technique is used extensively in a later section. This plot is utilized later to arrive at Figure 25 in Section II C. The lowest value recorded was 18,000 psi while the highest value reached by a single filament was 590,000 psi. The numerical average value of all the tests was 357,000 psi.

These filaments, which had received all the various processing manipulations necessary to form composites, showed a slight weakening when compared to virgin material tested in the as-deposited condition.

The variability of strength properties encountered in filamentary materials as a function of both initial forming and processing damage made statistical testing on a sample to sample basis a necessity. Therefore, further filamentary testing results are scattered throughout the report as the needs arise.

2. *EPOXY EVALUATION*

During present epoxy-filament composite studies it was necessary to devise a means to adjust the bond strength between filament and matrix. A valid approach would be to vary the plasticizer content of the formulation. Just such an approach was tried. Table XI summarizes the formulation compositions while Figure 14 presents the tensile strength of each formulation at two different strain rates (2 in./in./min and 0.02 in./in./min.).

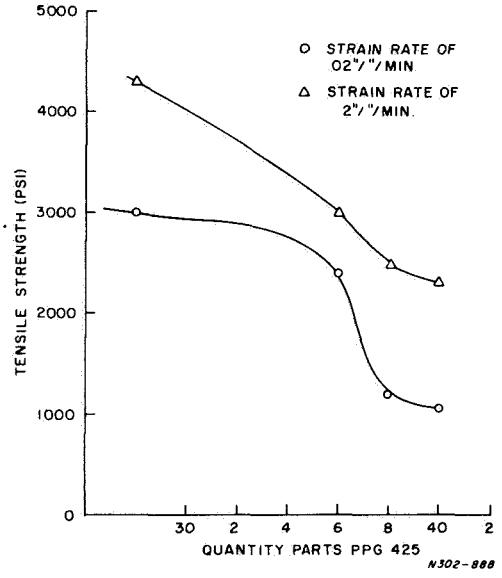

Figure 14. *Variation of Tensile Strength of Epoxy Novalac as a Function of Plasticizer Content (PPG425)*

TABLE XI. EPOXY NOVALAC FORMULATIONS STUDIED

Epoxy Designation	DEN 438	PPG 425	MNA	BDMA
PPG (30)*	52**	30	36	1
PPG (36)	52	36	36	1
PPG (38)	52	38	36	1
PPG (40)	52	40	36	1

*Standard formulation

**Numbers in all columns represent quantity parts

It was found that the bond strength could indeed be varied using this technique. However, as discussed in a later section, the crack sensitivity of the more heavily plasticized materials, increased at a much faster rate than the bond strength decreased, so that the overall effect was a fracture behavior which did not change markedly.

The problem of varying bond strength independent of epoxy chemistry (and therefore basic tensile strength) was solved, however, by treating the surface of the filaments with graphite or Teflon so that intermittent bonds would form. These materials are inert in the Novalac formulations and it is to be noted that many other organic or inorganic lubricants or sizings (such as MoS_2, WS_2, etc.) could be equally effective. Thus, a system was devised which can vary the bond strength of the epoxy formulation which had been standardized in previous work [1]. This isolation or separation of the bond strength variable from the many parameters which affect composite strength is an important result of this years' effort.

C. Aluminum Matrix Composite Systems

Prior work has shown that the strength predicted by the rule-of-mixtures was achieved in many continuous B_4C/B/W composites. It was also shown that B_4C/B/W filaments are ideal for aluminum-based composites, since they are capable of maintaining their chemical and mechanical stability at high temperatures. Also, studies with thin epoxy-filament samples had delineated the fracture modes to be expected in composite materials.

Thin Al-B_4C/B/W specimens were fabricated to extend the epoxy-filament work to metal matrix systems. Also, 50 v/o continuous filament B_4C/B/W-Al composites of various geometric designs were fabricated to study the tensile and fatigue behavior of large composites at both room and elevated temperatures. A group of aluminum composites containing chopped B_4C/B/W filaments in discontinuous array as reinforcements were also made.

1. Al-B_4C/B/W SINGLE, 5 AND 10-FILAMENT COMPOSITES CONTAINING CONTINUOUS FILAMENTS

a. Fabrication

A technique previously described[7] was used to produce single, five and 10-filament continuous composites. Briefly, 2 in. long by 1/8 in. wide by 0.025 in. thick aluminum strips were laminated together by hot pressing at 550 C for 10 minutes at 10,000 psi in a steel die. The filaments were incorporated into the resulting laminate before pressing by alternately laying 0.006 in. diameter aluminum wires and filaments so that the single filament array was centered in the laminate while the 5 and 10 filament arrays were equi-spaced in the cross section of the laminate. A series of three different filament surface treatments were used: including, as-deposited filaments (uncoated); sputtered with iron (coated); and graphite coated filaments (graphite).

Typical specimens produced by this method were approximately 0.030 in. thick, 0.135 in. wide and 2 in. long. All subsequent tensile tests were performed on an Instron tensile machine at strain rates of 0.02in./in./minute and 2 in./in.minute with 1 in. gauge length.

b. Results

Owing to very large scatter in the results obtained by tensile testing low volume $B_4C/B/W$-Al specimens, only a few very general remarks seem warranted. The tensile strength results are shown in Figure 15 and the total elongations to failure are shown in Figure 16. The extent of filament break-up as a function of surface treatment is shown, for single-filament specimens, in Figure 17.

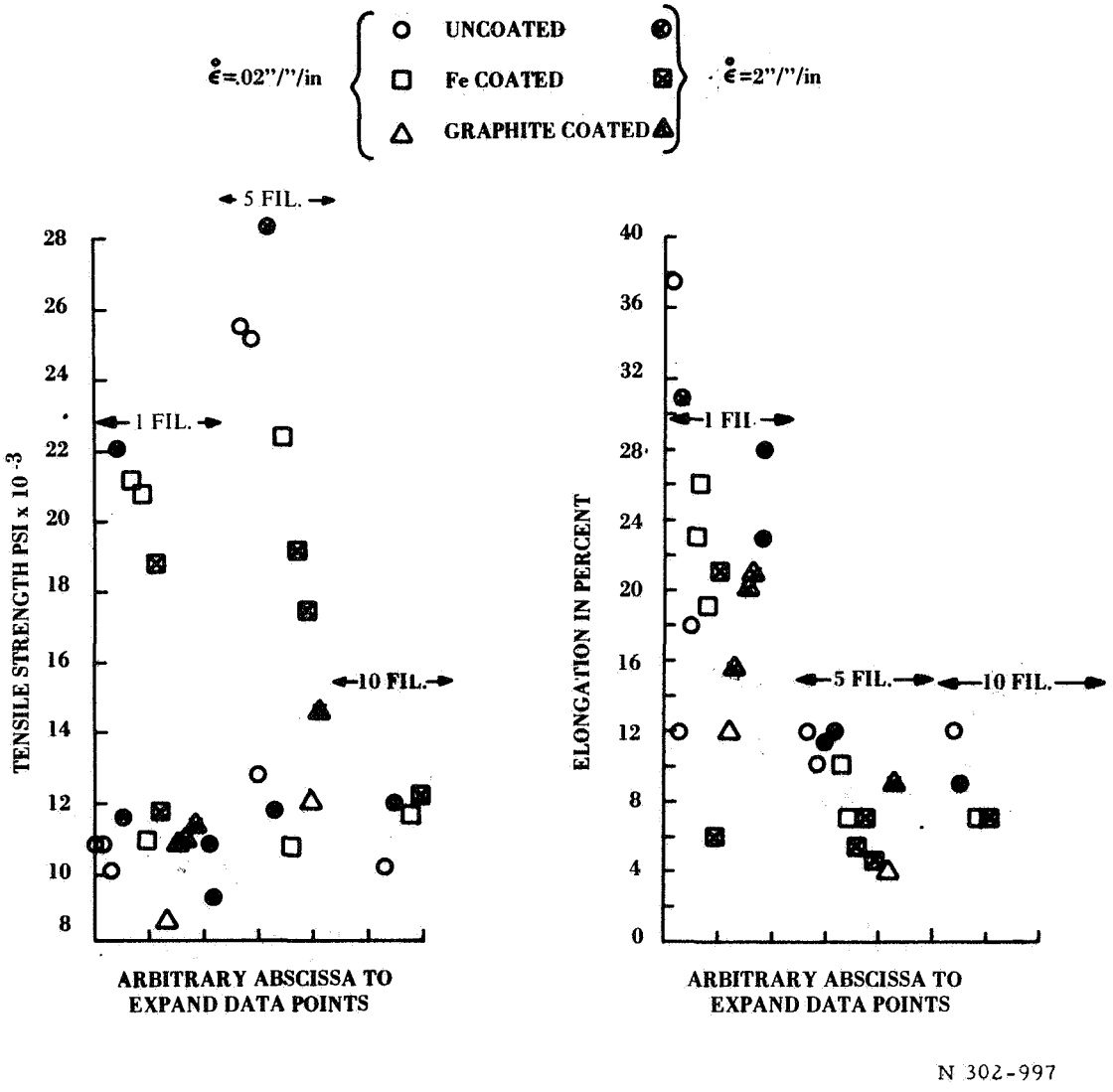

Figure 15. The effect of surface treatments on the tensile strength of low volume fraction $B_4C/B/W$-aluminum specimens

Figure 16. The effect of surface treatments on the tensile elongation to failure in low volume fraction $B_4C/B/W$-aluminum specimens

Although the data are limited, it would appear that a graphite coating reduces the bond strength while iron coating increases it (see Figure 17). It is also quite evident that filament break-up was confined to single-filament specimens; that is, 5 and 10-filament specimens exhibited only 1 break per filament, regardless of the kind of surface treatment. Figure 18 is typical of failure in multi-filament specimens (matrix etched away to show the filament integrity). Note that the breaks appear not to be randomly distributed.

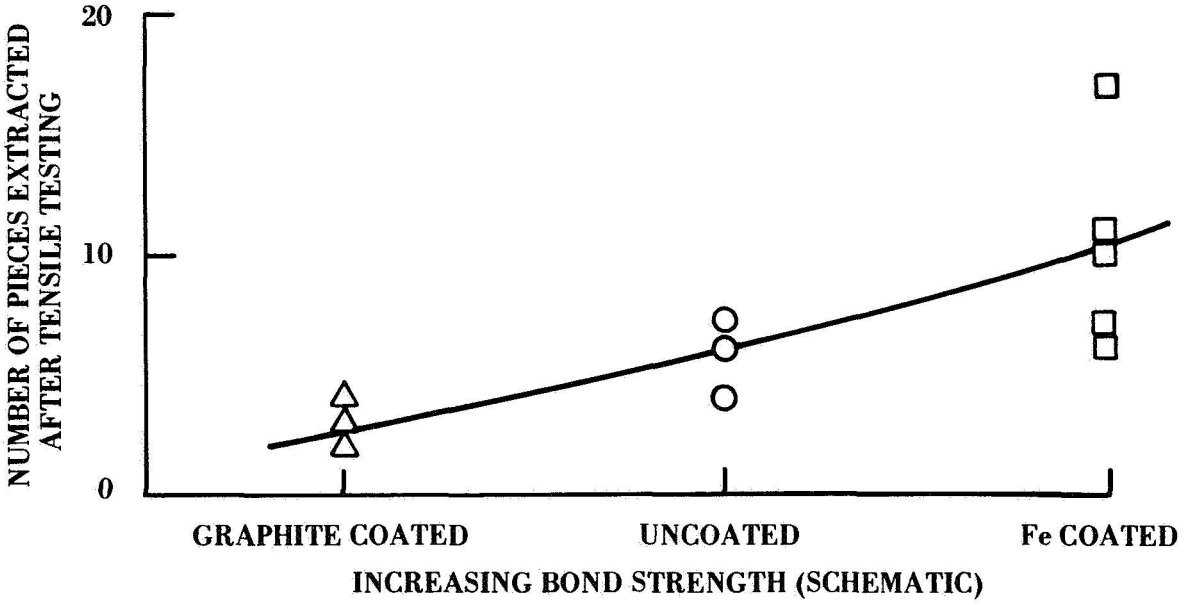

Figure 17. The effect of surface coatings on filament break-up in single filament B_4C/B/W-aluminum specimens

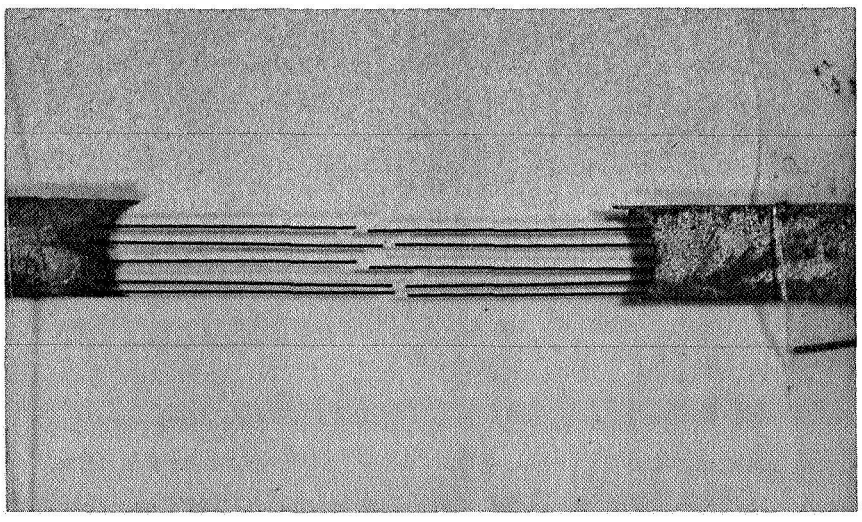

Figure 18. Typical 5-filament specimen after tensile failure (matrix dissolved to show filament integrity)

Figure 19 contains a pair of load elongation curves for single-filament specimens and shows the abrupt load changes which are associated with filament break-up. Perhaps the least ambiguous of the scattered tensile test results (see Figures 15 and 16) is the effect of configuration on elongation to failure. Most of the single-filament specimens are slightly less ductile than plain aluminum specimens. The multi-filament specimens are markedly less ductile than aluminum and also less ductile than most of the single-filament specimens. Apparently, the concentration of filament failures (see Figure 18) induces what in a homogeneous specimen would be designated as premature necking.

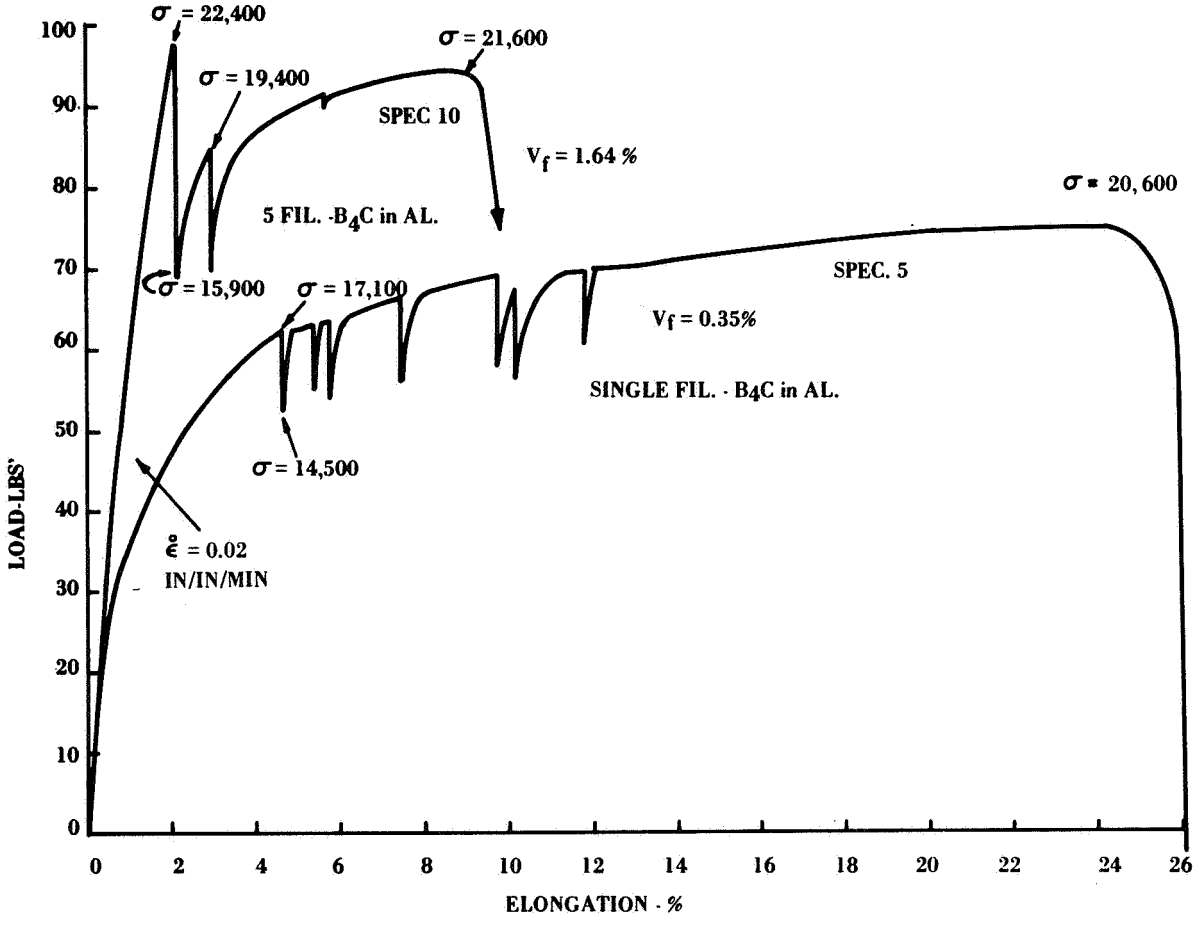

Figure 19. Typical load-elongation curves for single and five-filament B4C/B/W-aluminum specimens

The cumulative damage rationale for composite strengthening involves the proposition that reasonably extensive filament break-up (at weak regions in brittle filaments) will not preclude reasonable composites strengths. These data, while not definitive, indicate the phenomenon of filament break-up will not occur in B4C/B/W-Al composites having useful volume fractions. As will be discussed later, this has been confirmed for 50 volume percent composites which are quite strong without the cumulative damage phenomenon.

2. *CONTINUOUS ALUMINUM COMPOSITES*

a. Fabricate

The technique of others [12] was adopted to produce B_4C/B/W-aluminum test samples which would be suitable for high temperature testing. First attempts to utilize graphite inserts in a graphite mold to form the gauge section of a tensile bar (see Figure 20) failed because of the large difference

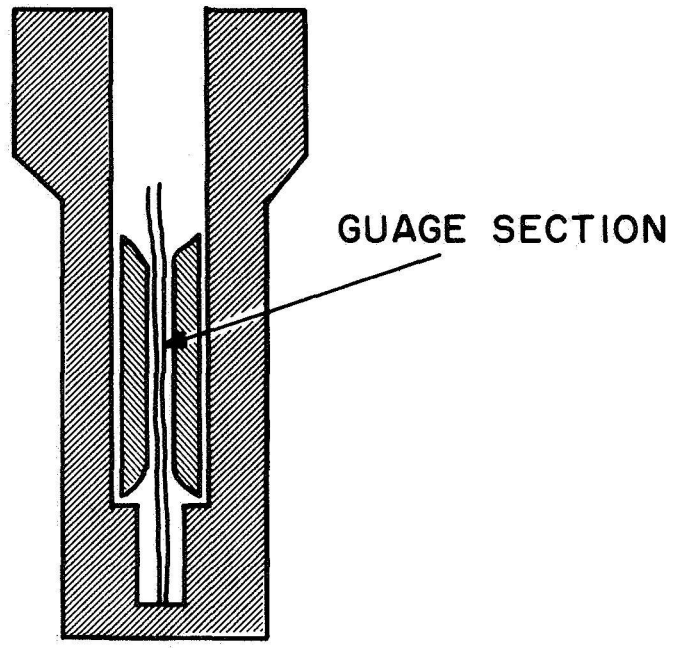

Figure 20. Schematic Diagram of Graphite Mold – Graphite Insert Assembly

in thermal expansion between aluminum and graphite which consistently produced tensile failure of the specimen at the fillet on cooling. A modification was made which solved this problem. A 2 in. long, 1/4 in. O.D. steel tube (SAE1020) with an I.D. of 0.080 in. was filled with filamentary material and the assembly was infiltrated with molten aluminum at 700 C in a hydrogen atmosphere. A one inch gauge, 0.080 in. diameter section was then ground from the center of the composite casting forming a usable specimen geometry (see Figure 21).

Specimens formed by this method were to be used for high temperature testing including uniaxial tension, creep and fatigue.

However, attempts to use these specimens for high temperature tensile tests resulted in pull out due to insufficient shear area in the grips. These specimens were adequate for room temperature testing and were used to study the room temperature fatigue properties of these materials.

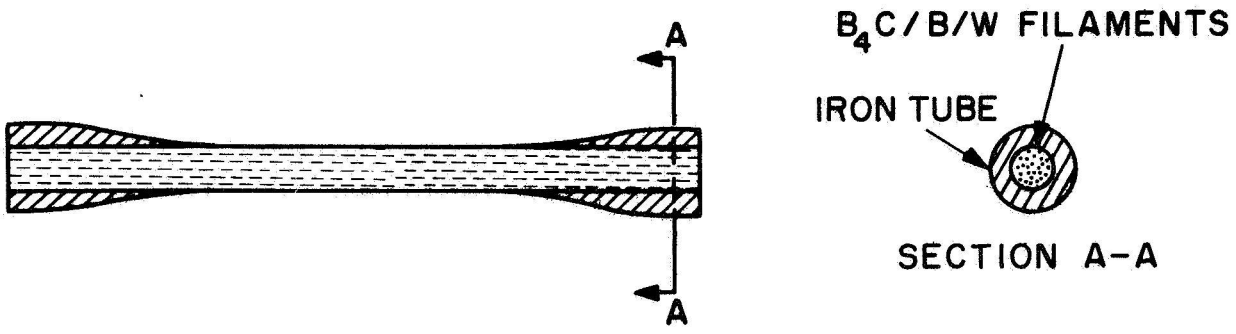

Figure 21. Sketch Showing Fabrication Technique for Al-B_4C/B/W Tensile Bars Suitable for High Temperature Testing

Others [13] had designed a flat tensile bar mold for liquid infiltration such that part of the filament containing volume could be physically held in serrated grips. The flat tensile bar is better illustrated by Figure 22. The iron strips were incorporated in the mold cavity so that the number of filaments

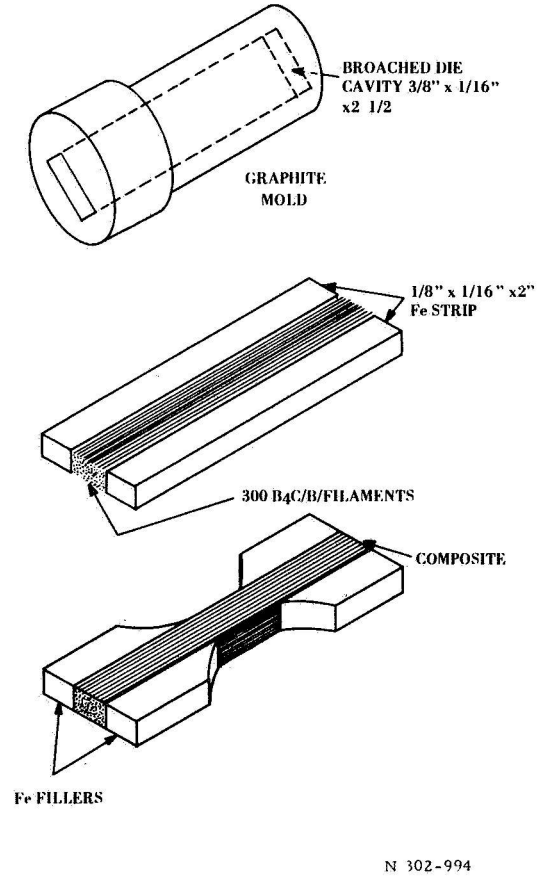

Figure 22. Schematic view of flat tensile bar molding and bar design

needed to completely fill the cavity was reduced by 2/3 as a filament conservation step. All tensile bars were designed to contain 50 volume percent B_4C/B/W filament. This composite section of the specimen measured 1/16 in. x 1/8 in. x 2 in. and contained 300 filaments. After removing the iron from the test section, it is seen that a tensile bar containing a 1 in. gauge section of Al-B_4C/B/W composite can be formed. Unfortunately, this design also proved incapable of testing at high temperatures and indeed also pulled out at room temperature. A reduced section in the composite area was also tried (Figure 23) so that only 1/3 of the original composite cross section remained

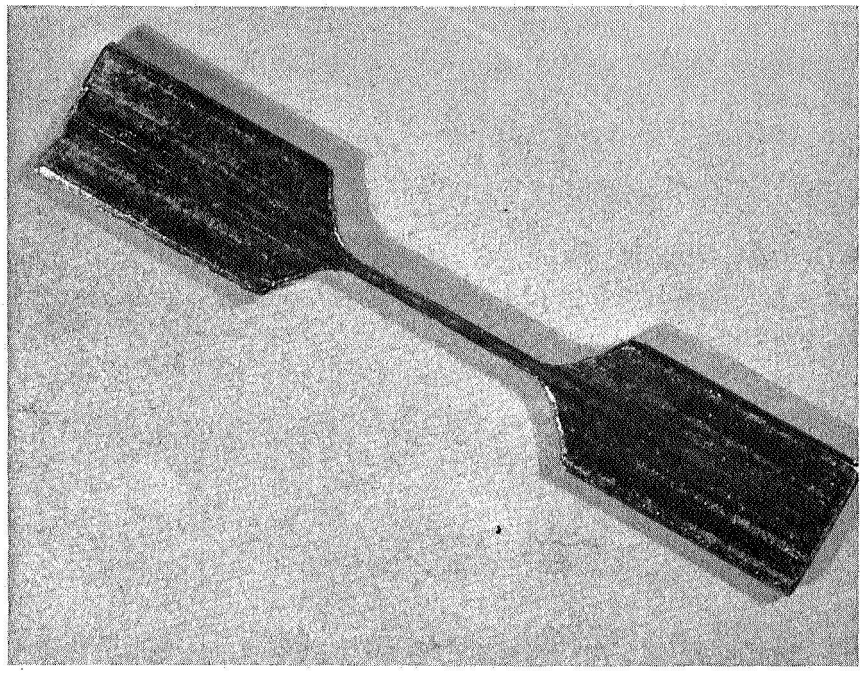

Figure 23. Flat tensile specimen containing reduced composite cross-section

(~100 filaments) still without success. The twelve specimens fabricated were salvaged for room temperature measurements by stripping the iron slabs from the grip area and resorting to the technique [7] of inserting the composite bar into aluminum grip tabs with epoxy adhesive.

Further specimen designs were tried with increased shear area still without success. It appears that with pure aluminum as a matrix material, high temperature testing would necessitate very long specimens which could not be fabricated with the present infiltration apparatus.

b. Tensile Test Results

Table XII contains a summary of the tensile test results obtained on the salvaged 50 volume percent continuous B_4C/B/W-aluminum composites.Tensile tests were performed on an Instron machine. All specimens were tested at a strain rate of 0.02 in./in./Minute, unless otherwise designated in the table. (All specimens which pulled out of the grips, but were not otherwise damaged, were re-tested.)

Tensile data at 500 C, although recorded, is only a measure of the stress necessary to overcome the specimen shear area in the grips. All high temperature tests pulled out in this manner. Data obtained on specimens tested at 2 in./in./minute strain rate also proved invalid because of inadequate pen response on the Instron. A simple exercise using 1/16 in. diameter drill rod specimens showed that the machine was only capable of reliably testing specimens at strain rates of 0.5 in./in./Minute or less.

Figure 24 is a plot of all the room temperature tensile data for 50 v/o continuous

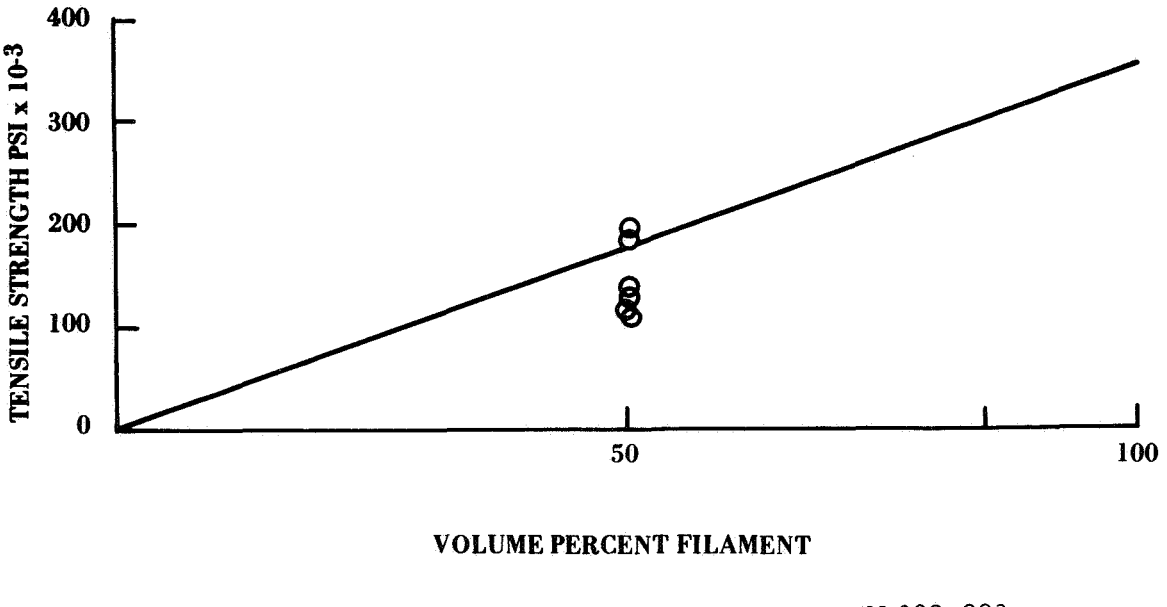

Figure 24. Room temperature tensile strength of 50 v/o continuous B4C/B/W-aluminum composites compared to the predicted value using the rule-of-mixtures based on the average filament strength of 357,000 psi

B_4C/B/W-aluminum composites at 0.02 in./in./minute strain rate, accumulated during this study period. Included in the figure is the predicted (rule-of-mixtures) strength of composites using the average value of filament strength as reported in an earlier section. As can be seen, the value scatters both above and below the predicted value of 175,000 psi.

c. Discussion of Results

The tensile test data on continuous composites fell both above and below the rule-of-mixtures predictions. Considerations of "mechanical compatibility" (see section IID-4) might be invoked to explain sub-average results, but the higher strength observed requires additional considerations. As a beginning, it is useful to examine the matter of bundle vs. composite strength expectations.

The effect of the filament strength distribution on the expected bundle strength is shown in Figure 25. The strength distribution was obtained by extracting 96 filaments from a B_4C-Al composite and testing each individual filament in tension (Section II B). The strength values were arranged in the order of increasing strength, and the median of each group of eight specimens were plotted using data from Figure 13 (see also Figure 25) and the solid line, then, represents the estimated strength distribution for 100 specimens. The abscissa shows the number of filaments (in a bundle of 100) which would be broken as the stress *per unbroken* filament increased. The dashed-lines in Figure 25 show the stress per filament at constant load and they curve upward because the stress on the unbroken filaments increases as the number of filament failures increase. The intersection of these curves with the ordinate is the average stress on the 100 filaments if none had been broken.

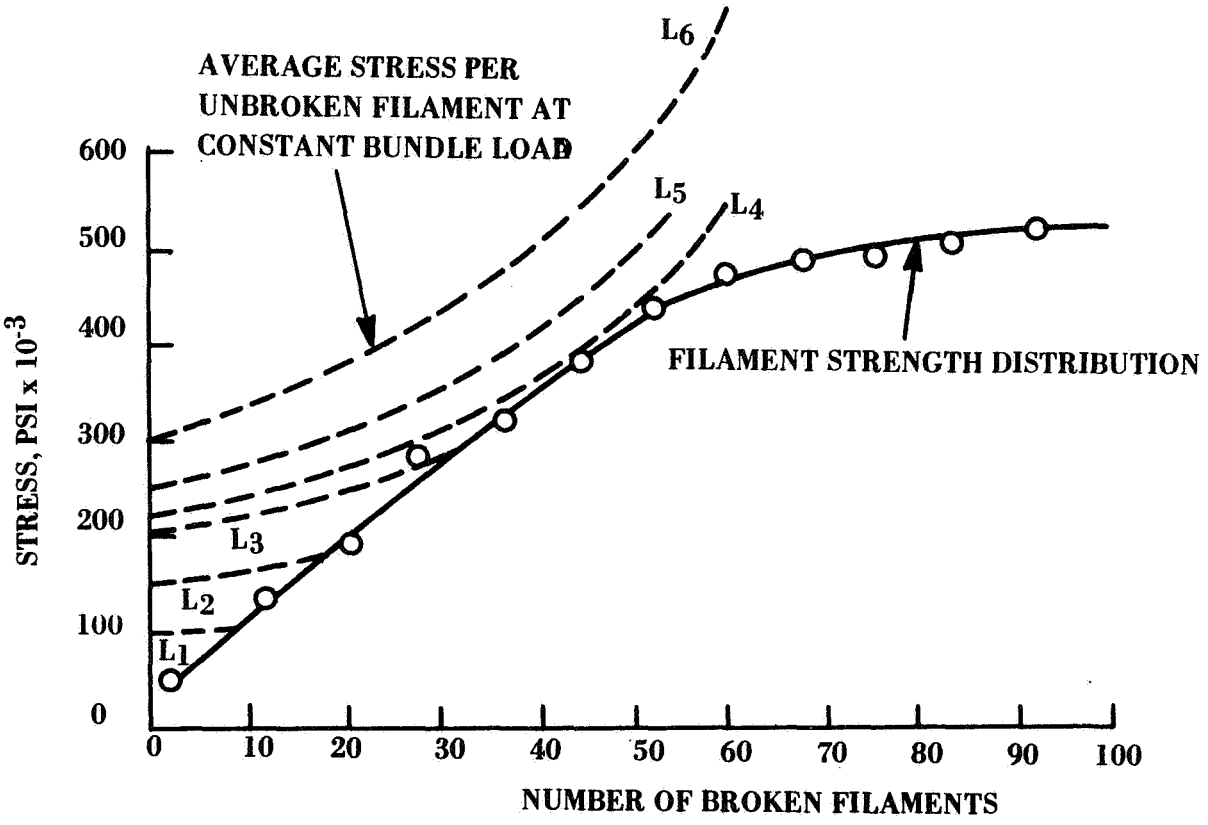

Figure 25. The effect of filament strength distribution on bundle strength

From an examination of Figure 25, it is possible to hypothesize a load deflection curve for the filament bundle. It is assumed that filaments will continue to fail at a constant load until the strength of the unbroken filaments becomes greater than the rising stress occasioned by failure of the weaker filaments. The bundle will fail at a load characterized by a dashed curve tangent to the strength distribution curve (L4 in Figure 25). This is, in this case, a load equivalent to an initial average stress of 220,000 psi/filament which will cause the bundle to fail catastrophically, because the stress per unbroken filament is above and increasing more rapidly than the strength of the remaining unbroken filaments.

Since the number of broken filaments will increase from approximately 2% at 50,000 psi to approximately 42% at the onset of catastrophic failure, the stiffness of the bundle will continue to decline as the load rises during the tensile test. The effect of filament failure (from Figure 25) on stiffness is also taken into account in synthesizing the bundle (non-linear) load-elongation curve in Figure 26. It is interesting to note that this non-linearity would not be easily distinguished from approximate 0.3% uniform plastic deformation in a ductile material. The flat transition region at the top of the curve would be expected to continue so long as the slope of the curve for rising stress on unbroken filaments was equal to the slope of the filament strength distribution curve (at the point of tangency in Figure 25). In this transition region, of accelerating filament breakage, the rapidly decreasing bundle stiffness precludes a bundle load increase (in a constant cross-head motion test).

There are several significant similarities and differences between the hypothetical bundle (see Figure 26) and the behavior of a B $_4$C/B/W-aluminum composite shown in Figure 27. Composite No. 9 (see Figure 27) contained 100 B$_4$C filaments (same batch as filament used in strength-distribution work, shown in Figure 25) in an (infiltrated) aluminum matrix (see Table XII). The data for the plain aluminum was obtained on a specimen of approximately the same cross-section. The comparison is summarized in Table XIII.

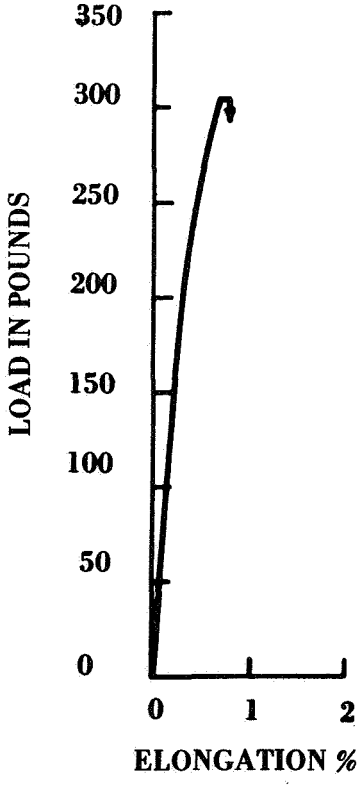

Figure 26. Synthesized load/deflection curve for a bundle of 96 filaments (from Fig. 13)

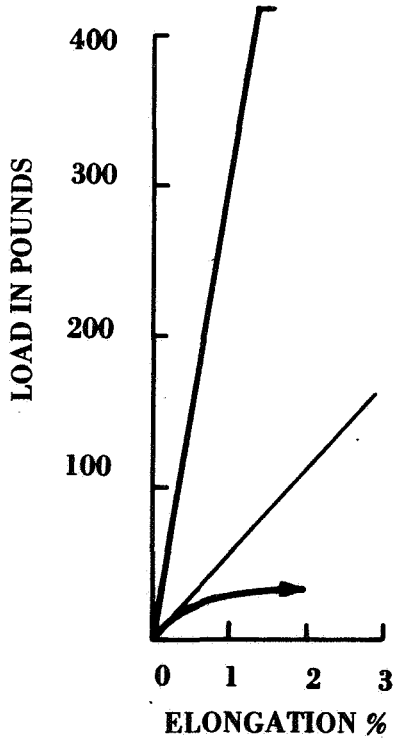

Figure 27. Load/elongation curves for specimen # 9 and pure aluminum

The stiffness difference need not be regarded as significant when comparing hypothetical with real tests owing to the "softness" of tension testing machines.

TABLE XII. TENSILE TEST RESULTS OF 50 v/o CONTINUOUS B_4C/B/W-ALUMINUM COMPOSITES

Spec. #	Load (Lbs.)	Tensile Strength (psi)	% Efficiency (as coated values of 375,000)	% Efficiency (after processing 357,000)
1 (1)	---	---	---	---
2	330	141,000	0.75	0.79
3 (2)	---	---	---	---
3 (4)	135	55,000	---	---
4	230	110,000	---	---
5 (2)	187	67,800	---	---
6 (5)	---	---	---	---
7 (6)	480	198,000	105.00	111.0
8 (7)	307	116,000	---	---
9	420	186,500	100.00	105.00
10 (3)	310	131,000	---	---
11 (2)	---	---	---	---
12	Not tested			

(1) Specimen lost during machining
(2) Tested at 500 C – pulled out of grips
(3) Tested at room temperature – pulled out of grips
(4) Tested at 2 in/in/min. strain rate
(5) Etched out filaments after infiltration cycle
(6) Cycled to 500 C once
(7) Tested at 0.5 in/in/min. strain rate
(8) The % efficiency is the tested tensile str./filament divided by the average value determined statistically.

TABLE XIII. COMPARISON OF HYPOTHETICAL BUNDLE OF 100 B_4C/B/W FIBERS WITH COMPOSITE SPECIMEN

Load Deflection Characteristics				
Sample Decription	Stiffness	Shape	Transition Region	Max Load per Filament, lbs
Hypothetical Bundle	Based on Elastic Modulus	Non-linear	Flat	3.05
Composite 9	Less stiff than bundle	Linear	Flat	4.20 (3.92)[1] (3.45)[2]

[1] Load sharing by Al in plastic range

[2] Load sharing by Al elastic deformation extrapolation

It seems reasonable to assume that the shape differences in the load-elongation curves are significant. The results suggest one of two possibilities: (1) filaments break in increasing numbers as the load rises, but being well-bonded, their contribution to stiffness is not appreciably diminished or (2) few, if any, filaments break prior to catastrophy at stresses predicted by the bundle model. In either event, it is interesting to note that the introduction of a ductile matrix reduces the apparent ductility of a bundle of brittle filaments.

Both the hypothetical bundle and the real composites exhibit a flat load-deflection transition region at the onset of catastrophic failure. The remarkable shape similarity indicates that the catastrophic mechanism is similar for both.

The experimental composite is approximately 38% stronger than the hypothetical bundle and in another case (see Spec. 7, Table XII) 57% stronger. These values may be reduced by taking into account the load bearing capacity of the aluminum matrix (see Figure 27) in which case the composites are only 28% or 48% stronger. Even more conservative is to consider that the aluminum does not deform plastically (as indicated) but shares the load in proportion to its elastic behavior; in this case, the composites are still 11% or 13% stronger than the bundle. Fabrication and experimental difficulties are often necessary to explain away less-than-bundle strengths; but, rational explanations seem necessary to explain composites which are stronger than bundles.

Superior results for composites can be rationalized by recalling a common characteristic of brittle filaments. Owing to a statistical distribution of flaw severity, short lengths are often stronger than

longer gage lengths. In consequence, strength distributions obtained on 1-inch gage lengths are adequate only for bundle models, because a single failure precludes any further load sharing by the broken filament. However, if broken filaments continue to reinforce (as long as they exceed the critical length), and breaks are randomly located, composites can be stronger than bundles owing to the higher strength of the broken remnants. In such a situation, the specimen would remain stiff and be stronger than the bundle as is the case here. This "cumulative damage" model is, then, consistent with the observed mechanical behavior but it appears completely incompatible with another experimental observation: multiple filament B_4C/B/W-Al specimens almost never exhibit more than one break per filament and these breaks are not randomly located but situated at or very near to the region of catastrophic failure.

The fact that there is no direct evidence of cumulative damage shows that a number of randomly situated weak regions of filament do not bear their share of the load and that conventionally obtained strength-distribution data is inadequate for predicting composite behavior. The problem is to explain why weak regions of filament do not fail until after the average filament stress far exceeds the strength of the weak region. In what follows a model is suggested based on a different elastic strain distribution in the composite relative to that in a single filament test.

Filament defects may be small internal cracks having high (tip) stress concentrations. Since the net effect (for strength of single filaments) is equivalent to a local reduction in cross section, it is depicted as such for convenience in Figure 28A. Under this load. this filament will have an inhomogeneous elastic strain distribution along its length, the ratio of maximum to minimum being inversely proportional to the ratio of the respective cross-sectional areas. Failure in the tensile test will occur when the maximum elastic strain (located at the smallest cross-section) becomes equal to the fracture strain. However, when two such filaments are well-bonded to three defect-free filaments the strain inhomogeneity in the defect region will be markedly reduced by virtue of the strain constraint imposed by the neighboring filaments (as indicated in Figure 28B). Therefore, the 5-element specimen will sustain a greater nominal average stress before the fracture strain is reached at either defect. When one of the defects finally fails, the highest elastic strain in the specimen will be in the neighboring filaments in the region of the failed defect, not at some other 5-element defect region. This reasoning is numerically illustrated by assuming values of elastic modulus and a high and low strength shown in Figure 28. In summary, the elastic strain inhomogeneities characterizing loaded single filaments are reduced (by interaction constraints) when the filament is incorporated in a well-bonded composite. This reduces the strength-scatter and increases the average strength predicted on the basis of single-filament tests. This accounts for higher-than-average (predicted) composite strengths and is consistent with the one-break-per-filament observation. This model differs from conventional cumulative damage models in four respects: (1) useful load redistribution occurs prior to, not after, failure of weak regions; (2) it does not depend upon an inverse strength-gage length relationship; (3) it is consistent with few breaks per filament; and, (4) it predicts specimen failure nearly coincident with the first filament failure. The details of the example (Figure 28) were chosen to explain above- average strength. If the two defects were lined up in a single plane but still separated by defect-free filaments, the composite would exhibit average or near average strength. If, however, the two defects were adjacent, their common boundary would

no longer have the same constraint against inhomogeneous deformations and the composite would exhibit less-than-average strength.

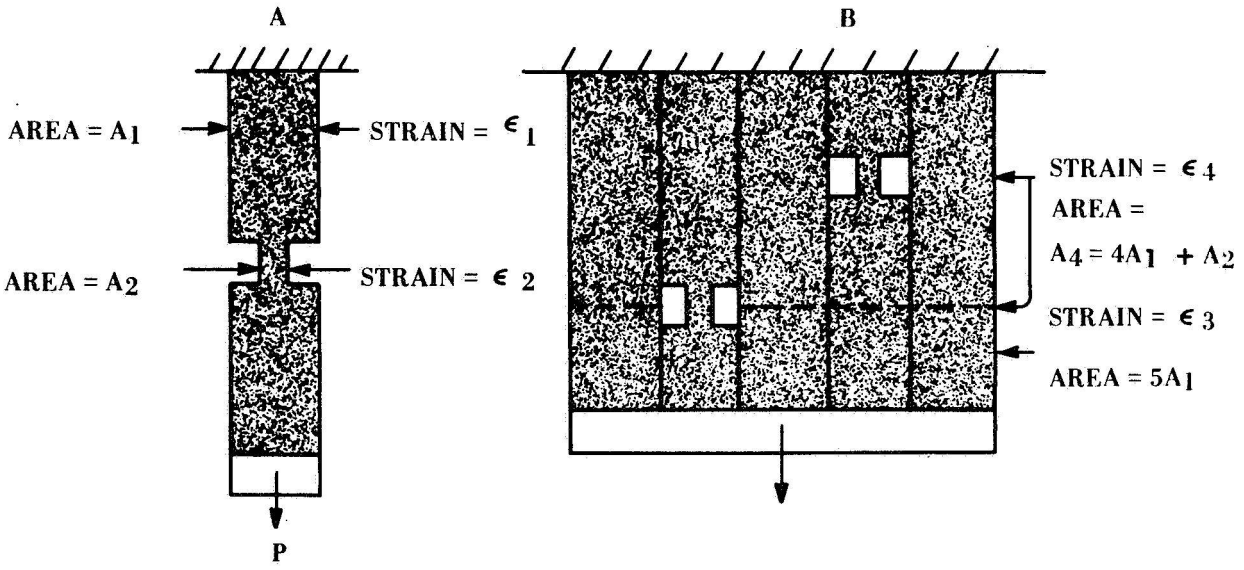

If max strength is 550,000 psi and elastic modulus is 55 x 10^6 psi, $\epsilon_f = \epsilon_2 = \epsilon_4 = 10^{-2}$.

If nominal minimum strength is 55,000, ($\epsilon_1 = 10^{-3}$) in single filament test,

then $\epsilon_2/\epsilon_1 = 10^{-2}/10^{-3} = 10 = A_1/A_2$ and $\epsilon_3/\epsilon_4 = 4/5 + 1/5\ A_1/A_2 = 41/50$

$\therefore \epsilon_3 = 41/50 \times 10^{-2}$ (when $\epsilon_4 = \epsilon_f = 10^{-2}$)

and the nominal stress/filament in composite,

$$\sigma_c = \epsilon_3 E = 41/50 \times 55x104 \quad 451{,}000 \text{ psi}$$

The average of individual filament strength

$$\sigma_a = \frac{3 \times 550{,}000 + 2 \times 55{,}000}{5} = 352{,}000 \text{ psi}$$

If above 5 element configuration was unbonded (bundle) the nominal stress per filament,

$$\sigma_B = 3/5 \times 550{,}000 = 330{,}000$$

Figure 28. Schematic representation of model to account for composite strength greater than rule-of-mixtures predictions

Thus, the model chosen is consistent with the scatter of tensile data shown in Figure 24.

A more illustrative description of the inhomogeneous strain criteria is now discussed.

As seen in Figure 29 the strain in filaments 1 and 3 is

$$\epsilon_1 = \frac{e_1}{L_o}$$

and the strain in the E_2 portion of filament 2 is

$$\epsilon_2 = \frac{e_2}{L_o} \cdot$$

Thus, the shear strain is

$$\gamma = \frac{\frac{e_2}{2} - \frac{e_1}{2}}{a} = \frac{e_2 - e_1}{2a} \cdot$$

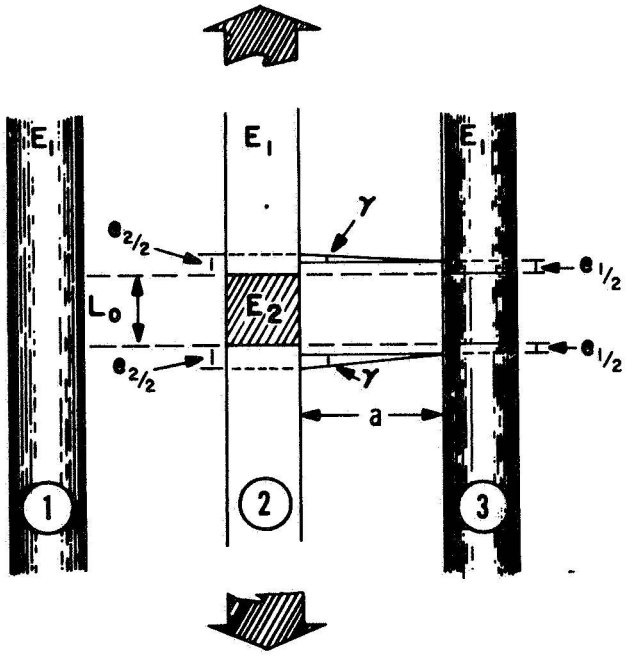

N 303-087

Figure 29. A Detailed Model for Inhomogeneous Strain

For the center filament to experience the strain ϵ_2, the shear strain in the matrix must be at least γ. At the same time the matrix must experience the same tensile strain ϵ_1 at the outer filaments (if bonded) and the same tensile strain ϵ_2 at the center filament (if bonded).

$$\tan \gamma = \gamma = \frac{e_2 - e_1}{2a} \tag{a}$$

or

$$\gamma = \frac{e_2 - e_1}{L_o} \cdot \frac{L_o}{2a}$$

$$\gamma = (\epsilon_2 - \epsilon_1) \frac{L_o}{2a}$$

or

$$\Delta\epsilon = \epsilon_2 - \epsilon_1 = \frac{2a\gamma}{L_o} = \frac{2a}{L_o} \frac{\tau}{G}. \tag{b}$$

The incremental difference in strain which the adjacent filaments experience is directly proportional to the spacing of filaments and the shear stress in the matrix and inversely proportional to the length of the weak section and the shear modulus of the matrix.

For a flaw length L_o on the order of the spacing a, such that $a/L_o = 1$, one can determine the strain difference $\Delta\epsilon$ which can occur for a given matrix material without fiber failure. For aluminum alloy $\tau_{max} = 30$ ksi and $G = 4x10^3$ ksi.

$$\Delta\epsilon = 2\ (1)\ \frac{(30)}{4x10^3} = 0.015^*\ \text{in/in or } 1.5\%\ \text{strain.}$$

For a resin matrix $\tau_{max} = 4000$ psi and $G = 250000$ psi

$$\Delta\epsilon = 2\ (1)\ \frac{(4000)}{250\,000} = 0.032^*\ \text{in/in or } 3.2\%.$$

*Note that these are the strain difference increments which the matrix will allow to occur in two adjacent filaments.

This means that an aluminum matrix material can allow strain differences in adjacent fibers of up to 1.5% before the matrix will exceed its limiting elastic shear strain γ for $a/L_o = 1$ (beyond which excessive yielding of the matrix occurs and the weaker fiber fails). If the difference in fracture strains of adjacent filaments over the flaw length, L_o is greater than 1.5%, the matrix can effectively prevent the weaker filament from failing. If, however, the difference in fracture strains of the adjacent filaments is less than 1.5%, the aluminum matrix will not be stiff enough to prevent the fracture of the weaker filament (for $a/L_o = 1$).

In the case of the epoxy matrix material, the difference in local fracture strains must be greater than 3.2% for the matrix to prevent fracture of the weaker filament. This is why one would expect to see more weak fiber fractures in an epoxy matrix than in aluminum, since the 3.2% differential local fracture strain between adjacent filaments is probably never exceeded in very high modulus filaments when $a/L_o = 1$.

Further, the limiting strain differential given by

$$\Delta\epsilon = \frac{2a}{L_o}\,\gamma \tag{c}$$

is directly proportional to the spacing a and the limiting shear strain γ of the matrix. This means the greater the spacing and the more flexible the matrix, the greater the allowed strain differential (no matrix restriction).

Also, the shorter the gage length L_o over which the local strain is measured, the greater the allowable axial strain differential in that gage length. Therefore, when the flow region is very small ($L_o \to 0$) compared to the fiber spacing a, great deal more local strain differential is allowed to occur without fracture because the fraction $2a/L_o$ is quite large in equation (c).

It is therefore possible for a very small flaw in a filament to have a considerably reduced local modulus (or very high local strain tendency) and yet not fail at that location, because the adjacent filaments are close enough and the matrix is stiff enough to prevent inhomogeneous strain (and fracture) from occurring at that point.

Using the inverse approach one can use the known spacing a and the length of flow section L_o, together with the experimentally determined difference in filament fracture strain $\Delta\epsilon$, to compute the required matrix shear strain γ to prevent individual fibers from failing (i.e., prevent cumulative damage). Inverting equation (c)

$$\gamma = \Delta\epsilon\,\frac{L_o}{2a} \quad . \tag{d}$$

Where $\Delta\epsilon, L_0$ and a are known for a given composite. However, $\Delta\epsilon$ is a local fracutre strain and somewhat difficult to measure.

Note, when G = 0 (bundle with matrix of air) γ is infinite and the differential strain allowable is infinite. That is, the filaments can fail when they reach their local fracture strain with no constraint imposed by adjacent filaments or matrix.

3. *DISCONTINUOUS ALUMINUM-B_4C/B/W COMPOSITES*

Bundles of chopped B_4C/B/W filaments, between ½ in. to ¾ in. long, were infiltrated with aluminum to form composites 0.062 in. diameter x 2 in. long, each containing nominally 50 v/o filaments. The specimens were removed from a multi-cavity mold and aluminum grips were attached [1]. The tensile results are presented in Table XIV and Figure 30. Tensile tests were performed on an Instron tensile testing machine at a strain-rate of 0.01 in./in./min. Unlike the continuous specimens tested, Table XIV shows that predicted rule-of-mixtures values have not been achieved by the discontinuous composites made thus far.

Figure 30 is included to give a graphical view of the relation between the predicted values of composite strength and the actual values measured.

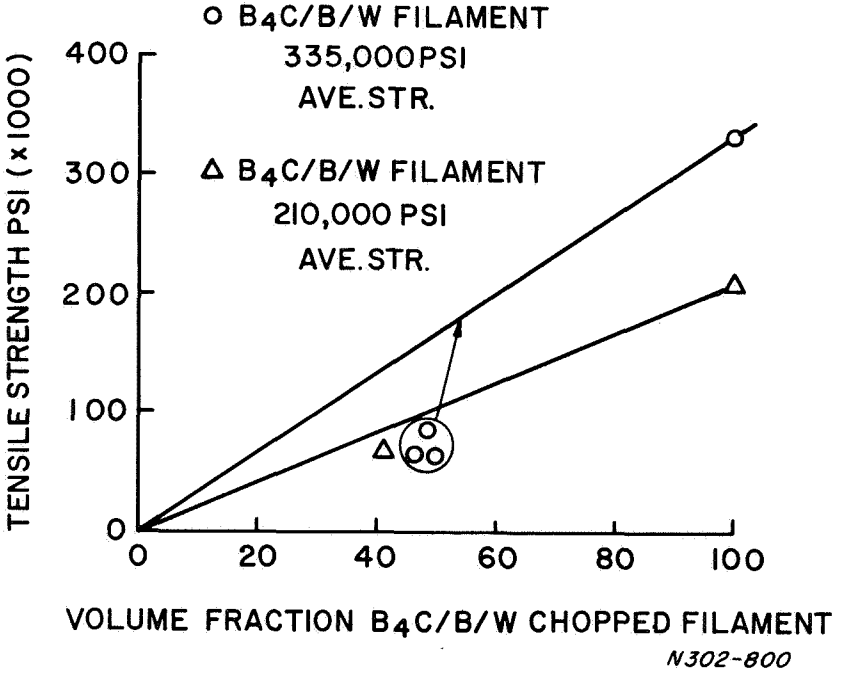

Figure 30. Tensile Strength vs. Volume Fraction for Discontinuous Aluminum-B_4C/B/W Fibers

In summary the limited data thus far indicates that a greater portion of the calculated strength has been realized from specimens using weaker filament (compare No. 18 with 13, 14, 17 Table XIV). The comparisons can be meaningful if matrix limitations are interfering with the reinforcing mechanism of stress transfer efficiency between filaments. That is, the inability of the matrix to deform plastically in the vicinity of the filament ends may lead to premature failure of the composite below its predicted strength value. Then, of course, as stronger and stronger filaments are put into the composite, the predicted value would necessarily be a lower and lower percentage of that value. There are other mechanisms which can also cause premature failure as stronger and stronger filaments are utilized. One has to do with the magnitude of energy release as adjacent filaments breaks and the resulting effect of this energy on neighboring filaments. Another has to do with the stress concentrations which occur as adjacent filaments fail. The energy release mode has been studied using epoxy based composites and is described in another section of this report. The stress concentration mode has been advanced by Zweben [14] as part of a study of the failure of boron-epoxy composites of high boron filament volume fraction.

Another consideration is the inhomogeneous strain criteria advanced for continuous filament composites. As will be shown in the next section, data on continuous filaments containing broken filaments extrapolate to the efficiency value most seen for discontinuous composites at 100% broken filaments (50% maximum).

It must be realized that such few specimens as studied here make the above hypothesis highly speculative at the present time.

TABLE XIV. ROOM TEMPERATURE TENSILE STRENGTH OF DISCONTINUOUS B_4C/B/W ALUMINUM CONTAINING COMPOSITES

Spec. No.	Tensile Strength(s) psi	v/o Fibers	~Theoretical(S_c) (psi)[a]	Eff. % $s/S_c \times 100$
13[b]	65,000	50.0	167,000	39.0
14[b]	85,000	49.2	165,000	51.5
17[b]	69,700	46.8	157,000	44.0
18[c]	62,500	41.0	86,000	

(a) Based on Rule-of-Mixtures, ignoring the matrix contribution

(b) Avg. Fiber strength 335,000 psi

(c) Avg. Fiber strength 210,000 psi

4. *EXPERIMENTS RELEVANT TO THE INHOMOGENEOUS STRAIN HYPOTHESIS*

The "inhomogeneous strain" hypothesis suggested experiments which would test its validity. It was speculated that if composites could be fabricated without damage and the resulting specimens tested in tension at stress levels corresponding to between 85 and 100 percent of their predicted rule-of-mixtures tensile strength, without specimen failure or individual filament failure, the model derived from this hypothesis would be representative of composite mechanical behavior. As will be described, the results were consistent with this hypothesis; however, they were not definitive, owing to shifting filament strength scatter from specimen to specimen and some fabrication damage.

A graphite mold, containing six 1/16 in. diameter by 2 in. deep cavities was packed with B_4C/B/W filaments so that each cavity contained 50 v/o filaments (112 filaments). The filaments were infiltrated with liquid aluminum by the standard method, described earlier (720 C for 3 minutes). The resulting six composites were removed from the mold and five of the rods were epoxy-cemented into steel grips [1] for further room temperature tensile testing. The remaining rod was digested in a 50/50 HCl-H_2O solution as a control.

Statistical strength studies were made of chopped 2 in. long B_4C/B/W material and included the starting material (designated as-coated), a group of specimens which had been soaked for two hours in 50/50 HCl-H_2O solution, designated soaked, and the digested composite No. 6 new. Number 6 new was also examined for filament breakage. The tensile data for these three samples are presented in Figure 31. (The method of plotting the individual tensile values in increasing order was a convenient method for comparison purposes, with a bundle, and is used throughout this report.) The data show that (1) this particular batch of B_4C/B/W was weaker than those previously used (197,000 psi average vs. 375,000 psi average); (2) the HCL-H_2O soak had little effect on the strength of the filaments; and (3) further processing of this material by liquid infiltration weakened it from the virgin condition of 197,000 psi average to after processing average strength of 158,000 psi. Further, (see Table XV) the processed material sustained 22 filament breaks as a result of the temperature cycling and/or aluminum infiltration process.

The average filament strength of 158,000 psi was used to determine the stress levels to which the remaining 5 composites would be subjected so that the tensile values reached would span the 85-100% range mentioned earlier. The results of these tests are shown in Table XV. The specimens (1 new through 5 new) were then digested in 50/50 HCl-H_2O solution and the number of broken pieces recorded. It is to be noted that tensile values both higher and lower than the predicted rule-of-mixtures strengths were reached (assuming 158,000 psi average filament strength). However, the goal of no broken filaments was not achieved. To have been an unambiguous confirmation of the ("inhomogeneous strain") hypothesis, there should have been no broken filaments and the individual strengths should have been essentially identical with those for virgin specimens. As indicated in Table XV, the untested sample (No. 6 new) exhibited 20% filament breakage but similar specimens, which had been loaded, exhibited the same amount (No. 3 new) or less (No. 4

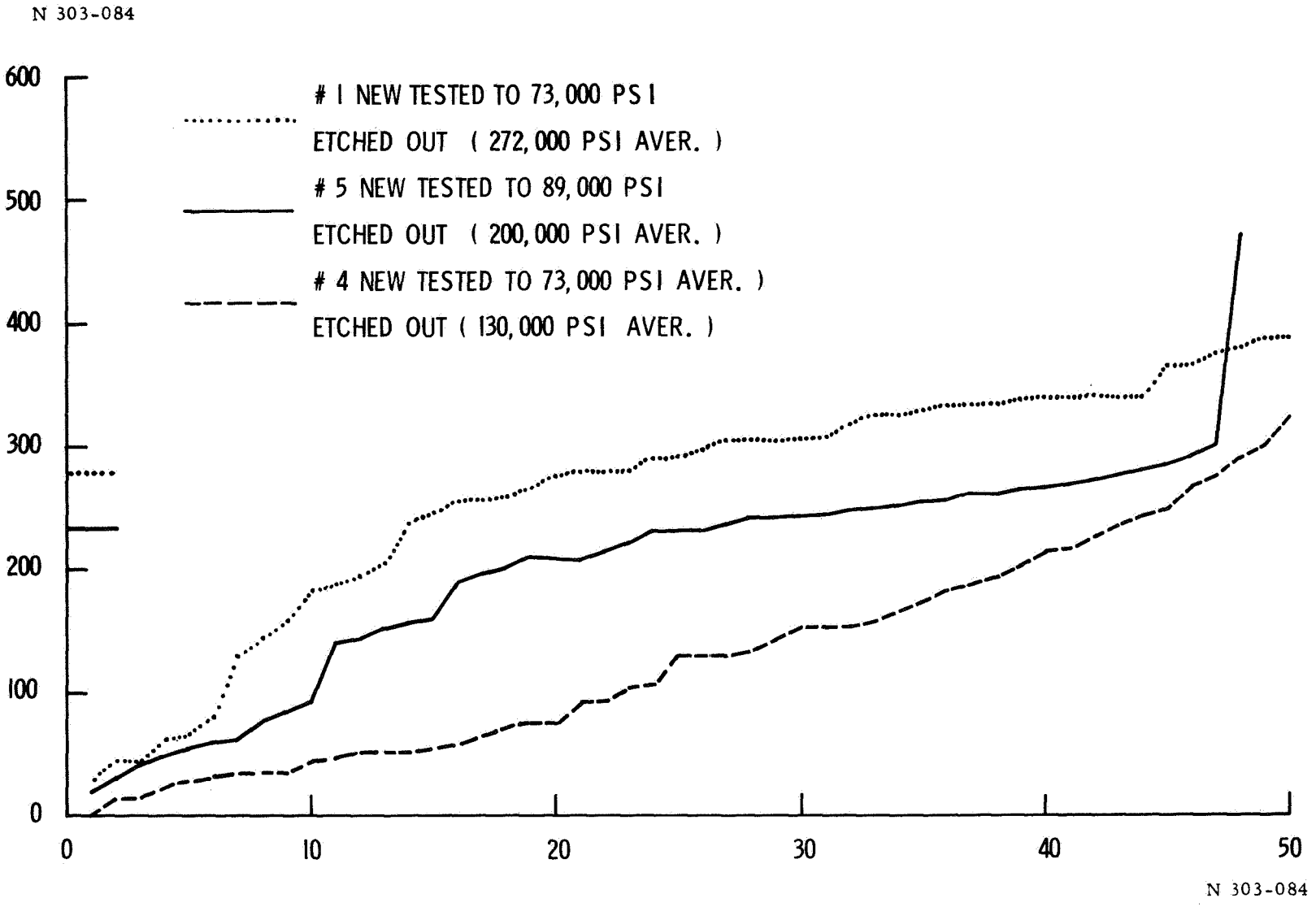

Figure 31. Tensile Data on Virgin, HCl-Soaked and Spec. No. 6 New (Etched) $B_4C/B/W$ Filaments

new) filament breakage. Therefore, it is evident that fabrication damage is quite variable and can obscure the one-break-per-filament prediction of the hypothesis.

A statistical sample of the pre-tested composites filaments (No. 1 new, No. 4 new, and No. 5 new) tensile properties were obtained and are shown in Figure 32. As can be seen, the specimen with the least amount of breakage (No. 4 new) most closely approximated the "untensiled" distribution (No. 6 new) while the other samples showed an increasing average strength due to the smaller number of remaining filaments. Number 1 new which contained 54 broken filaments had the highest remaining average strength (272,000 psi average), which was almost 50% greater than the virgin value of 197,000 psi average. The strength of the extracted unbroken filaments can thus be seen to be greater than or less than that of virgin specimens; thus filament strength-scatter also introduces ambiguities in the results. In consequence, any interpretation of the data must be a qualified one.

One way of considering the data, which is interesting and suggestive, is to assume that any broken filaments (in those specimens unloaded prior to failure) were broken during fabrication (minimum 12-½% maximum 48%). If it is further assumed that broken filaments carried no load at all (bundle behavior), it would follow that the average stress per unbroken filament (in the composites) is greater than the average strength of the individual (extracted) filaments. In the absence of broken filaments, this would be considered to be unambiguously consistent with the "inhomogeneous strain" hypothesis. If, as is the case, a significant number of broken filaments is present, the results could also be interpreted to indicate that the broken filaments share part of the load (i.e., exhibit cumulative damage behavior). The results which come nearest to distinguishing between the cumulative damage and inhomogeneous strain hypothesis are those for specimen No. 4. In this case, both the nominal stress per filament (146,000 psi) and the stress per unbroken filament (166,000 psi) was significantly higher than the average strength of the extracted filaments (130,000 psi). At least in this case, the composite was clearly stronger than predicted from the rule of mixtures (applied to extracted filaments) and exhibited only a few uninvolved (with specimen failure) filament breaks.

Some of the results with regard to filament efficiency are also suggestive, if not definitive. The "Nominal Efficiency" values (in Table XV) are probably conservative since the specimens were not loaded to failure, this is indicated by the arrows on the open symbols in Figure 33. Probably the most important inference from Figure 33 (a plot of Nominal Efficiency vs. the number of broken filament, which may be attributable to fabrication damage) is that discontinuous composites are likely to be inherently inferior to continuous filament composites. Other data, previously obtained, substantiate this impression. These additonal data were obtained by testing to failure both continuous and (deliberately) discontinuous specimens. It was assumed that the strongest of the older data was associated with the least and the weakest with the most fabrication damage, and the respective efficiencies were plotted (solid symbols) to correspond with the filament damage of 12½% and 48% (observed in the recent work). Of course, the discontinuous specimen was regarded as a specimen having 100% filament damage prior to testing (that is, at least one break/filament). It

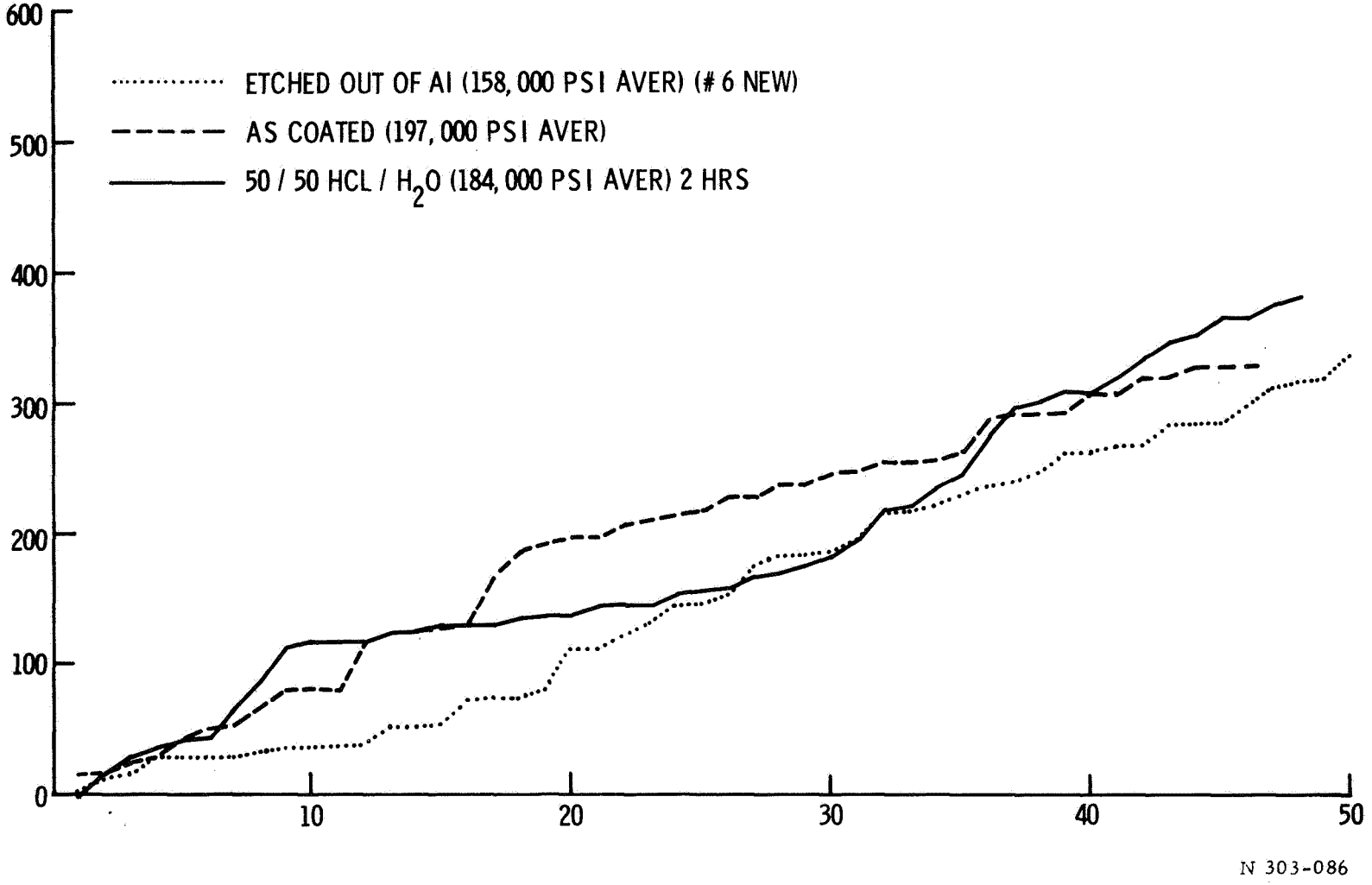

Figure 32. Tensile data on Samples No. 1 New, No. 4 New, and No. 5 New

TABLE XV. TEST RESULTS FOR 50 v/o CONTINUOUS B_4C/B/W-Al COMPOSITES

Spec. No.	Nominal Stress per Filament in Composite when Test was Stopped psi	Efficiency = Stress per Filament in Composite / $\bar{\sigma}$, Average Filament Strength*			Fraction of Filaments Broken After Extraction from Composite %	Stress per Unbroken Fil. and Strength of Unbroken Fil. psi/psi	
		Nominal ($\bar{\sigma}$ = 197,000 psi) Virgin Fil.	Adjusted ($\bar{\sigma}$ = 158,000) Extracted Fil.	No. of Filaments Broken After Extraction			
1 New	146,000	0.74	0.925	34	48	280,000/272,000	1.03
4 New	146,000	0.74	0.925	14	12 1/2	166,000/130,000	1.28
5 New	178,000	0.91	1.13	28	25	238,000/200,000	1.19
2 New	166,000	0.84	1.05	39	35	254,000/not tested	
3 New	152,600	0.78	0.96	22	20	190,000/not tested	1.20
6 New	not tested	---	---	22	2-	not tested/158,000	

*Virgin specimens $\bar{\sigma}$ = 197,000 psi Virgin Specimens Etched in 50% Hcl $\bar{\sigma}$ = 184,000

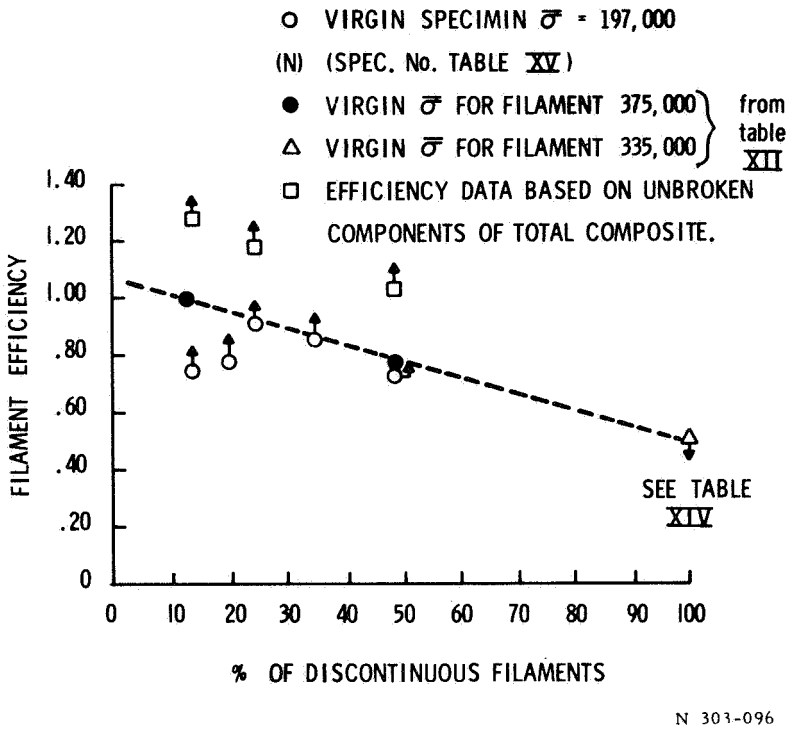

Figure 33. The Effect on Filament Efficiency of the Degree of Filament Discontinuity in $B_4C/B/W$-Al Composites

should be noted that the data for the discontinuous reinforcement is the best, not the typical result for this kind of reinforcement. These data and assumptions suggest that discontinuous composites are inherently inferior to continuous composites and that the gap widens with improved fabrication techniques (few unintentional breaks in fabrication) and possibly with decreased scatter in filament strength.

5. *FATIGUE STUDIES OF ALUMINUM-50 v/o $B_4C/B/W$ COMPOSITES*

A Total of six fatigue bars were fabricated to standard dimensions, see Figure 34. The composites were tested in tensile and compression cycling (double cycle fatigue) on a Baldwin SF-01-U Universal Fatigue Testing machine at room temperature.

A summary of the results is shown in Table XVI. Because of the limited number of samples available and also the limited time available, only a cursory type study was made. The data was not exceptional in that the fatigue values obtained were not outstanding when compared to many aluminum alloys. There is an obvious need for more work in this area.

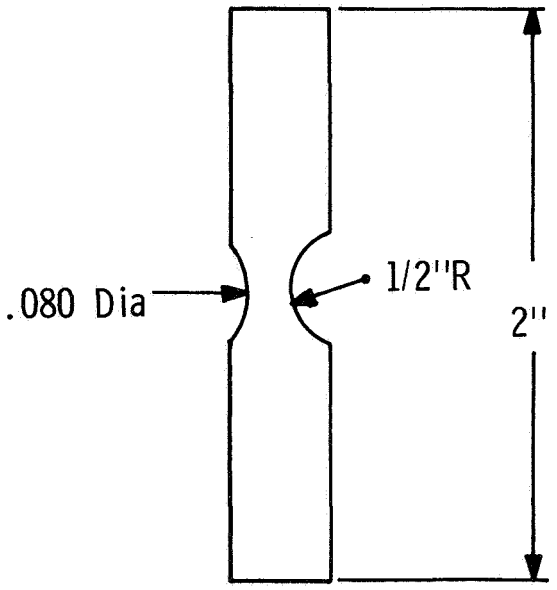

N 303-085

Figure 34. Schematic Diagram of a Typical ¼ in. Diameter Fatigue Bar

TABLE XVI. RESULTS OF DOUBLE CYCLE FATIGUE TESTS ON CONTINUOUS ALUMINUM - 50 v/o B_4C/B/W COMPOSITES

Sample	Load PSI	Cycles	Remarks
F1	60,000	4×10^3	Test Completed
F2	-----	-----	Broke During Maching
F3	40,000	-----	Broke in Loading
F4	40,000	-----	Broke in Loading
F5	36,000	2×10^3	Test Completed
F6	25,000	548×10^3	Test Completed

D. Epoxy Novalac Matrix Composite Systems

1. FABRICATION TECHNIQUES

Prior work [1] demonstrated the value of using thin specimens. The incorporation of brittle filaments into an epoxy matrix which approximates a metal in its mechanical (stress-strain) behavior would also offer certain advantages because of its transparency. A search was made of epoxy systems and a formulation attributable to V. Mazzio [15] was finally standardized. The epoxy formulation used was based on DEN 438 and has been adequately described elsewhere [1]. Formulations which were softer than the selected material (by the addition of more plasticizer) had poor bonding strength, while harder material was barely "ductile" and consistently failed at the first filament break. The curing cycle and the mold release agent were also found to be important variables which had to be controlled in order to consistently duplicate a given epoxy-filament tensile behavior. Briefly, composites were fabricated by a process wherein a thin, partially cured layer of resin was laid down, on top of which another thin layer of liquid resin was placed. Aligned filaments were then placed on top of the liquid layer. Because of their greater density, the filaments sank to the partially cured layer. The entire assembly was final cured and then specimens are sawed from the resulting laminates.

2. TENSILE BEHAVIOR OF SINGLE FILAMENT-EPOXY NOVALAC SPECIMENS

a. Materials and Test Methods

The observed and expected effects of filament strength and moduli differences on composite performance has been discussed in previous reports. In order to more fully clarify the strength-modulus-strain rate effects, tensile tests have been made at a high and a low strain rate using continuous single filament composites. Four filament materials were used which, as a group, cover the strength range of less than 50,000 psi to more than 500,000 psi and the modulus range from about 10×10^6 to 60×10^6 psi. All of the filaments exhibited brittle failure in tensile tests and in the composite specimens. The E-glass filament had a low modulus and was the weakest filament. The tungsten wire, embrittled by heat treatment (described elsewhere in this report), was stronger than the E-glass, but was the weakest of the three high-modulus materials tested. Two groups of boron (on tungsten substrate) filaments were tested; the weaker was designated "normal" and the stronger was designated "strong". The "strong" filaments were, on the average, more than twice as strong as the "normal" filament and, perhaps more important, the weakest "strong" filament was approximately 40% stronger than the strongest "normal" boron filament. The tensile test results for the filament materials and for single filament-epoxy specimens is shown in Table XVII. Stress-elongation curves for the filament-epoxy specimens are shown in Figures 35 and 36. Representative fracture cross sections are shown in Figures 37 and 38.

In the interpretation of these tests it is necessary to qualify quantitative results by pointing out that the specimens were made by casting and then hand grinding. Therefore, there are variations in thickness and gage length in each specimen and from specimen-to-specimen. Area measurements

TABLE XVII. TENSILE TEST RESULTS FOR CONTINUOUS SINGLE BRITTLE FILAMENTS IN AN EPOXY NOVALAC MATRIX (GAGE LENGTH ~ 1 INCH)

Spec. No.	Filament Material	Nominal Strain Rate (in./in/min.)	Strength, Max. Load/A_o (psi)	Total Elongation to Failure, (%)	No. of Non-Catastraphic Filament Breaks	REMARKS
529	E-Glass[1]	0.02	3010	> 16.5	35	Not failed - Test stopped
530	E-Glass[1]	2.0	4250	11.3[5]	38	
529 (reloaded)		0.02	3010	11.5	-	
449	Brittle Tungsten[2]	0.02	3900	14.7	6	No disk snaped cracks but observed on load defl. curves
450	" "	2.0	2460	1.3[5]	5	
521	B/W-Normal[3]	0.02	2920	3.7	6	1st Break at 2080 psi 6th Break at 2580 psi
522	" "	2.0	2620	1.4[5]	0	
518	B/W-Strong[4]	0.02	2340[6]	2.1	1	1st Break at 2300 psi
519	" "	2.0	2770	1.5[5]	0	
541A	Plain Epoxy	0.02	3030	>17.8	-	Not failed - test stopped
541B	Plain Epoxy	2.0	4360	20.3[5]	-	Failure Origin at Surface

High, Low and Average Tensile Strength (5 Spec.) of (See Table V)

	High	Low	Avg.
(1) E-Glass Filaments	48,000	22,400	30,500
(2) Brittle Tungsten Filament (WCA)	99,000	54,900	74,200
(3) Boron on Tungsten Filament-Normal	350,000	62,500	200,000
(4) Boron on Tungsten Filament-Strong	582,000	485,000	541,000

(5) Best Estimate-pen response precludes accuracy at small strains and high chart speeds

(6) Believed to be (ambiguously) low in view of filament tensile strength.

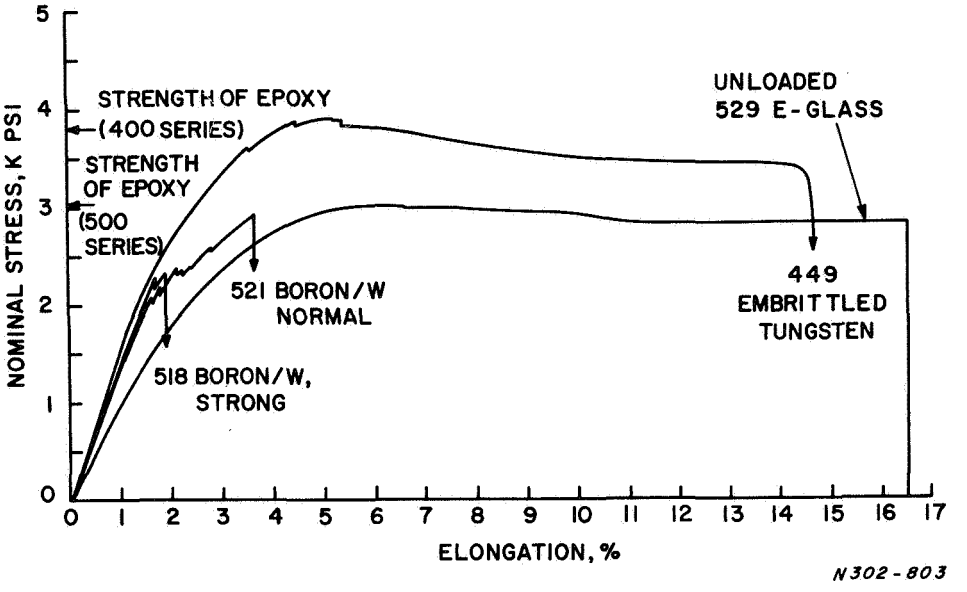

Figure 35. *Stress-Elongation Curves for Single-Filament-Epoxy Specimens Tested in Tension at 0.02 in./in./min.*

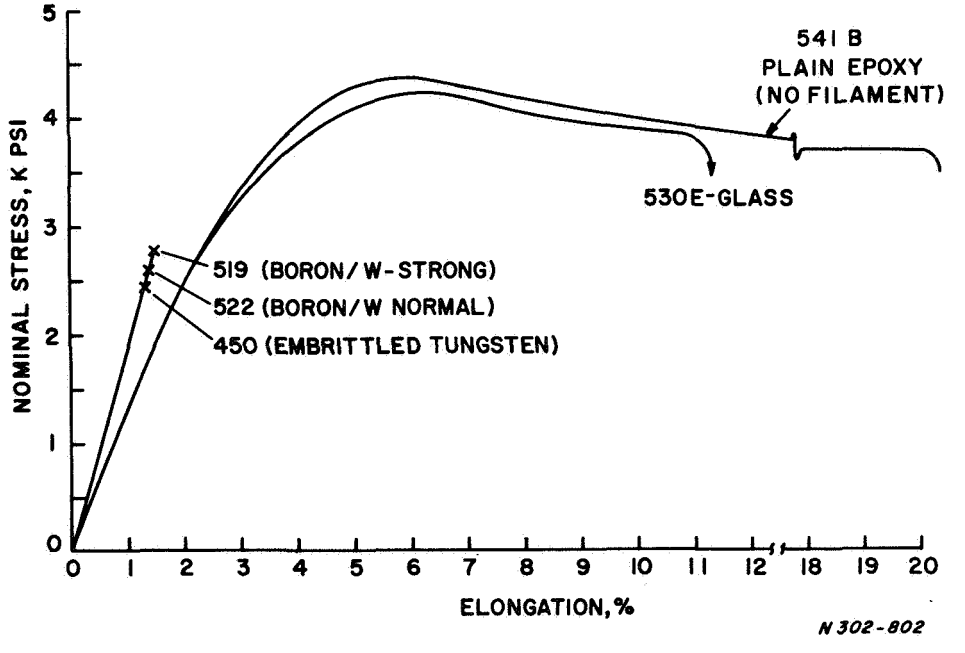

Figure 36. *Stress Elongation Curves for Single-Filament-Epoxy Tested in Tension at 2 in./in./min.*

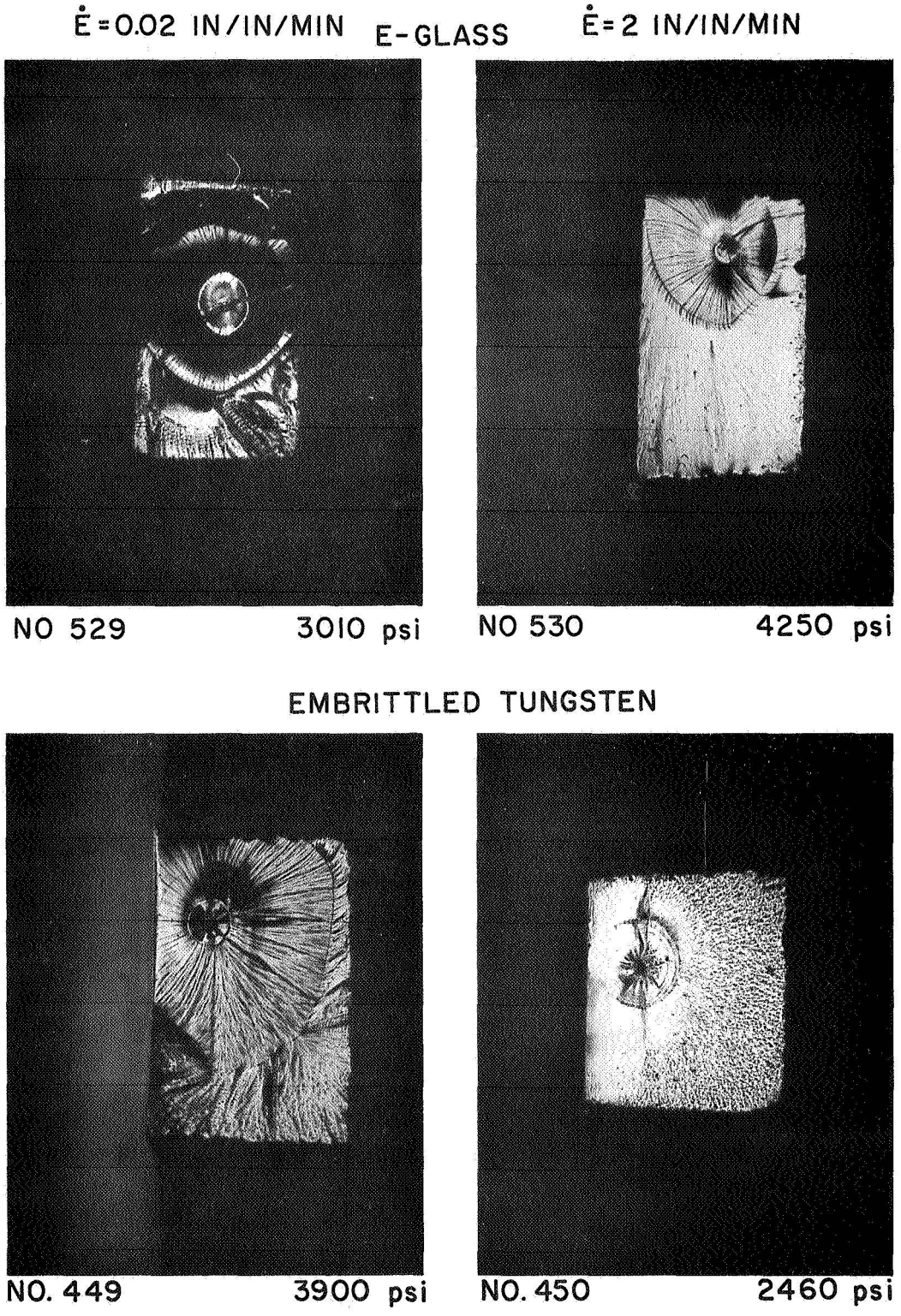

Figure 37. *The Effect of Strain Rate on Fracture Mode for Single-Filament-Epoxy Specimens — Weak, Brittle Filaments (17X)*

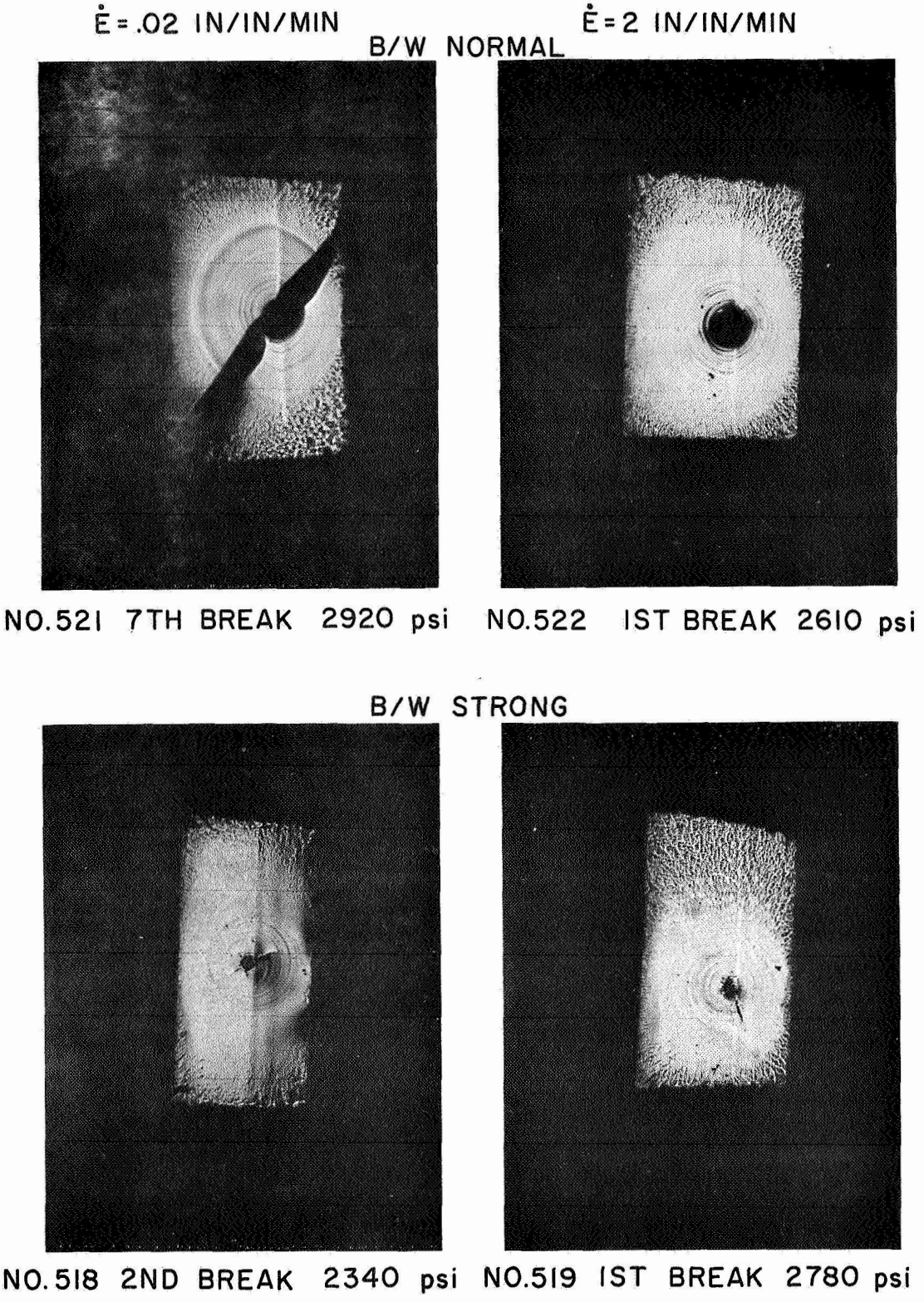

Figure 38. *The Effect of Strain Rate on Fracture Mode for Single-Filament-Epoxy Specimens — Strong, Brittle Filaments (17X)*

were made at the center of the gage length and it was assumed that the gage length was (the nominal) 1-inch long. Small differences in stress and elongation are of less significance than the qualitative differences in behavior, including fracture modes, to be described.

b. Discussion of Results

An important result of these tests is the relationship of filament strength to the shape of the stress-elongation curve as a function of strain rate. All of the single filament-epoxy specimens exhibit non-linearity in the stress-elongation curves at the lower strain rate (0.02 inch/inch/min). On the other hand, at the higher strain rate (2.0 in/in/min); all curves are linear to failure except for the E-glass-epoxy and plain epoxy specimens. This observation is represented more quantitatively in Figure 39. The upper curve (Figure 39) shows that, at the lower strain rate, the total elongation to

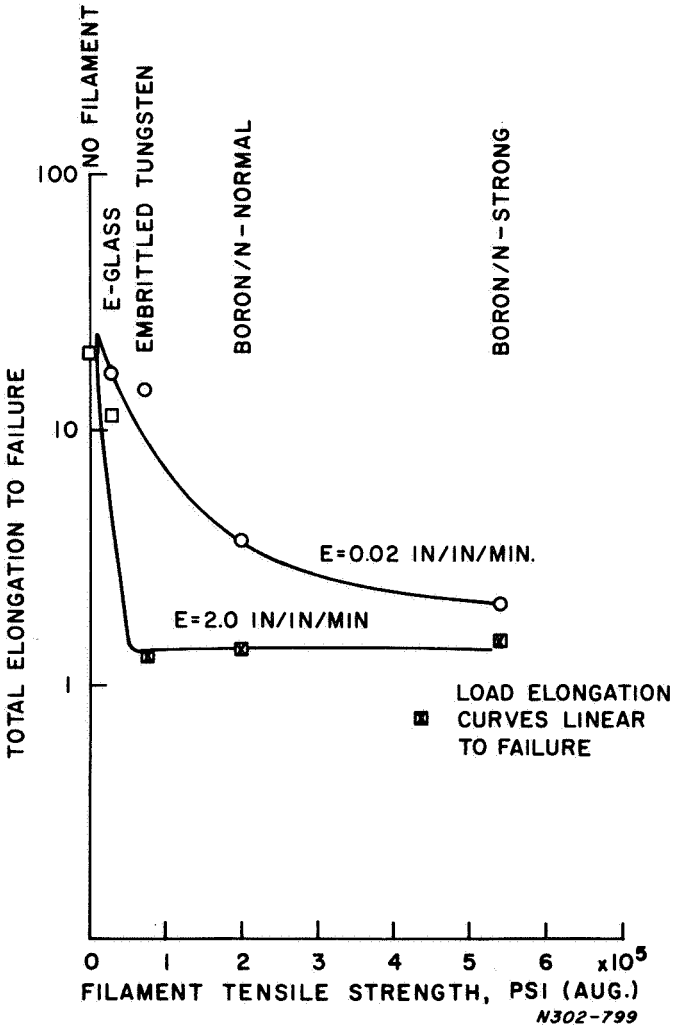

Figure 39. The Effect of Filament Tensile Strength on the Total, Elongation to Failure in Single-Filament-Epoxy Specimens

failure of filament-epoxy specimens decreased with increasing filament tensile strength. The lower curve shows that, at the higher strain rate, all of the filament-epoxy specimens were completely brittle except for the weakest and least stiff E-glass. Although the inelastic deformation of an epoxy is, in many important respects, different from that of metals, it is interesting to also consider an analagous parameter, the uniform inelastic elongation (equivalent, in metals, to the uniform plastic deformation). This "apparent" uniform elongation, the elongation from the linear portion of the curve to the maximum load (stress) on the specimen, is shown in relation to filament strength and strain rate in Figure 40.

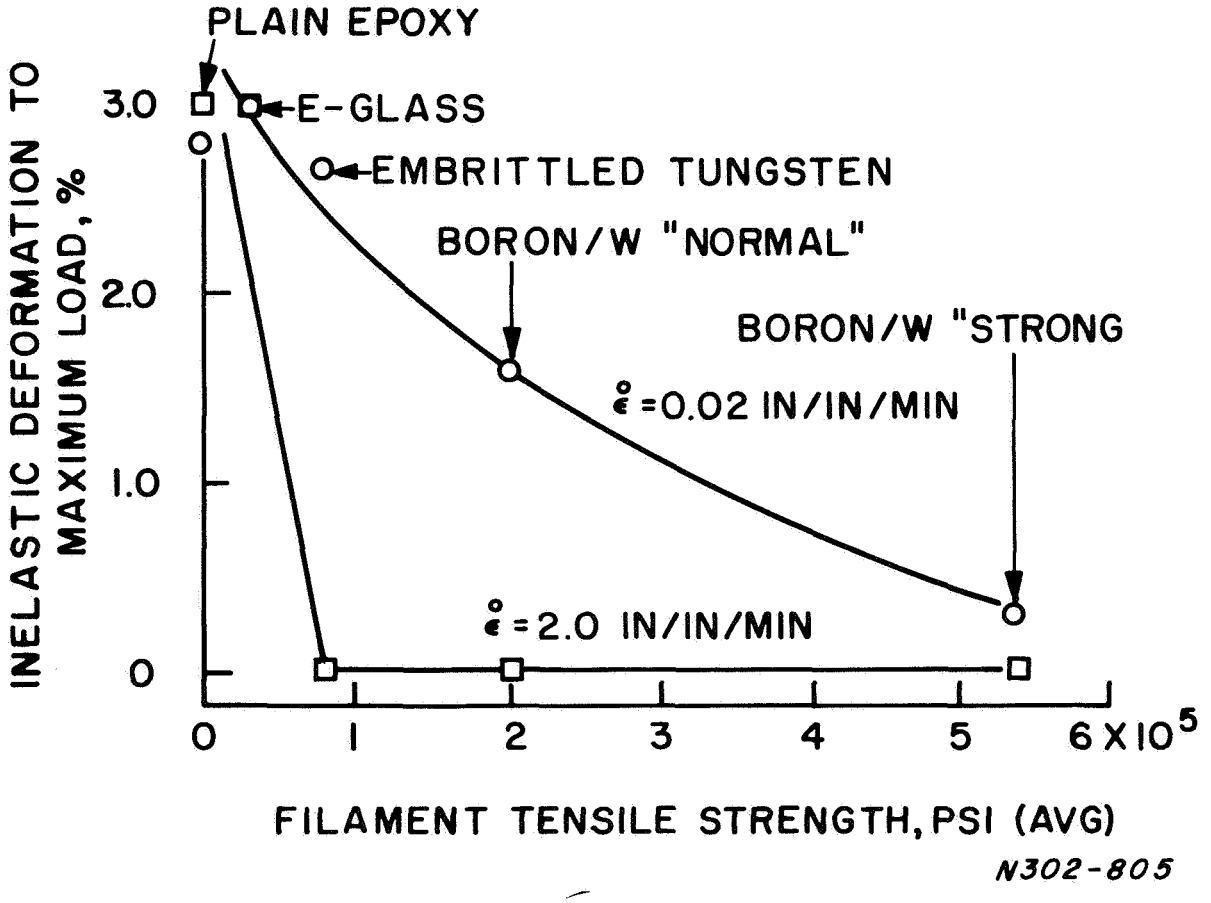

Figure 40. *The Inelastic Elongation to Maximum Load as a Function of Filament Tensile Strength in Single-Filament-Epoxy Novalac Specimens*

In many of these specimens, a number of cracks are formed prior to the formation and growth of the catastrophic crack (Table XVII). Owing to the stress concentration at the tip of these non-catastrophic cracks, they grow. This slow growth along with some loss of specimen stiffness (owing to filament break-up) is responsible for some of the non-linearity of the load-elongation curves. The behavior of each specimen will be discussed below with reference to strength, elongation and fracture mode.

The E-glass-epoxy specimen was very similar to the plain epoxy specimen with respect to strength and inelastic deformation to maximum load (Fig. 36) in the test at the low strain rate (0.02 in/in/min). At the higher strain rate ($\dot{\epsilon}$ = 2.0 in/in/min) the elongation to maximum load was the same but the elongation subsequent to maximum load and, therefore, the total elongation was greater for the plain epoxy. This indicates that at least one of the 38 internally generated cracks grew faster than the surface-originated crack in the plain epoxy specimen. (Figure 41A and B) shows profiles of some non-fatal cracks. It is evident that some unbonding can occur (Figure 41B) as cracks grow beyond their minimum size (shown in Figure 41A).

It is also evident that the matrix crack is initially formed and grows asymetrically in the case of E-glass-epoxy specimens (Figure 41A and 41B). This occurs because the failure in the E-glass filament usually originates at the filament surface; this is clearly apparent on the specimen fracture surface (Figure 42A). It will be noted, in Figure 41, that the radius of the smallest matrix crack in the E-glass-specimen (Figure 41A) is somewhat smaller than that in the embrittled tungsten specimen (Figure 41C). However, because the former is one-sided, the new matrix area created in the case of the tungsten-epoxy specimen was approximately 4 times that created in the E-glass-epoxy specimen. It seems reasonable to suppose that differences in 1) the filament fracture modes, 2) the elastic moduli and 3) the filament sizes account for the differences in the amount of matrix fracture area.
At both the high and the low strain rate, the fracture surfaces of E-glass-epoxy specimens have large areas exhibiting radial markings. These large areas are created subsequent to the formation of the very small smooth region adjacent to filament fracture (Figure 43A). As discussed in the Summary Report [1], matrix crack propagation is believed to be very fast in the smooth regions and relatively much slower in the radially marked regions. From this it is concluded that E-glass-epoxy specimens fail in two steps. First, a very small area of matrix is rapidly cracked adjacent to each filament failure. Second, these cracks slow down and propagate much more slowly during which time the load-elongation curve behaves inelastically. In summary, the cracking of an E-glass filament is not sufficiently energetic to propagate rapidly enough to embrittle the epoxy or significantly affect its strength.

In contrast to the E-glass-epoxy specimens, the behavior of embrittled tungsten-epoxy specimens is markedly strain rate dependent. At the lower strain rate ($\dot{\epsilon}$ = 0.02 in/in/min.) these specimens behaved similarly to E-glass-epoxy and plain epoxy specimens with respect to inelastic elongation (Figure 35*). The number of discontinuities in the load-elongation curve indicated the formation of six non-catastrophic failures, but none of the disk shaped cracks were observed in the specimen profile. Instead there appeared to be small cracks in the filament and considerable unbonding (Figure 43A). Apparently the only disk shaped crack in the specimen was the one leading to final failure, shown in Figure 43B (and Figure 35). The smooth (high speed fracture region) of this crack is very nearly the same size as the minimum sized crack in the specimen tested at the higher strain rate.

*The greater strength of this specimen reflects the greater strength of the epoxy used in the 400 series of specimen numbers.

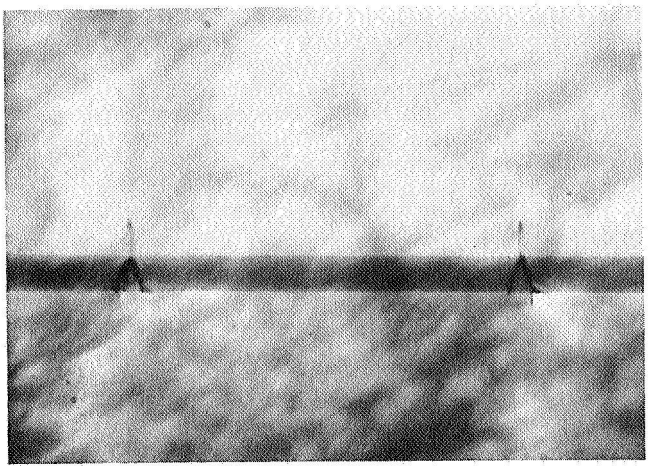

NO. 530 - E GLASS
MAXIMUM RADIUS OF
MINIMUM SIZE
CRACK = 5.3×10^{-3}

A

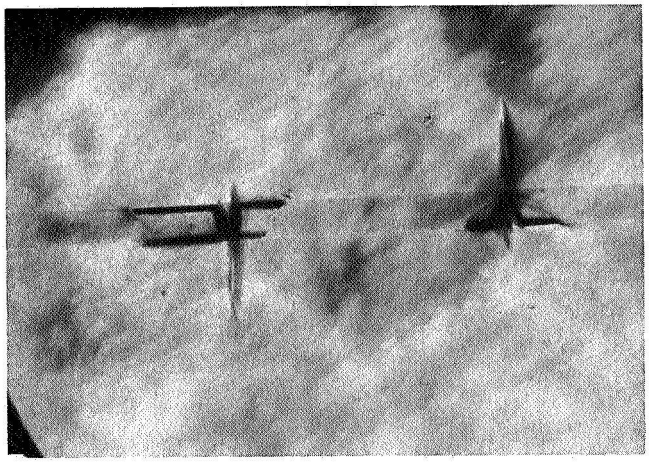

NO. 530 - E GLASS

NOTE UNBONDING

B

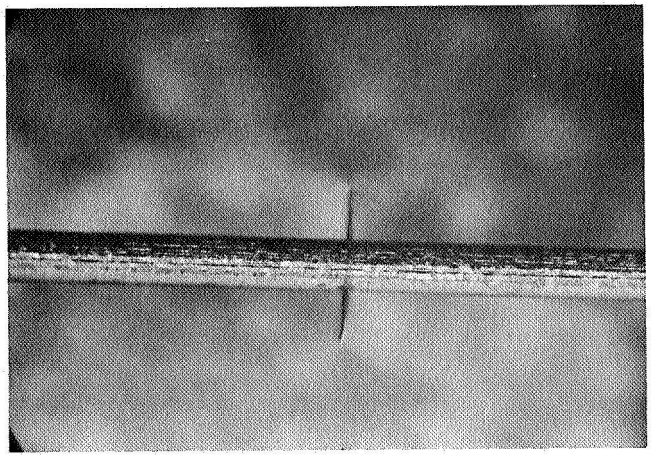

EMBRITTLED TUNGSTEN

NO. 450

MAXIMUM RADIUS OF
MINIMUM SIZE
CRACK = 7.0×10^{-3}

C.

Figure 41. *Profile of Filament-Matrix Cracks Created at a Tensile Strain Rate of 2 in./in./min. (58X)*

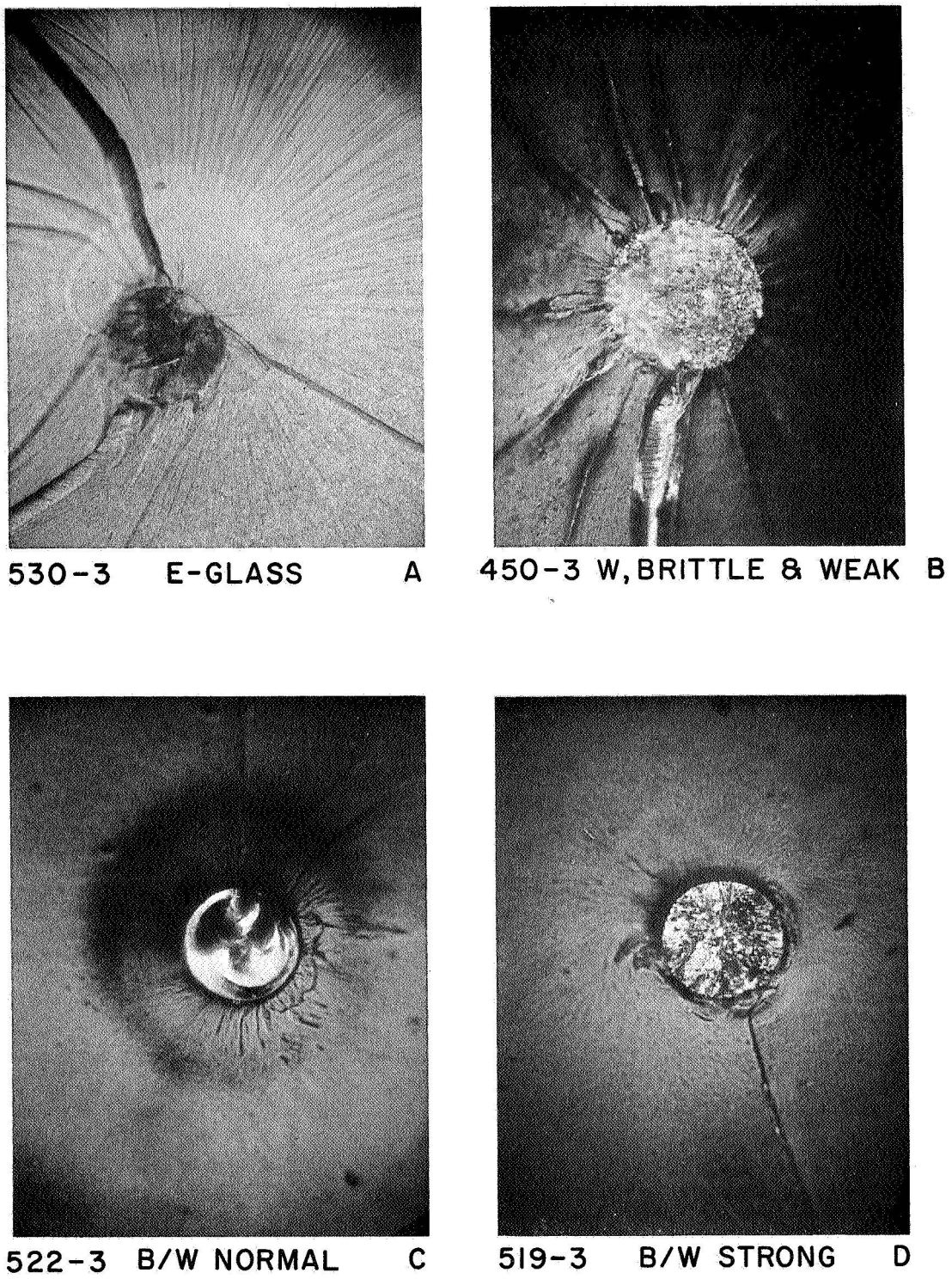

Figure 42. Typical Filament-Matrix Fracture Surface in Specimens Tested at 2.0 in./in./min. (202X)

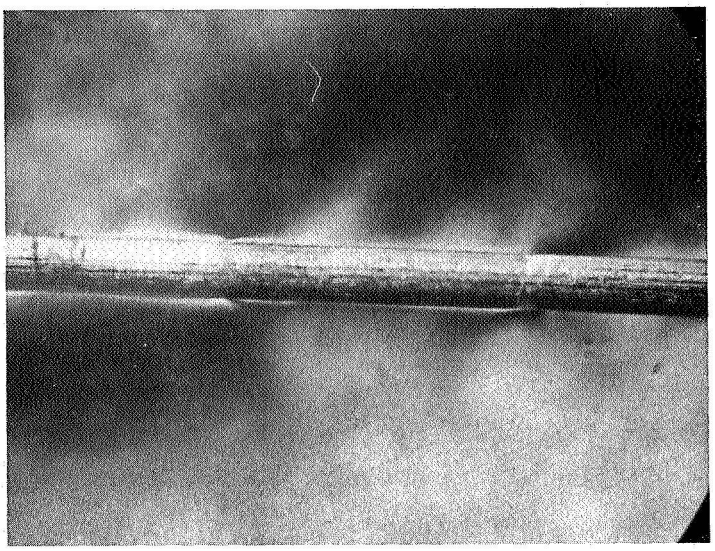

SPECIMEN:
NON-CATASTROPHIC
FILAMENT CRACKS
AND UNBONDED REGIONS

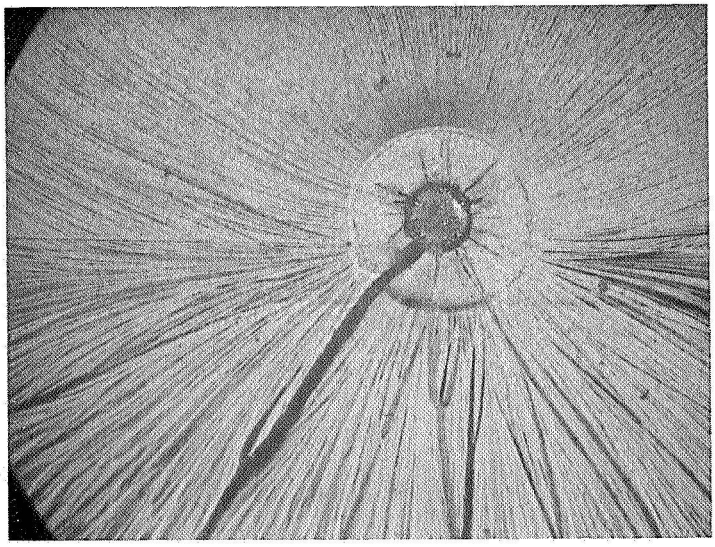

FRACTURE SURFACE
SHOWING REGIONS OF
RAPID (SMOOTH) AND
SLOW (RADIALLY MARKED)
MATRIX CRACK
PROPAGATION

Figure 43. *Failure in Embrittled Tungsten-Epoxy Specimen Tested at 0.02 in./in./min. (58X)*

From these observations, it is evident that, unlike the E-glass-epoxy specimen, most of the low strain-rate filament failures in the embrittled tungsten do not produce matrix cracks. However, it is also clear that the crack which eventually slowly propagates to specimen failure does originate as a high speed crack adjacent to a filament failure in a manner similar to failure in the E-glass-epoxy specimens at both strain rates. The extent of this similarity becomes apparent by comparing specimens No. 449 and 530 in Figure 37. In summary, there are a number of similarities in the mechanical behavior and fracture mode of E-glass-epoxy specimens at both strain rates and embrittled tungsten specimens tested at the low strain rate.

The behavior of the embrittled tungsten-epoxy specimen tested at the higher strain rate is markedly different from its low strain-rate behavior. At the higher rate, the stress-elongation curve is linear to fracture and all of the non-fatal cracks are disk shaped and exhibit a minimum size (Figure 41C). The fracture surface is relatively free of the overall radial markings. The few heavy radial markings originate at fracture level differences in the filament and soon disappear as they extend into the matrix (Figure 37 and Figure 42B). In short, the smooth fracture surfaces are much more like those characterizing the boron/W filament-epoxy specimens at both strain rates than they are like the same tungsten-epoxy specimens tested at the low strain rate (see Figure 37 and 38).

Of the four filaments tested, the embrittled tungsten-epoxy specimens exhibit the greatest sensitivity to the test strain rate with respect to both mechanical behavior and fracture mode.

At the lower strain rate, the boron/W-epoxy specimens exhibited some non-linearity (Figure 35). The amount of inelastic deformation to maximum load (Figure 40) is rather small and some of it might be attributable to a loss in specimen stiffness associated with filament break-up (particularly in the case of "normal" filament). Non-catastrophic disk-shaped cracks are present and these have undoubtedly grown to some extent by the slower mode associated with radial markings in the matrix. (The fracture mode in boron-epoxy specimens was discussed in detail in the Summary Report [1].) The specimen fracture surfaces, however, are free of the radial marking. (Figures 37 and 38) This indicates that the catastrophic filament failure occured at a stress high enough to maintain the rapid (smooth) mode of matrix crack propagation.

At the higher strain rate ($\dot{\epsilon}$ = 2.0 in/in/min), both "normal" and "strong" boron-epoxy specimens were unambiguously and completely brittle. The load-elongation curves were linear to failure (Figure 36), and the first filament crack formed propagated to failure in the rapid fashion (Figure 38).

The filament fracture surfaces shown in Figure 42C and 42D are noticeably different. The "normal" filament fracture surface is smoothly conchoidal, a feature commonly observed in low-strength boron filament failures. The fine scale roughness of the "strong" filament is not commonly observed and it may be characteristic only of very strong filament.

c. Summary and Interpretation of Results

For purposes of clarity and perspective in comparing the effect of filament properties and test conditions on the mechanical behavior of the epoxy matrix, the results have been concisely restated, (Table XVIII) in the form of a "qualitative-quantitative" summary. This brief restatement is not rigorous because it omits possibly important qualifications (discussed previously) and includes judgments based, in part, on previously documented work (see in particular Summary Report, Ref. 1).

TABLE XVIII. QUALITATIVE-QUANTITATIVE SUMMARY OF TENSILE TEST RESULTS ON SINGLE CONTINUOUS BRITTLE FILAMENT-EPOXY SPECIMENS

Property or Behavior	Low-Modulus Low Strength E-Glass	High Modulus Low Strength Embrittled Tungsten	High Modulus High Strength	
			Boron/W "Normal"	"Strong"
Estimated Modulus, (psi)	10×10^6	53×10^6	60×10^6	60×10^6
Tensile Str. Avg. (psi)	30,500	74,200	200,000	541,000
Specimen Str. Relative to Strength of Plain Epoxy at				
$\dot{\epsilon} = 0.02$	Same	Same	Same	Same(?)
$\dot{\epsilon} = 2.0$	Same	Less	Less	Less
Specimen Inelastic Deformation Relative to Plain Epoxy				
$\dot{\epsilon} = 0.02$	Same	Same	Less	Less
$\dot{\epsilon} = 2.0$	Same	None	None	None
Fracture Mode				
Non-Catastrophic Filament Cracks				
$\dot{\epsilon} = 0.02$	Many	Few	Few	Few
$\dot{\epsilon} = 2.0$	Many	Few	None	None
Catastrophic Crack Prop.				
$\dot{\epsilon} = 0.02$	Rapid then slow	Rapid then slow	Rapid	Rapid
$\dot{\epsilon} = 2.0$	Rapid then slow	Rapid	Rapid	Rapid

The question to be generalized about is: "What is the effect, on the mechanical behavior of a matrix, of internal cracks created by the fracture of an embedded brittle filament?" The general answer, from this work, is: Both test conditions and filament properties can have a profound effect on the mechanical behavior of the matrix. It seems, therefore, reasonable to conclude that: Predictions of composite performance based only on a knowledge of the conventional properties of individual components can be only fortuitously valid.

Table XVIII shows that the weak, low-modulus E-glass had little or no effect on the strength or the deformation of the epoxy matrix. Therefore, in principle, the performance of these composites should be predictable on the basis of knowledge of the behavior of the individual components.

Performance predictions for composites made using high-modulus weak filaments are another matter. The single filament specimens are markedly strain rate sensitive. Since higher volume fractions may be equivalent, in some respects, (see Summary Report, Ref. 1) to high strain rates, useful composites might be both weaker and more brittle than predicted on the basis of tests on the separate components.

Performance predictions for composites made using high-modulus, high strength filaments are, indeed suspect. The boron/W filaments adversely affected the inelastic elongation, characteristic of the epoxy at the low strain rate. At the higher strain rate, the epoxy was completely embrittled and markedly reduced in strength by the formation of a single filament crack. While the situation could not be worse at usable volume fractions, it seems unwarranted to predict that it would be improved. The expectation is, then, that reinforced composites (of this epoxy) would fail brittlely at the first filament failure.

3. TENSILE BEHAVIOR OF FIVE FILAMENT-EPOXY NOVALAC SPECIMENS

a. Materials and Test Methods

In order to study filament interaction affects over a range of filament properties, a number of 5 filament-epoxy specimens were tested at two strain-rates. The materials selected were those used for the single filament tests and, in addition, two ductile filaments, aluminum and tungsten. The dimensions of these five-filament specimens were such that, though small, the volume fraction is appreciable (of the order of 1/2%). The tensile test results are shown in Table XIX.

b. Discussion of Results

In many respects, the results on 5-filament specimens were similar to those on single filament specimens. However, in several very important respects there was obvious filament interaction. All of the filament-epoxy specimens incorporating brittle filaments were strain-rate sensitive in one way or another. For example, all of them exhibited brittle failure at the higher strain rate, even the low strength low modulus E-glass. The specimens incorporating ductile filaments were at least as

TABLE XIX. TENSILE TEST RESULTS FOR 5-FILAMENT-EPOXY NOVALAC SPECIMEN GAGE LENGTH ~ 1 in.)

Spec. No.	Filament Material	Nominal Strain Rate (in/in/min.)	Strength Max Load/A_o (psi)	Inelastic Elongation to Max. Load (%)	Number of Non-Catastrophic Cracks
410	E-Glass	0.1	3750	3.9	~165
411	E-Glass	2.0	3620	Nil	~100
404	Brittle Tungsten	0.1	3850	1.1	12 disk-shaped cracks
405	Brittle Tungsten	2.0	1480	Nil	4 disk-shaped cracks
406	B/W Strong	0.1	4630	0.1	1 disk-shaped crack
407	B/W Strong	2.0	4550	Nil	0
409	0.004" Aluminum	0.1	3590	4.7	Ductile extension of Al-No cracks
408	0.004" Aluminum	2.0	4900	3.5	Ductile extension of Al-No cracks
403	0.005" Ductile Tungsten	0.1	8000	4.0	No Disk-shaped cracks
402	0.005" Ductile Tungsten	2.0	9020	4.0	No Disk-shaped cracks
412	Plain Epoxy	0.1	3770	3.2	
441B	Plain Epoxy	2.0	4950	3.4	

"ductile" as the plain epoxy. The inelastic deformation to maximum load and the specimen tensile strength as a function of filament strength are shown in Figure 44 and 45 respectively. Only the strongest brittle filament was capable of increasing the strength of the epoxy at the lower strain rate and no brittle filament-epoxy specimen was stronger than the plain epoxy at the higher strain rate. The weak ductile aluminum had no effect on the epoxy strength at either strain rate, but the strong ductile tungsten reinforced the epoxy at both strain rates. Some detailed comments on behavior and fracture mode follow.

The 5-filament E-glass-epoxy specimens, as distinct from their single filament counterparts, are sensitive to the test strain rate. At a strain rate of 0.1 in/in/min the 5-filament specimen had approximately 33 non-catastrophic cracks (per filament), nearly the same as in the case of the single

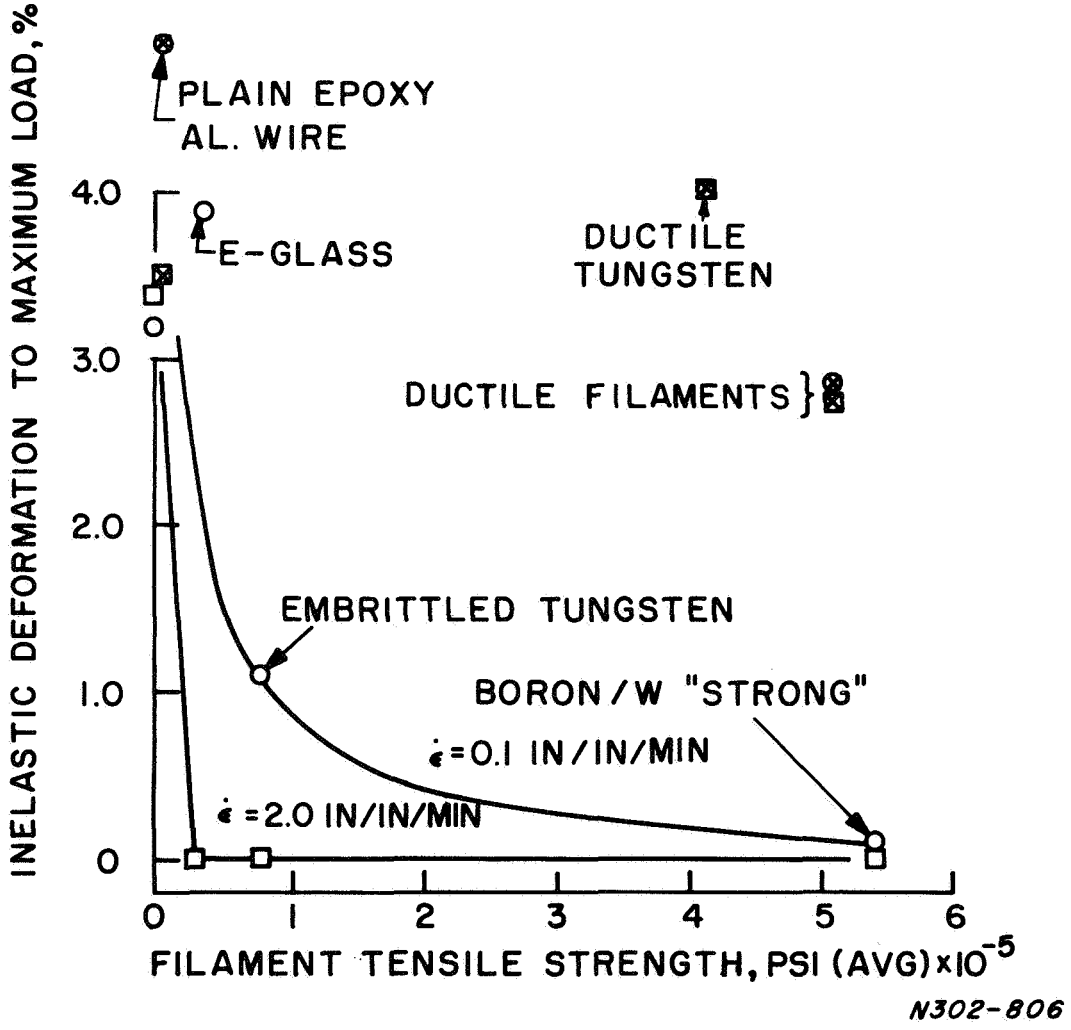

Figure 44. *The Inelastic Elongation to Maximum Load as a Function of Filament Tensile Strength in 5-Filament-Epoxy Novalac Specimens*

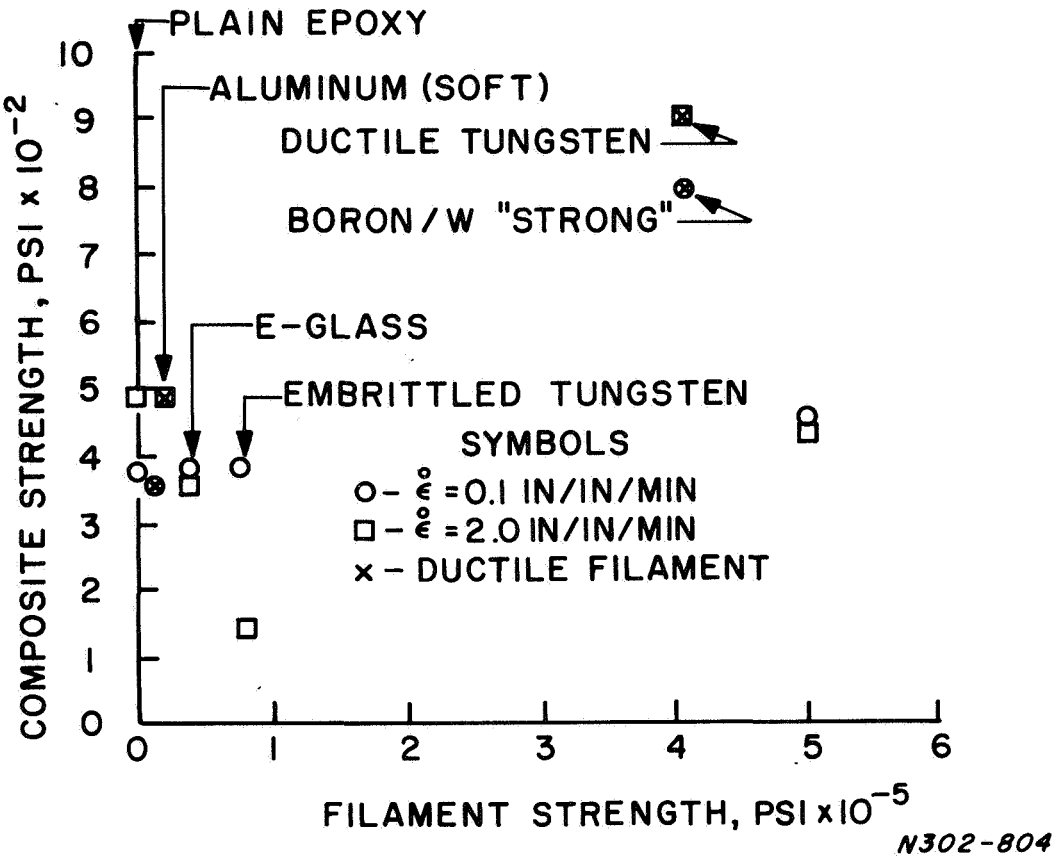

Figure 45. *The Tensile Strength of 5-Filament-Epoxy Novalac Specimens as a Function of Filament Tensile Strength*

filament-epoxy specimen at 0.02 in/in/min (Table XVIII). The strength and inelastic elongation to maximum load are very nearly the same as for plain epoxy tested at the same strain rate. Unbonding is evident in Figure 46, and when this occurs as an alternate to matrix tensile crack propagation it promotes strength and "ductility". In short, the behavior of the five element specimen tested at $\dot{\epsilon}$ = 0.1 in/in/min is similar to that of the single-filament specimen tested at $\dot{\epsilon}$ = 0.02 in/in/min.

On the other hand, the 5-filament specimen tested at $\dot{\epsilon}$ = 2.0 in/in/min exhibits 40% fewer non-catastrophic breaks per filament and no inelastic elongation (Table XIX) and there was little or no evidence of unbonding (Figure 47). The filament breaks were very non-uniformly distributed. Matrix fracture started at the filament having the fewest failures (in the center of the specimen) and propagated entirely by the rapid (smooth) mode (Figure 47). Not only was this specimen completely brittle, it was considerably weaker than plain epoxy. This contrasts strikingly with the single filament specimen, which performed very much like the plain epoxy at $\dot{\epsilon}$ = 2.0 in/in/min. In summary, the work with E-glass epoxy specimens demonstrates that matrix properties may be adversely affected by filament interactions and that this is clearly identifiable with the fracture mode.

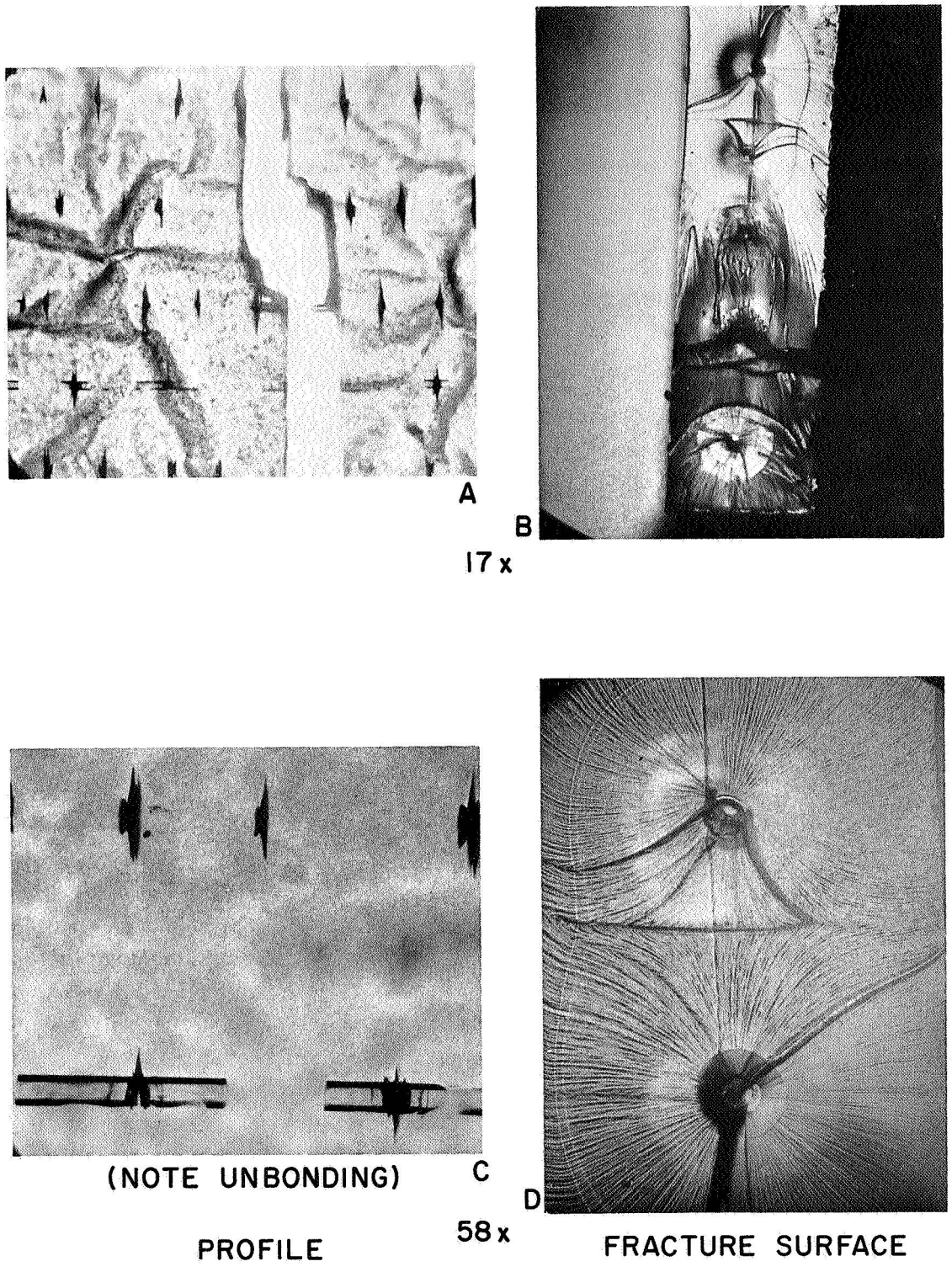

Figure 46. *Profile and Fracture Surfaces of 5-Filament F-Glass-Epoxy Novalac Specimen Tested in Tension ϵ = 0.1 in./in./min. (Specimen No. 410)*

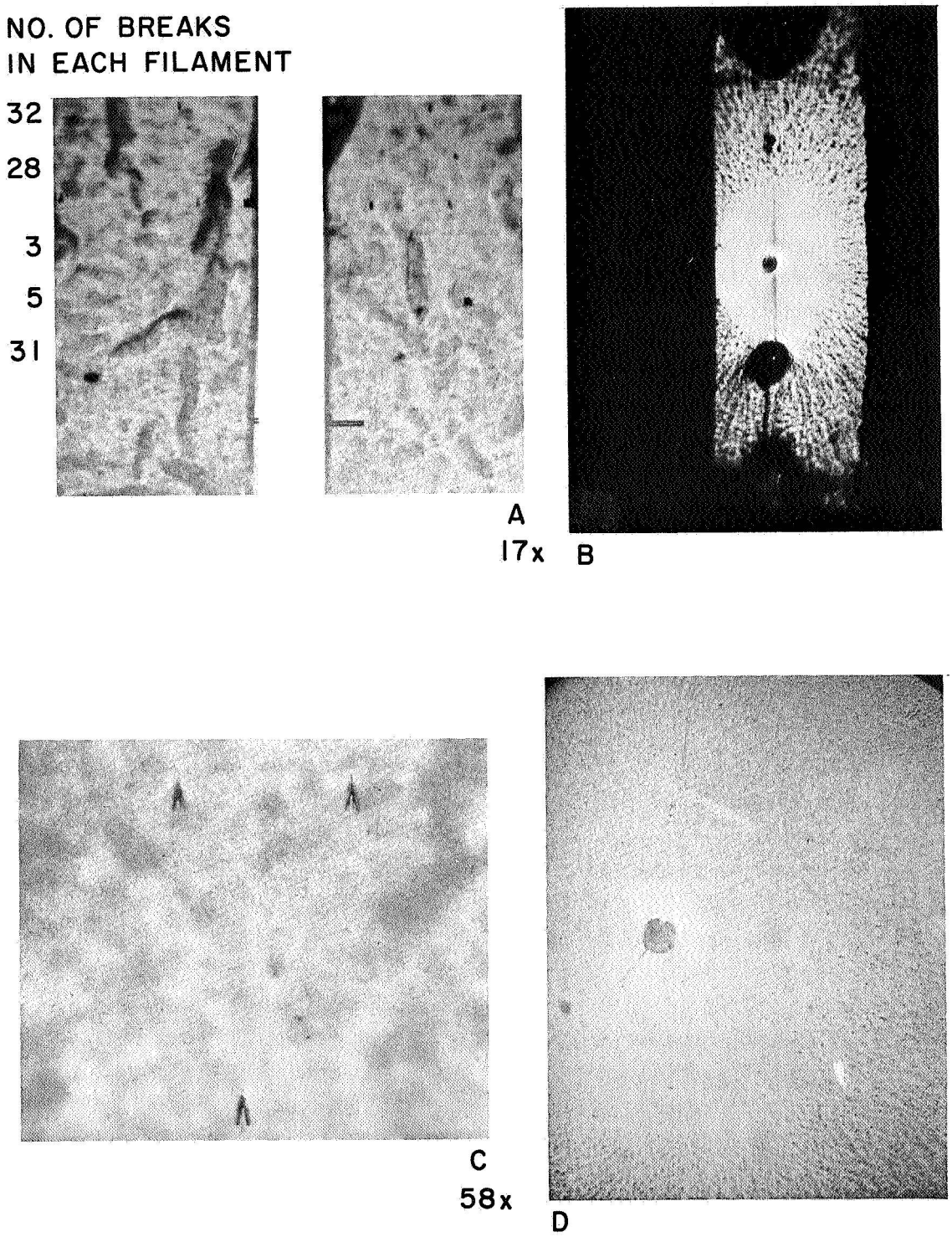

Figure 47. *Profile and Fracture Surface of 5-Filament E-Glass-Epoxy Novalac Specimen Tested in Tension at ϵ = 2.0 in./in./min. (Specimen No. 411)*

The 5-filament embrittled tungsten-epoxy specimens were markedly strain-rate sensitive as were their single-filament counterparts. At the lower strain rate (0.1 in/in/min), the 5-filament specimens were at least as strong as the plain epoxy, but they exhibited only 1/3 the inelastic deformation to maximum load. This is probably related to the fact that non-catastrophic cracks were disk-shaped matrix tensile cracks, not unbonding as in the case of the single filament specimen tested at a lower rate ($\dot{\epsilon}$ = 0.02/in/in/min, Table XVIII).

At the higher strain rate ($\dot{\epsilon}$ = 2.0 in/in/min), the 5-filament specimen exhibited a total of 4 disk-shaped non-catastrophic cracks (80% fewer cracks than the counterpart single filament specimen on a per/filament basis; see Table XVIII). This suggests that, as weak as these filaments are, only a small fraction of the filament potential was utilized. Figure 48 shows photomicrographs of the profile and fracture surface of this specimen. The dark parabolic markings opening toward the left hand side (Figure 48B) indicates that final fracture originated in the right-hand filament and propagated toward the left. It is evident that the center filament failed at a point remote from the surface, because it generated a non-catastrophic crack (visible in the upper part of Figure 48A) and was pulled from its original location during catastrophic failure. It is quite possible that three of the filaments (two on the left and one on the right-hand side of the center filament) had generated non-catastrophic cracks which, of course, offered little or no resistance to crack propagation when the right hand filament failed. On the other hand, the fracture surface appearance is also consistent with the proposition that the catastrophic crack was momentarily retarded by the (unbroken) filaments in its path. In either event, time did not permit any crack growth by the slow mode characterized by a multitude of closely spaced radial marking. In summary, the 5-filament specimens show, again, that these weak and high modulus filaments are the most intense sources of matrix failure.

The 5-filament Boron/W ("strong") epoxy specimens exhibited essentially brittle behavior at both strain rates. Only one non-catastrophic crack was sustained at $\dot{\epsilon}$ = 0.1 in/in/min and that was near the fracture region; none occurred at $\dot{\epsilon}$ = 2.0 in/in/min. The specimen was stronger than the epoxy at the lower strain rate showing that some "reinforcement" occurred at even this low volume fraction(0.7%). The strength at the higher strain rate was slightly less than that of the matrix. The first crack was catastrophic and, therefore, this specimen was matrix limited. Higher volume-fraction specimens would undoubtedly be stronger. However, they would also be expected to fail at a strength less than an equivalent unbonded bundle of filaments (unless the filament strength was scatter-free), because the matrix is unable to redistribute the load in a non-catastrophic manner. This is evident on the fracture surface of the specimen tested at 0.1 in/in/min, see Figure 49A. The first failure, on the right hand side, generated a rapidly moving crack in the matrix. This crack first rapidly reduces the specimen area. More important (for higher volume fraction specimens), it concentrates the stress at the adjacent filament as shown by the cusp at the second filament. When this filament fails, the crack again increases in area and its velocity increases. The original crack passes to each side and down stream of the third filament before it too fails, as shown by the dark V-shaped marking. Thus, the process is an accelerating one, each filament adding its stored energy to the rapidly increasing stress on the unfractured portion of the specimen.

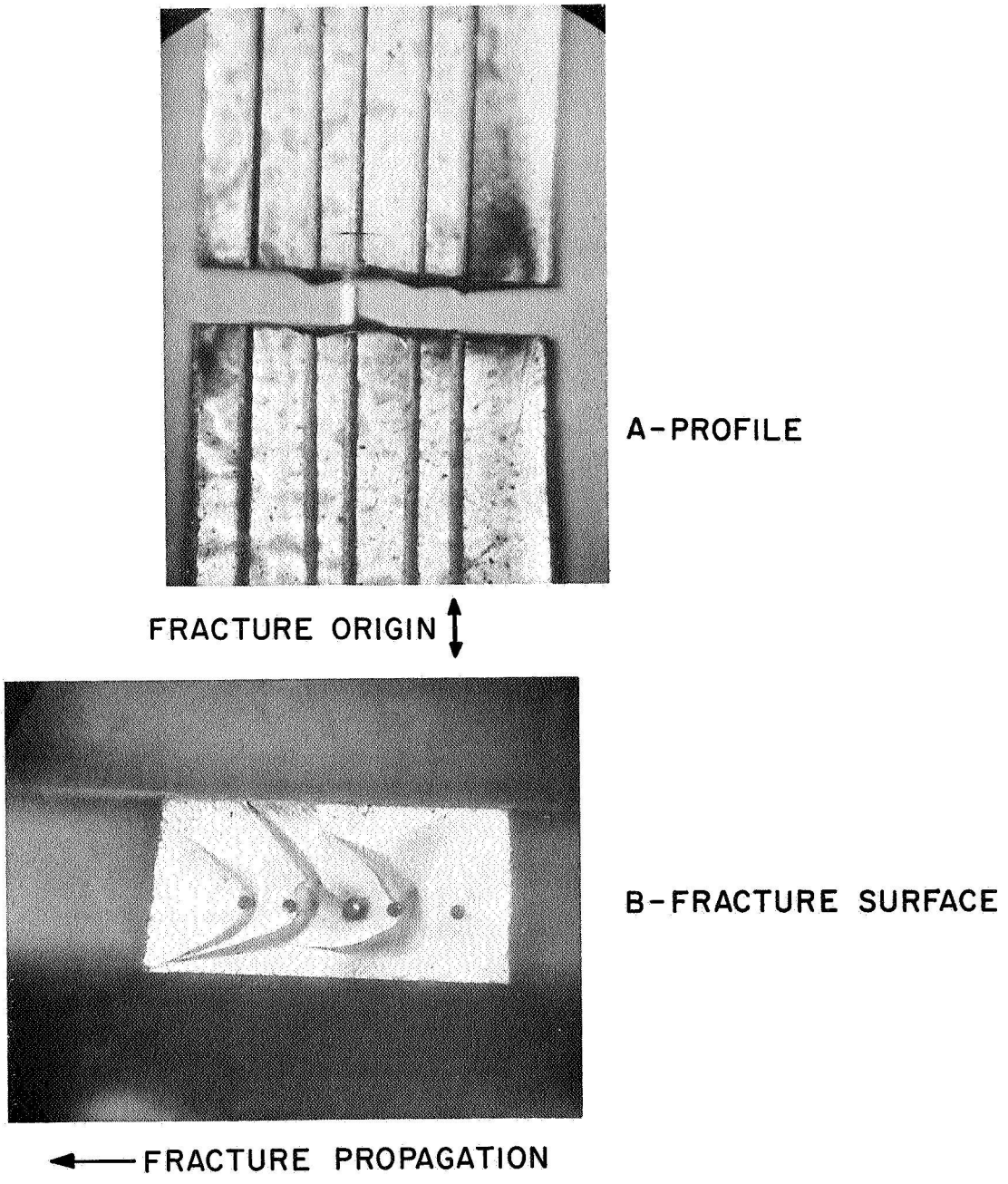

Figure 48. *Profile and Fracture Surface of 5-Filament Embrittled Tungsten-Epoxy Novalac Specimen (No. 405) Tested in Tension at ϵ = 2.0 in./in./min. (17X)*

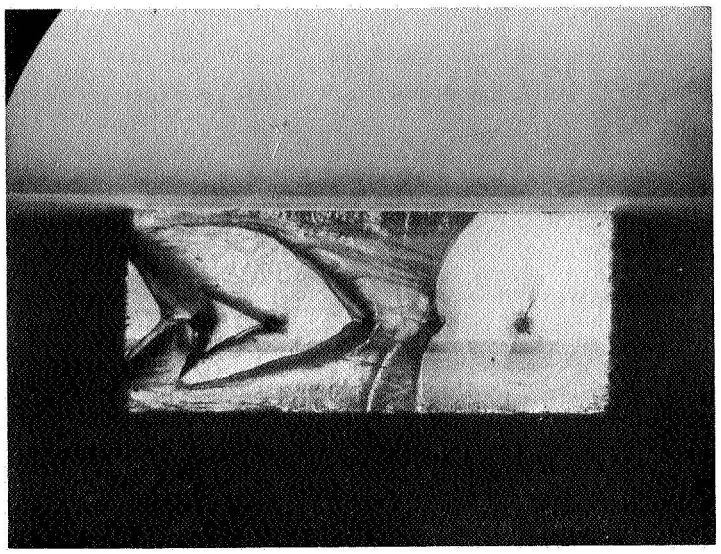

BORON/W "STRONG"
SPEC 406
$\dot{E}$=0.1 IN/IN/MIN

A

FRACTURE PROPAGATION

FRACTURE ORIGIN

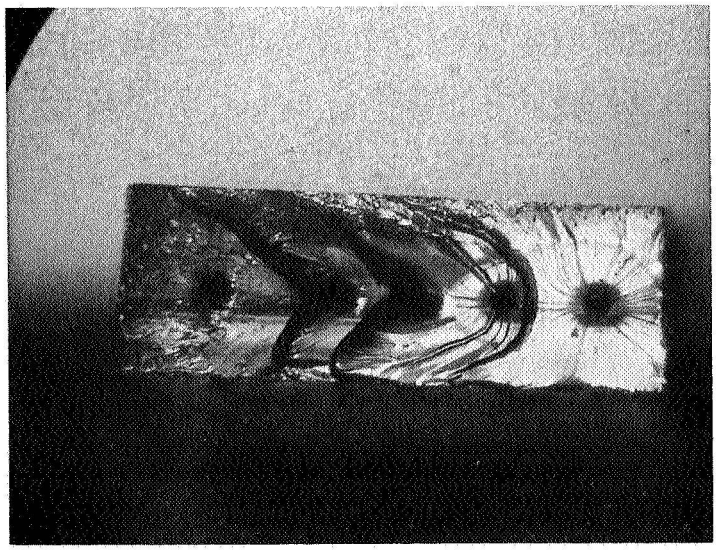

DUCTILE TUNGSTEN
SPEC 402
$\dot{E}$=2.0 IN/IN/MIN

B

Figure 49. *Fracture Surfaces of 5-Filament-Epoxy Specimens Showing the Effect of Filament Ductility on Crack Propagation in the Matrix (17X)*

In summary, the high modulus-high strength composite is matrix limited in that the matrix cannot redistribute the load in a non-catastrophic manner. Such composites are filament limited by the lower region of the filament strength scatter band.

The specimens containing ductile materials behave in a manner which might relatively simply be predicted from the properties of the individual components, aluminum, tungsten, and epoxy.

The 5-filament aluminum-epoxy specimens are almost indistinguishable from plain epoxy at either strain rate because the aluminum is too weak ($\sim$ 8,000 psi) to reinforce (at low volume fraction) and too ductile to generate matrix cracks.

The 5-filament ductile tungsten-epoxy specimens are strong enough (410,000 psi) to reinforce, but are too ductile to generate brittle matrix cracks. It was pointed out in an earlier Report [1] that a slowly propagating inclined crack is generated in the matrix when a ductile tungsten wire necks down and breaks. Figure 49B shows how specimen failure occurs. The first tungsten wire to neck down and fail (right-hand side of Figure 49B) produces a free end. Owing to a good bond, this free end generates a matrix crack which grows slowly, as indicated by the radial markings. As this crack grows the specimen area is reduced. The adjacent filament bears slightly more than its share of the load, and may also be subject to some superimposed bending stress, and it is the second filament to fail. It also generates a slowly growing radial crack which, when it intersects the original crack, gives rise to the dark parabola. The third filament fails in a similar manner, but the independent crack growth is much less in extent owing to the rising stress and increasing speed of the first two cracks. This is even more true for the fourth filament but the fact that it failed independently is indicated by the dark parabolic marking. The final filament was overwhelmed by virtue of its location in a high stress (low area) region.

c. Summary and Interpretation of Results

All of the brittle 5-filament specimens were strain-rate sensitive in one way or another. Strength, relative to plain epoxy, and/or the "ductility" was reduced as the strain rate was increased. The most important single result was that E-glass, which was not stain-rate sensitive in the form of a single filament specimen became markedly so in the form of 5-filament specimens. It is also evident that the combination of weaknesses and high-modulus (the embrittled tungsten filament) is a most serious disadvantage if brittle filaments are used. This indicates, again, that the property of importance for brittle high-modulus filaments is the strength level of the lower region of the scatter band.

Ductile filaments may or may not reinforce, depending on their average strength, since local premature failures do not propagate catastrophically in the matrix. The soft weak aluminum did not materially contribute to the strength of 5 filament specimens, but the contribution of the ductile tungsten is fully that which would be predicted by the "rule of mixtures",

4. *MECHANICAL COMPATIBILITY MODEL*

An attempt has been made to develop a simple schematic model for the graphic rationalization of expected composite behavior, see Figure 50. Most of the detail of this model is based on the

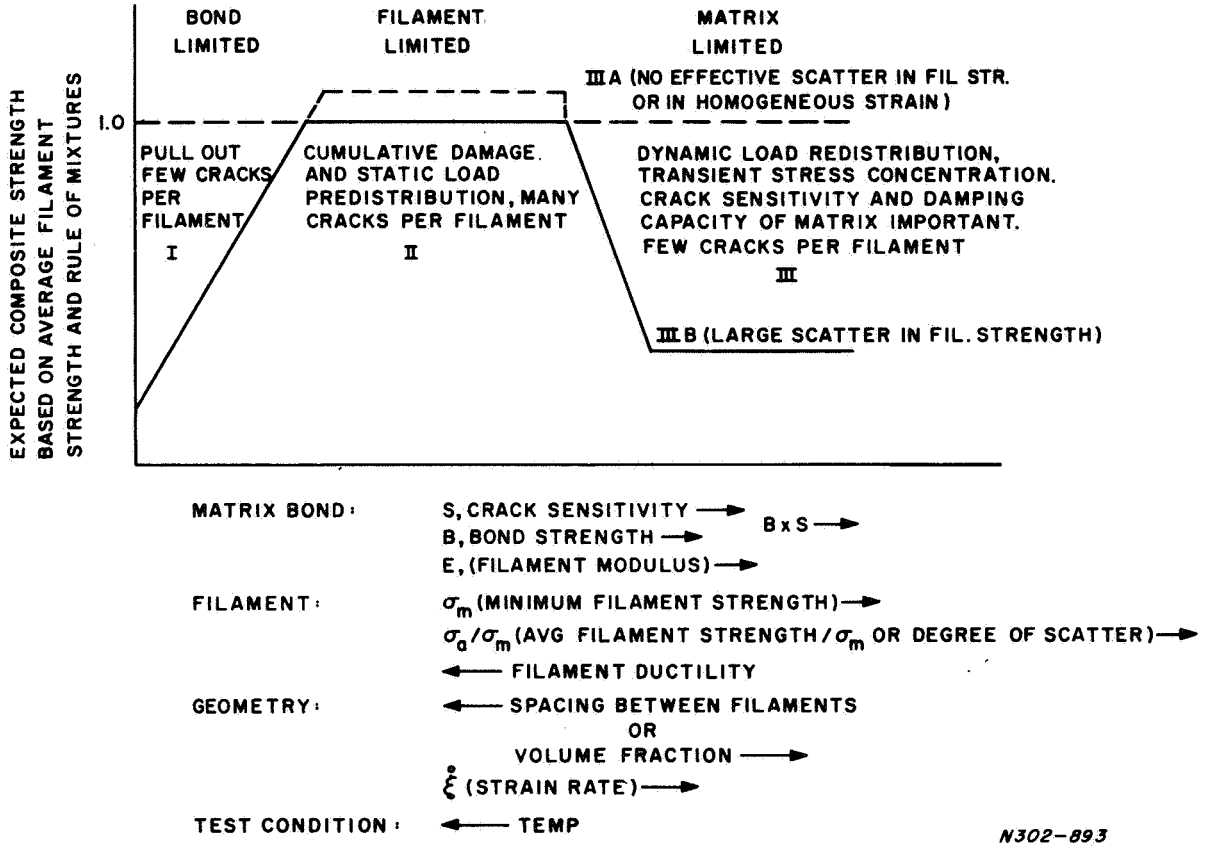

Figure 50. *A Schematic Model for the Graphic Rationalization of the Effect of Materials Properties, Specimen Configuration and Test Conditions on the Performance of Composites*

mechanical behavior and fracture phenomenology of simple filament-epoxy specimens tested during the course of this contract. The purpose of the model is to provide a qualitative frame of reference within which (1) a wide variety of test results can be rationalized and (2) more clearly critical experiments can be designed.

The ordinate on the diagram (Figure 50) represents the normalized composite strength, which would be expected from the rule of mixtures in its simplest form, as given by:

$$\sigma_c = \sigma_m (1-V_f) + \sigma_f V_f \qquad (e)$$

where σ_c,,σ_m and σ_f are the strengths of the composite, the matrix and the filament, respectively, and where V_f is the volume fraction of the reinforcing filament.

The abscissa of the diagram shows many of the parameters which determine when and to what extent the rule of mixtures will be obeyed. The interdependence of many of the important variables has been quite evident in much of the experimental work reported and is also evident in the work on bonding described in this report. For purposes of ready allusion to the interrelation of fundamentally mechanical, as distinct from chemical, aspects it seems warranted to make use of the phrase "mechanical compatibility". One might say that mechanical compatibility is satisfactory when premature filament failures do not adversely affect the ability of the matrix to redistriqute the load in the manner tacitly assumed by the rule of mixtures. These mechanical parameters have been categorized as relevant to (a) bond and matrix properties; (b) filament properties; (c) composite geometry; and (d) test conditions.

The directional arrows on the mechanical variables (abscissa, Figure 50) point in the direction of an increase in the property, dimension, etc. The effect of some of these variables will now be discussed.

At the top of the diagram, three regions of composite behavior are indicated: (1) Bond Limited; (2) Filament Limited; and (3) Matrix Limited. By definition, a Bond-Limited composite does not utilize the average strength of the reinforcing filament, because the bond fails at a stress below that required to break filaments of average strength. That is, although the matrix is capable of redistributing the load, the bond is too weak to transmit the load from the broken filament to the matrix. Fracture is characterized by only a few breaks per filament (at the weaker regions) and extensive filament pull out. Filament-Limited behavior is, of course, the most desirable type of behavior because the strength of the composite reflects, as predicted by the rule of mixtures, the average strength of the reinforcing filament. Such composites fail by cumulative filament damage (many cracks per filament) and are free of substantial matrix contribution to premature failure. This is not only inherently advantageous but it also is especially amenable to statistical sophistication in performance predictions. In this connection, Figure 50 shows a Filament-Limited region (IIA) above that predicted on the basis of average filament strength. This takes into account the fact that the strength of filamentary materials often increases as the gage length decreases. Thus, after many non-catastrophic failures, the gage lengths remaining in a composite may be stronger than those used in characterization tests of the filament. Matrix-Limited behavior is undesirable because the composite performance is often limited by the weaker of the two components, the matrix. Numerous examples of the loss of matrix integirty in filament-epoxy specimens have been discussed during the course of this work. Briefly recapitulated, the matrix may redistribute the load, arising from filament failure, in a manner (say, cracking) which adversely affects the strength of the composite. Composite failure is frequently brittle and the relatively few fractures per filament show that strength utilization is less than required. In Matrix-Limited behavior, composite strength is limited by certain "defects" rare enough to be regarded as insignificant in ordinary statistical characterization of separate composite components. The upper dashed line in the Matrix Limited region (IIIA) in Figure 50 shows that the matrix limitations are of little consequence if the filament strength is scatter-free.

5. *BOND STRENGTH – A COMPROMISE*

The model described still appears to be consistent with most of the data obtained during the course of the investigation. However, the attractiveness of the "inhomogeneous strain" hypothesis is such that it should be rationalized with the general model (Figure 50). In the "inhomogeneous strain" hypothesis it is postulated that when the volume fraction is sufficiently high, weak filament regions are so well "splinted" by strong regions that the former do not reach the fracture strain appreciably ahead of the latter. In other words, the act of incorporating filaments in a composite markedly reduces the strength-scatter characterizing tests of individual filaments. In consequence, the composite behaves as if its individual reinforcing components were nearly scatter-free, corresponding to the upper dashed line in region III A, Figure 50. That is, the composite to which the hypothesis is applicable are both strong and exhibit few breaks per filament. While this appears to indicate that the composite is filament limited,the capacity for effective splinting depends upon the modulus of the matrix; therefore, the composite is actually matrix limited in a complex fashion.

Much of the previously reported work done on filament-epoxy specimens has been concerned with limitations of the matrix capacity to redistribute load in the vicinity of filament failure in a manner consistent with the assumption of the rule of mixtures. In most instances, the filaments have been sufficiently well-bonded to insure that the energy released upon filament failure was transmitted through the bond and into the matrix. Thus, experimental work has been designed to demonstrate the critical nature of the filament-matrix bond, which is important for two reasons: (1) an understanding of the critical nature of the bond is necessary for a general understanding of composite performance, as will be discussed later; and (2) unbonding is a rather common practical problem in metal matrix composites and has lead to considerable efforts toward improved bonding.

Since unwanted unbonding had not been a major experimental difficulty in filament-epoxy specimens, special attempts were made to reduce bond strength in order to test the hypothesis that the maximization of bond strength may not be always necessary or even desirable. Figure 51 shows failure in a single filament-epoxy specimen in which the filament had been Teflon coated to drastically reduce the bond strength. Neither of the two filament cracks propagated into the matrix; long unbonded regions were evident, the extent of pull-out being evident from the fact that two ends project from the fracture surface. The final fracture started in the matrix at the edge of the specimen. As will be discussed later, the mechanical behavior of this specimen was similar to that of plain epoxy.

Figure 52 shows the fracture surfaces and profiles of single discontinuous filament-epoxy specimens. When both segments of the filament were graphite coated (Spec. 708, Figure 52), failure was by the slow propagation of a matrix tensile crack from an end of one of the filament segments. The other cracks in the filament segments resulted in local unbonding and/or slowly propagating (non-catastrophic) matrix tensile cracks; when closely coupled; the alternation (of unbonding and cracking) may be-characterized as a "slip-stick" fracture mode. This specimen was approximately as strong as plain epoxy (also true in tests at $\dot{\epsilon}$ = 2 in/in/min) and considerably stronger than the other

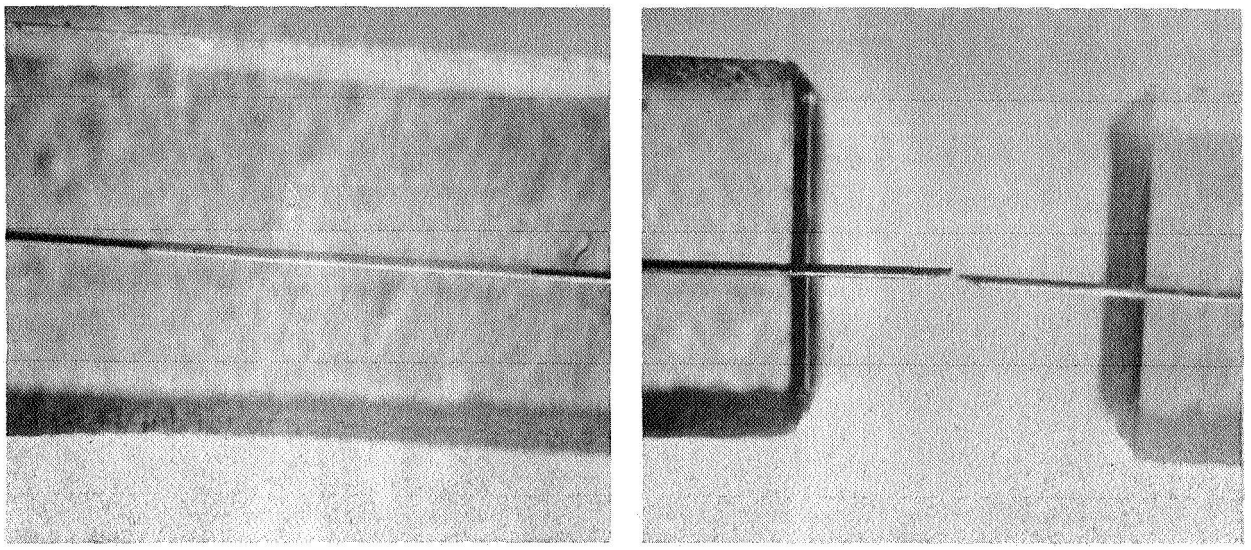

Figure 51. Profile of Failures in Teflon Coated Single B/W Filament-Epoxy Specimen Tested in Tension at ϵ = 2 in./in./min. (Specimen 715 - 17X)

discontinuous specimen (No. 712) having only one of the segments graphite coated. The latter failed in a brittle manner by the rapid propagation of a matrix tensile crack from a crack in the uncoated filament (as is evident in Figure 52); that is, this specimen was not significantly different from a continuous filament specimen similarly tested (see Spec. 518, Table XVII and Figure 38). In regard, then, to the mechanical behavior and fracture mode, the fact that these specimens had discontinuous, rather than continuous, filaments was of less importance than the bond strength.

From these results it seems reasonable to infer that discontinuous composites will be weaker than continuous composites when bond strengths are very low. At bond strengths inherently high enough to load the filament to fracture, the crack sensitivity of the matrix would become critical. A ductile crack originating at an early filament falure might not be as damaging as a larger one already present at a filament end in a discontinuous composite, and it would be weaker than a comparable continuous composite. However, when the bond strength is high enough to propagate the filament failure into the matrix in a brittle fashion, there would be little reason to expect the two kinds of composites to behave differently. This, of course, is not definitive because so many of the other variables (see Figure 50), which influence expected composite behavior, can also be expected to have relevance for the discontinuous-continuous comparison. The limited amount of evidence and many of the lines of reasoning that come to mind suggest that discontinuous composites are most likely to be as strong as continuous composites when both are weak and brittle (Region III, Figure 50).

Duplicate specimens (each containing a simple continuous graphite coated B/W filament in epoxy) were tested in tension at 2 in/in/min, a strain rate which always results in weak brittle specimens if the filaments are uncoated (that is, well bonded). The fracture surfaces and profiles are shown in Figure 53. In addition, each specimen had five non-catastrophic filament failures which exhibited

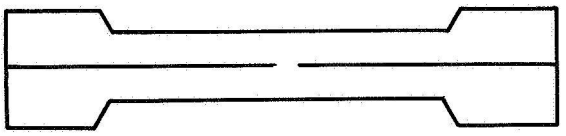

Both Filaments Graphite Coated
σ = 3120 psi (Spec 708)

One Filament Graphite Coated
σ = 2650 psi (Spec 712)

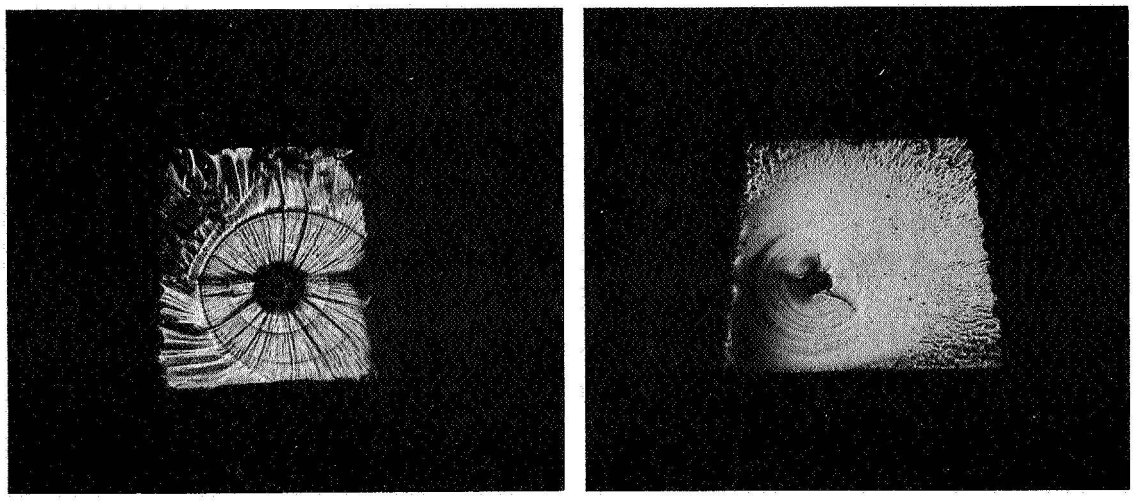

Fracture Surfaces (17X)

Failure in Uncoated
Filament Generated
Catastrophic-Matrix Crack

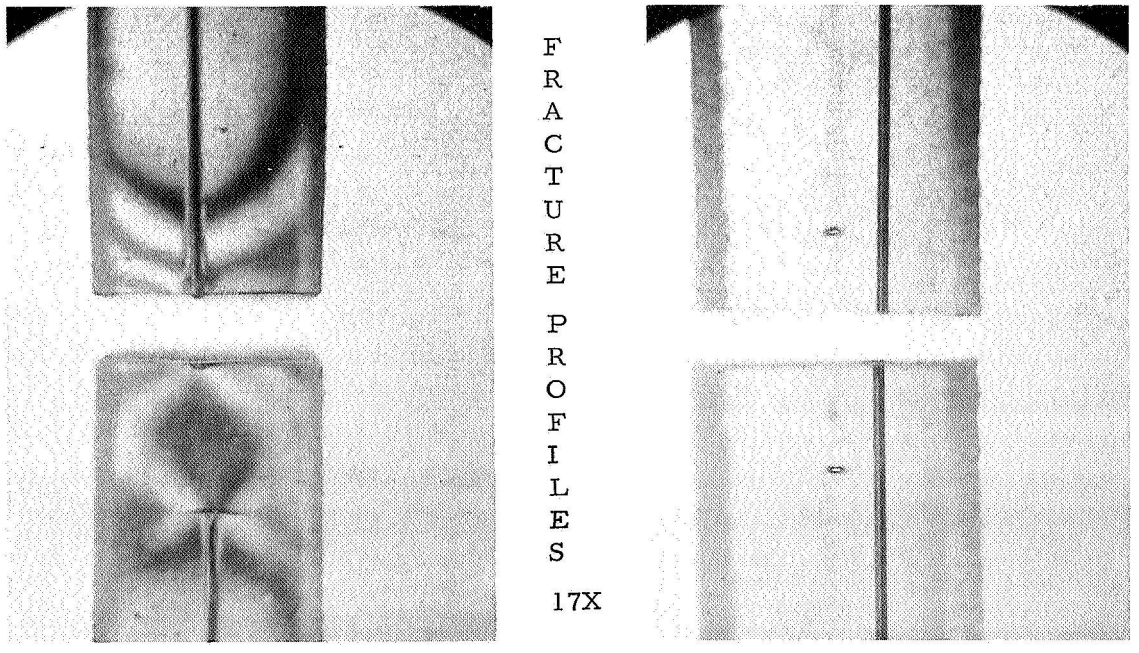

Figure 52. Discontinuous Single B/W Filaments Tested at ϵ = 0.02 in./in./min.

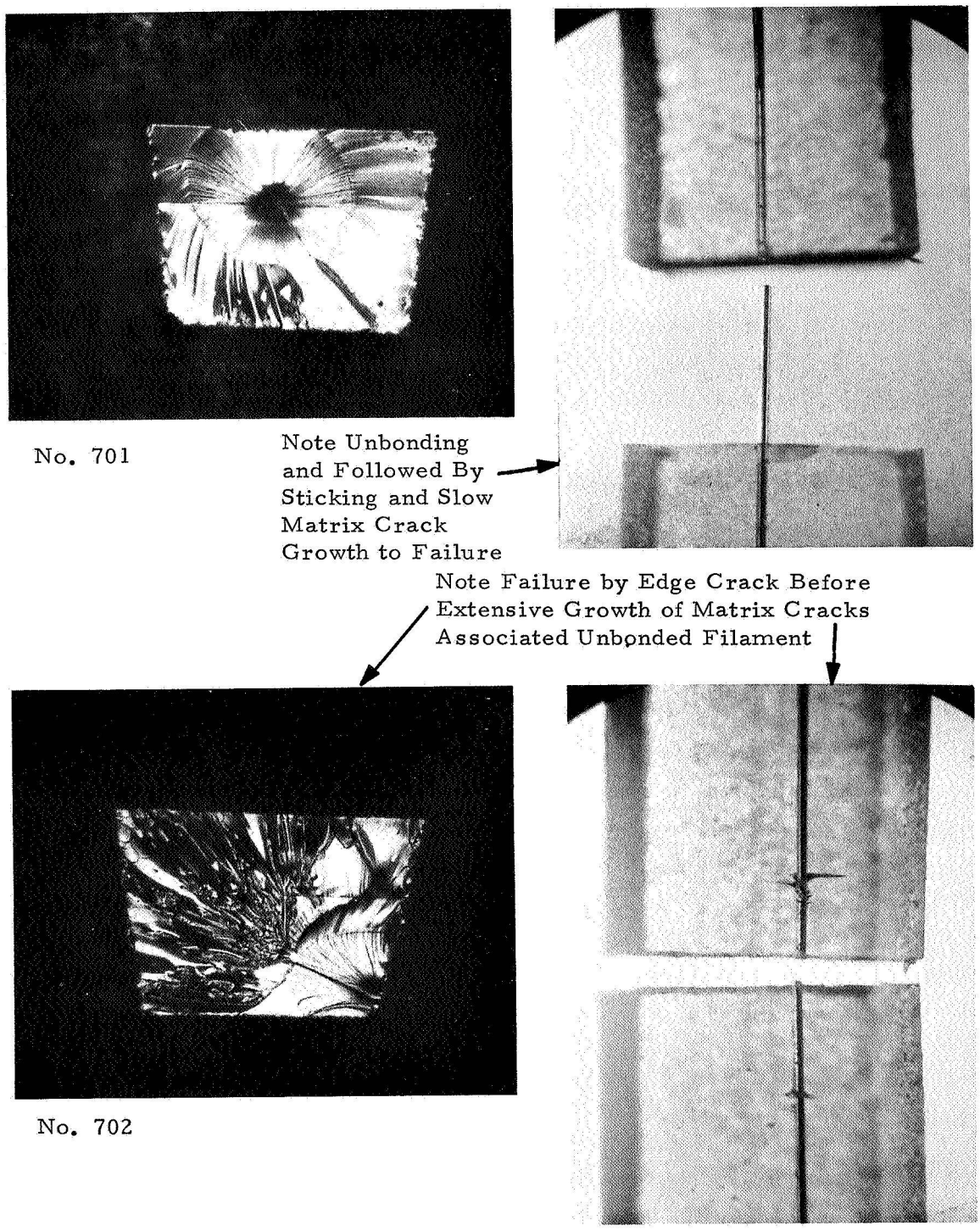

Figure 53. Graphite Coated, Continuous Single B/W Filament Tested at ϵ = 2 in./in./min. (17X)

the "slip-stick" fracture mode, an example of which is shown in Figure 54. It is evident (Figure 53) that considerable unbonding was associated with the catastrophic failure in Spec. 701; eventually it stuck enough to generate the fatal, slowly propagating, tensile crack (perhaps in a region of incomplete graphite coating). In the case of Spec. 702, two matrix cracks (associated with the "slip-stick" region evident in the profile in Figure 53) were in the process of growth. However, before either of these could propagate sufficiently to separate the specimen, a matrix crack originating at the specimen edge (see fracture surface, Figure 53) intervened catastrophically. The mechanical behavior of these specimens was similar and superior to specimens exhibiting unlimited unbonding (e.g., Figure 51) or very good bonding (e.g., Figure 52, Specimen 712).

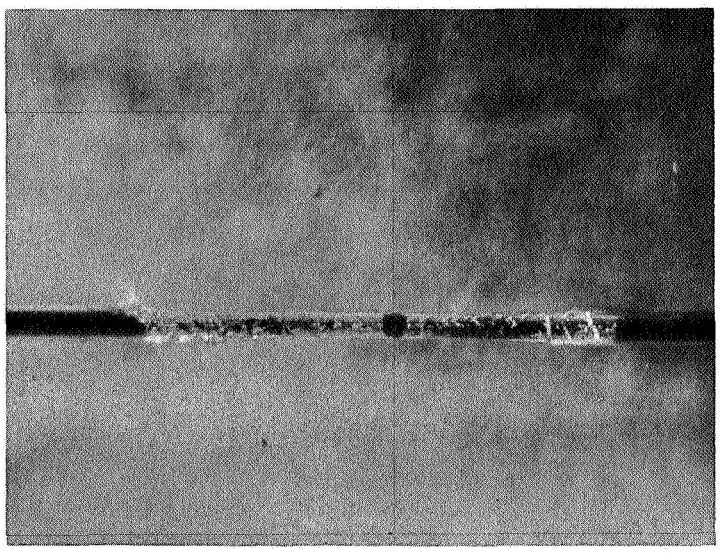

Figure 54. *A Typical Fracture Profile of One of Five Non-Catastrophic Cracks in Graphite Coated B/W Filament-Epoxy Specimen Tested at ϵ = 2 in./in./min. (Specimen 701 - 35X)*

The relationship between tensile behavior and bond strength for single filament-epoxy specimens is illustrated by the stress-elongation curves in Figure 55. The tensile tests were made at a strain rate of 2 in/in/min, a rate known to result in weak brittle behavior for well bonded specimens (see Table XVII and Figure 38). As expected, the well-bonded specimen (uncoated filament) failed at the first filament failure and was both brittle and weak relative to the plain epoxy. This specimen was "Matrix Limited" and is, thus, an example of failure in region III of the model (Figure 50). Spec. 715, having the teflon coated filament, exhibited two filament cracks and unlimited unbonding (Figure 54). It was slightly weaker than the plain epoxy (but not brittle) and can be regarded as an example of failure in region I of the model (Figure 50). Spec. 701 exhibited cumulative damage (many filament cracks prior to failure) and was somewhat stronger than the plain epoxy and may be regarded as an example of failure in region II of the model (Figure 50).

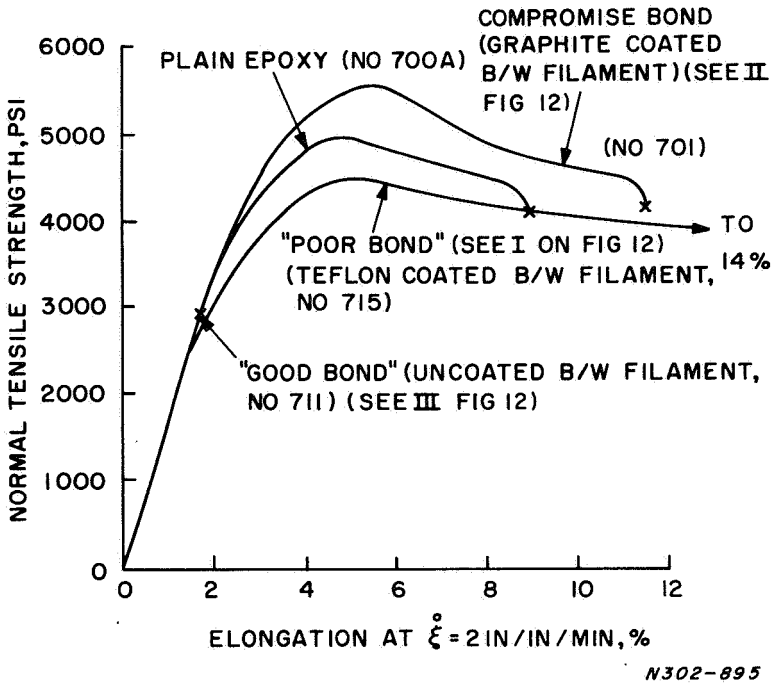

Figure 55. The Effect of Bond Strength on the Tensile Behavior of Single B/W Filament-Epoxy Novalac Specimens

It is evident from these results that the slip-stick mode of failure associated with early filament failure in graphite coated filament is preferable to either unlimited unbonding or to catastrophically "good" bonding. For this particular set of circumstances, the graphite coating is the best compromise bond. First, the bond is weak enough so that filament failure does not generate a rapidly propagating catastrophic matrix tensile crack. Therefore, the load can continue to rise as the filament breaks up and this insures some utilization of the stronger portions of the filament.

This point is, of course, crucial if "real" composites are to reflect the average rather than the lowest filament strength. Second, the bond is strong enough to "stick" and prevent the unlimited unbonding which also precludes load redistribution. In summary, the "slipping" prevents catastrophy and the "sticking" is necessary for effective load redistribution.

While the foregoing results are definitively applicable only to these specimen materials and configurations, they serve to emphasize the point that bond strength should be an appropriate, not necessarily the maximum attainable, value.The bond strength required will depend upon the matrix crack sensitivity, and it will be noted that the product of the two is identified as an important parameter in the model (Figure 50).

There are ambiguities in the nature of materials that may frustrate attempts to make statements

that are both rigorous and general. For example, in the case of epoxy Novalac, there is an ambiguity in the term "matrix crack sensitivity". In previous discussions [1] it was pointed out that this epoxy exhibits two kinds of tensile cracks. One propagates very rapidly, creating smooth surfaces; and may propagate to specimen failure while the load-elongation curve remains linear; therefore, it is logical to refer to this kind of crack as "brittle". The other kind of matrix crack propagate less rapidly or even quite slowly, creating linearly marked surfaces, and can do so during non-linear load-deflection behavior; this kind of crack propagation has, from time-to-time, been characterized as "ductile". When, by a change in formulation, the epoxy is made more flexabilized, it appears to become more resistant to the formation and/or propagation of "brittle" cracks but less resistant to the growth of "ductile" cracks. These divergent characteristics lead to some ambiguity in some early attempts to modify bond strength by changing epoxy formulation. The expedient of coating the filaments with graphite or teflon worked, because the bond strength could be changed independently of either of the two matrix crack sensitivities. The situation might be considerably more difficult to evaluate and control in metal matrix if, for example, bond-enhancing coatings diffuse into the matrix and adversely affect its capacity for plastic deformation or its crack sensitivity.

The relationship between tensile behavior and bond strength for single filament-epoxy specimens is shown in Figure 55. Five filament specimens (uncoated and Teflon coated) were tested to further document the bond effect. As expected, and in conformity with other well-bonded 5-element specimens, the specimens containing uncoated B/W filaments was weaker and more brittle than he plain epoxy (see Spec. 801 B, Figure 56 and Figure 55.) The poorly bonded specimen (Spec. 800B, Figure 56), was as strong as plain epoxy and exhibited a large elongation to maximum load, which occurred after non-catastrophic filament cracking. Although there were qualitative differences in the load elongation cures, the Teflon coated filament-specimen was quantitatively similar to the specimen containing ductile aluminum wires and clearly superior to the low modulus E-glass filament-specimen (see Spec. 408 and 411, Table XIX).

In summary, the "poor" bonding ameliorates the usual weakening and embrittling effect of a high-modulus, well-bonded, brittle filament and demonstrates the independent effects of bond strength and matrix crack sensitivity (referred to in the general model for composite behavior, Figure 50). The best bond is, of course, one which optimizes the combination of bond and matrix strengths, as previously discussed.

6. SUMMARY REMARKS ON MECHANICAL COMPATIBILITY

A study of the behavior of simple filament-epoxy specimens in uniaxial tension has been used to develop a generalized model (Figure 50) for explaining and predicting many effects of material properties, specimen configuration and test conditions on composite performance. It is abundantly evident that the many variables involved are strongly interrelated; therefore, it promises to be virtually impossible to predict composite performance from conventional data obtained by testing the separate components of an intended composite. Chemical compatibility is recognized to be an important attribute of successful composites, and it seems warranted to assert that what may be called mechanical compatibility is of comparable importance.

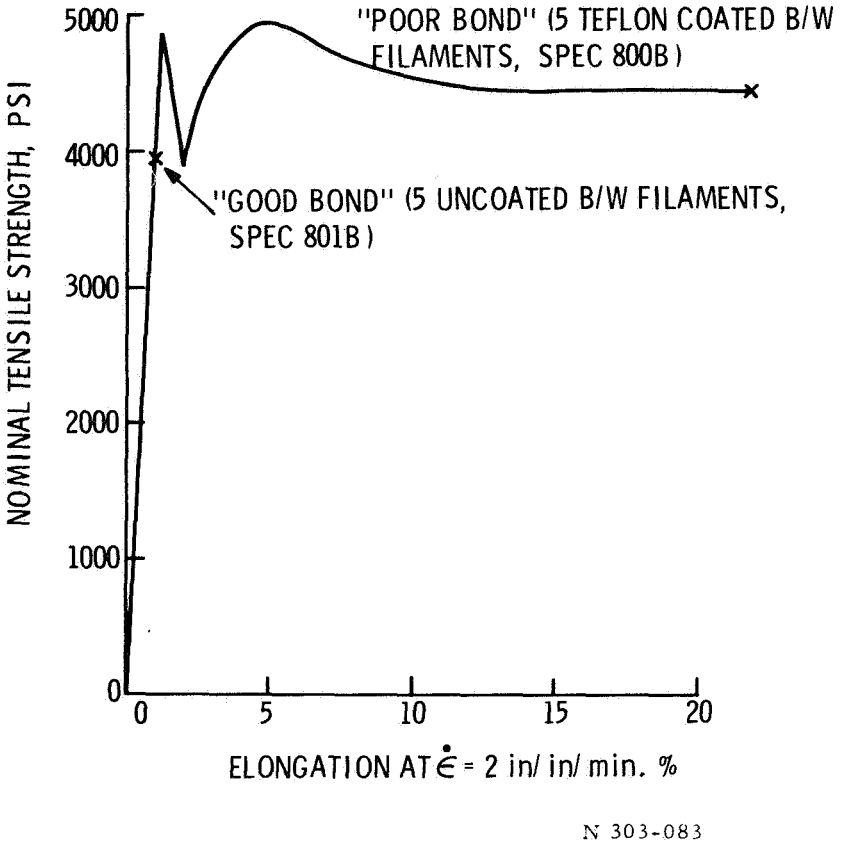

Figure 56. Nominal Tensile Strength vs. Elongation for "Good" and "Poor" Bonded 5-Filament B_4C/B/W-Epoxy Continuous Filament Composites

Given, on the one hand, a general understanding of the mechanical compatibility problem via the model and, on the other hand, an almost certain knowledge that highly specific information will be required to produce good composites using the filament-matrix systems, it seems warranted at this time to divert an increasing amount of effort to the study of other filament-matrix systems of interest.

E. Copper Matrix Composite System

Strain rate effects in composite materials are not well understood [1], especially in regard to metal matrices. Such studies (except for those on impact) are not generally discussed in the literature presumably because of the proprietary nature of the subject. It was felt then that because strain rate effects in epoxies produced composite weakening, a study of an ideal composite system, i.e., copper-tungsten, would be appropriate. However, as will be shown, the copper-tungsten system did not lend itself to a critical evaluation of this point because of metallurgical restrictions imposed on the wire components which resulted from thermal treatment.

Tungsten wire tensile properties fall into three categories:

(1) Strong and ductile with low strength scatter (as drawn)

(2) Strong and ductile with moderate strength scatter (annealed)

(3) Weak and brittle with high strength scatter (embrittled)

The critical attribute necessary (i.e., strong, brittle of high strength scatter) characteristic of the high performance filamentary materials B_4C/B/W, B/W etc. is thus seen to be unattainable.

1. FABRICATION TECHNIQUES

Two methods of infiltration were used to produce 2 in.-long, continuous filament Cu-W composites, all of which contained 50 v/o tungsten wire 0.005 in. diameter.

The first method tried was capillary rise. Briefly, an alumina tube about 0.080 in. inside diameter was packed with an appropriate number of tungsten wires. The packed alumina tube was then placed upright in a crucible containing copper, and the assembly was next placed in a hydrogen furnace at 1200 C. Molten copper was drawn into the tube and around the wires by capillary action. The volume fraction of wire was insufficient to produce complete filling of the voids between wires with molten copper. This method proved impractical from another aspect, since the tungsten wire treated similarly (called WCA in a previous section) proved to be totally brittle and very weak (Table IX).

The second method, liquid infiltration by the same technique developed for the alumina-B_4C/B/W composite materials, produced excellent appearing, dense composites. Briefly, a multiple cavity mold, containing 6 holes, 2 in. deep and 0.062 in. diameter, was packed with tungsten wires to a volume fraction of 50%. Copper was added to a reservoir at the top of the mold, and the assembly was evacuated and back-filled with hydrogen and held at 1200 C for 20 minutes.

2. TENSILE TEST RESULTS

Test specimens made by the capillary action method proved unacceptable because of the incomplete infiltration of copper within the composite and because of the drastic degradation of the mechanical properties of the tungsten wire (WCA). Specimens produced by the standard infiltration method were usable and were epoxied into alumina grips [1] having 1 in. gage lengths. They were tensile tested at various strain rates. The results of these tests are presented in Table XX.

A plot of the strength of the composites vs. strain rate is shown in Figure 57. An envelope of tensile values including the average value at each strain rate is plotted using the maximum and minimum values measured as limits. To help elucidate the discussion of these results, two additional bits of

TABLE XX. TENSILE RESULTS OF Cu-W COMPOSITES

Specimen No.	Tensile Strength (psi)	Strain Rate (in/in/min.)	Remarks
1	77,600	02	Grip break
2	50,000	2	Grip break
3	101,000	002	Grip break
4	72,000	002	Grip break
5	86,500	002	Grip break
6	62,500	2	Grip break
7	114,000	02	Grip break
8	32,600	2	Grip break
9	62,500	002	GL* break
10	121,000	02	GL break
11	168,000	20	Broke in grips
12	49,000	20	Broke in grips

*GL = gage length

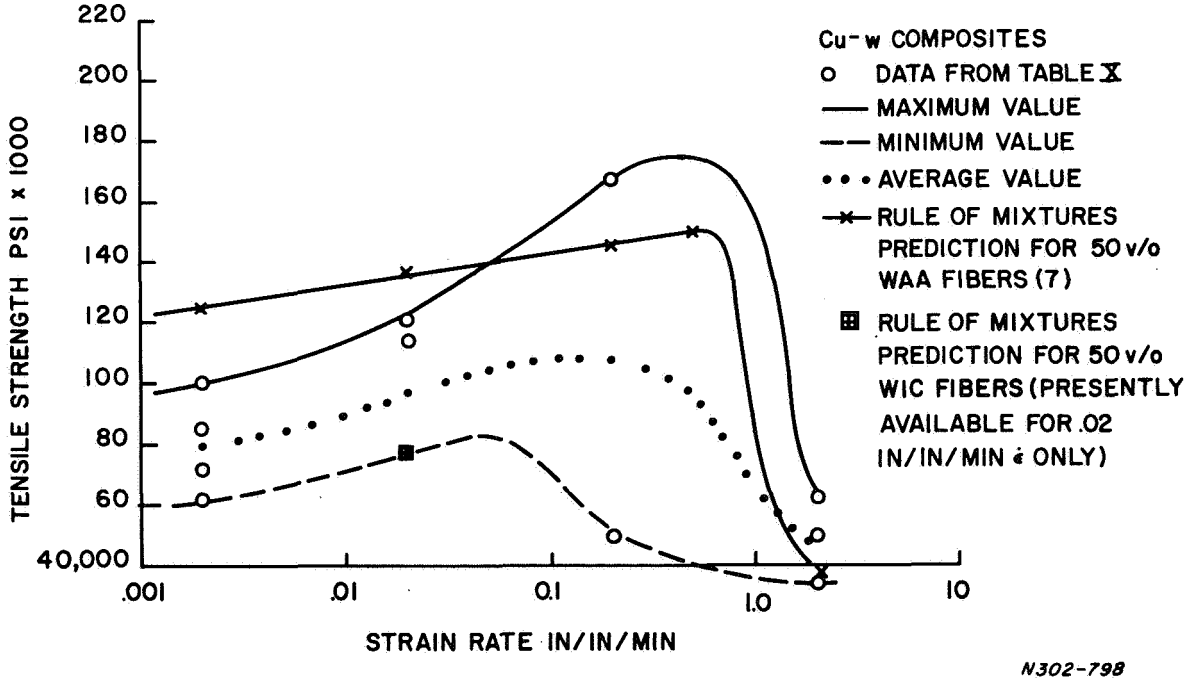

Figure 57. Room Temperature Tensile Strength as a Function of Strain Rate for 50% Cu-W Composites

data have been added. First, the rule of mixture predicted tensile value of a 50 v/o Cu-W composite composed of WIC tungsten wires (see Table IX) is included. These wires have received the identical thermal treatment as the tested Cu-W composites without the copper infiltrate. Second, a rule of mixture predicted tensile value of a 50 v/o Cu-W composite composed of WAA tungsten wires is included. These wires have received an annealing treatment of 1600 C for 16 hours in vacuum and were reported on previously [1].

By comparing the tensile behavior curves of the actual Cu-W composite with those of a hypothetical composite whose filament component behavior is known, it is seen that they have a similar shape. That is, a ductile-to-brittle transition occurs at a strain rate near 1 in/in/min. It is concluded then that the WAA wires and the WIC wires have similar tensile characteristics as a function of strain rate, although this similarity was not completely experimentally determined. Also, the tensile value of the predicted Cu-W composite using WIC wire is within the envelope of the actual data obtained.

Thus it is shown that although only a limited amount of experimental work was done, copper tungsten wires appear to follow a rule-of-mixtures tensile behavior independent of strain rate. Although this conclusion may be fortuitous, as discussed in Section II-D, it is also deduced that the copper-tungsten system obeys the general composite behavior hypothesis presented in earlier work [1]. Strong ductile fibers in a composite fail by cumulative damage (strain rates below 1 in/in/min) and weak brittle filaments also fail by cumulative damage (strain rate below 1 in/in/min). These results have been reported by others [15, 16]. However, this study was fortunate in that the ductile and brittle tungsten wire components of the composites occurred in identical specimens and at the same test temperature simply by changing the strain rate. It appears, then, that the original objective, viz., developing an ideal system to study the area of strong, brittle filaments of high strength scatter, cannot be reached because of material limitations of the Cu-W system.

III. CONCLUSIONS

1. The production of strong B_4C coated B/W or B/SiO_2 continuous filament is feasible. The material produced is chemically stable in molten aluminum allowing liquid infiltration techniques to be used for composite manufacture.

2. The characterization of composite components would be most valuable if their individual mechanical, physical and chemical properties could be determined in situ. Determination of various property parameters before further processing was a valuable but not definitive measure of how the final composite would behave. Testing of the filament component of composites after fabrication and testing (the matrix was dissolved by etching) always showed a deviation from the virgin results through either fabrication damage (breakage), fabrication weakening (temperature cycling) or both.

3. It was shown that metal matrix composites ($Al\text{-}B_4V/B/W$ and Cu/W) containing continuous filaments can be fabricated which utilize the strength potential of their components. A model (inhomogeneous strain criteria) was developed which seems to fit the observed tensile behavior of composites more rigorously than those developed by others [18] (cumulative damage models).

4. Discontinuous filament composite systems appear to reach a limiting value of about 50% of their potential of strong filament. This is indeed a severe limitation which could negate advantages envisioned using this approach.

5. Epoxy-filament composite studies have led to a number of observations and conclusions concerning composite behavior.

a. Epoxy-composite studies have delineated the three failure modes associated with filament failure.

b. A concept of mechanical compatibility has been advanced.

c. The role of bond strength and its effect on filament-matrix interaction and composite strength has been assessed and the concept of intermittant bond strength explored.

IV. RECOMMENDATIONS FOR FUTURE WORK

This study (NASw-1543) was proposed as a three year program; unfortunately, it was terminated after two years of effort. Some of the results and conclusions therefore, of necessity, are not definitive but rather suggestive and represent a research in progress report which should lead to a better understanding of the mechanical, chemical and physical behavior of composite materials.

The concept of mechanical compatibility has served to demonstrate the general effect of a number of variables which determine whether a composite will be bond limited, filament limited, or matrix limited. Maximization of a composite strength potential, utilizing the concepts developed, is an important goal for future work. Also, the inhomogeneous strain criteria has indicated that the filament-limited area of the compatibility model can be extended through the matrix-limited area by filament interaction (along with filaments of low strength scatter). Thus a more complete, definitive study of the inhomogeneous strain model appears warranted.

Suggestions for future experiments include: ductile-brittle tungsten wire arrays, more tensiled but not fractured experiments, lubricated filamentary arrays of large volume, etc.

ACKNOWLEDGEMENTS

Acknowledgement is given to Mr. William Laskow for his valuable assistance concerning the production of B_4C/B/W filament, composite testing and specimen preparation.

The authors also acknowledge the assistance and helpful suggestions of Messrs. R. Grosso, R. Mehan, Drs. M. J. Noone, E. Feingold and W. H. Sutton.

REFERENCES

1. A. Gatti, J. M. Berry, J. J. Gebhardt, J. V. Mullin, E. Feingold, "Investigation of the Reinforcement of Ductile Metals with Strong, High Modulus, Discontinuous Brittle Fibers", NASw-1543, Summary Report (Final Report), November 1967.

2. A. Gatti, R. Cree, E. Feingold, "Synthesis of Boron Carbide Filaments", NASw-670, Final Report, July 10, 1964.

3. A. Gatti, C. Mancuso, E. Feingold, R. Mehan, R. Cree. "Study of the Growth Parameters Involved in Synthesizing Boron Carbide Filament", NASA CR-251, July 1965.

4. A. Gatti, C. Mancuso, E. Feingold, R. Jakas, "Study of the Growth Parameters Involved in Synthesizing Boron Carbide Whiskers", NASw-1205, Final Report, March 1, 1966.

5. A. Gatti, E. Feingold, J. J. Gebhardt, J. M. Berry, V. A. Cordua, "Study of the Growth Parameters Involved in Synthesizing Boron Carbide Whiskers", NASw-1383, Final Report, November 1966.

6. D. L. McDanels, R. W. Jech, and J. W. Welton, "Metals Reinforced with Fibers", Metal Prog., Vol. 78, No. 6, pp. 118-121, Dec. 1960.

7. J. B. Higgins, A. Gatti and J. J. Gebhardt, J. Electrochem. Soc., to be published January 1969; AFML–TR–65–354, Part II, Aug. 1966, AF contract 33(615)-1644.

8. J. L. Hoard, "Borax to Boranes", ACS Monograph Series, #32, p. 42, 1961.

9. R. B. Reeves and J. J. Gebhardt, SAMPE 10, D–13 to O–24, 1967.

10. J. J. Gebhardt, GE TIS 67SD69, 1967.

11. R. Signorelli, Private Communication.

12. R. L. Mehan, R. Jakas, R. Grosso, "Behavior Study of Sapphire Wool Aluminum and Aluminum Alloy Composites", Contract No. F33615–67–C–1308, 1st Quarterly Report.

13. R. L. Mehan and R. Grosso, unpublished research.

14. C. Zweben, "Tensile Failure Analysis of Fibrous Composites", AIAA Paper No. 67–173, AIAA 6th Aerospace Sciences Meeting, New York, N.Y., January 22, 1968.

15. V. Mazzio, Unpublished Research.

16. A. Kelly and W. R. Tyson, "Tensile Properties of Fiber-Reinforced Metals: Copper/Tungsten and Copper/Molybdenum", J. Mech. Phys. Solids, Vol. 13, pp. 320–350, 1965.

17. J. V. Mullin, J. M. Berry and A. Gatti, "Some Fundamental Fracture Mechanisms Applicable to Advanced Filament Reinforced Composites", Journal of Composite Materials 11, 1, 82-103, January 1968.

18. B. W. Rosen, "Tensile Failure of Fibrous Composites", AIAA 2 No. 11, Nov. 1964.

APPENDIX A

INTERMITTENTLY BONDED FILAMENTS

In recent tests aimed at controlling the bond strength between filament and matrix, the mechanical application of graphite to the surface of boron filament has provided some interesting results. The "corn cob"-like surface of the filament causes nonuniform application of the graphite on the filament with a resulting pattern of intermittent coated and uncoated regions. This condition provides bonding in the low spots while the high points are shielded from the matrix by the graphite coating.

To better appreciate the experimental results it is important to analyze the way in which the reinforcing mechanism is influenced by this intermittent coating of the filament.

Figure 58 shows the surface of a boron filament at high magnification, and the knobby appearance is quite representative of all points along the length of the filament.

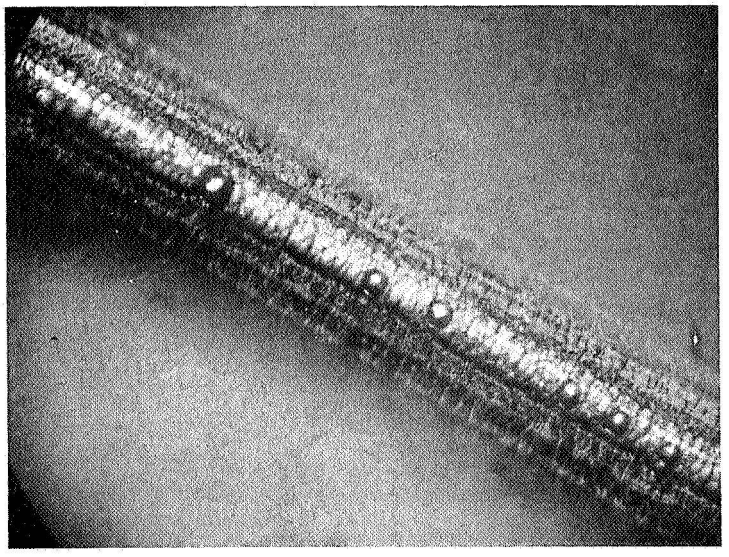

Figure 58. "Corn-cob" surface (202X)

The usual model used to describe the shear stress distribution at the interface in a uniformly bonded filament is shown in Figure 59. Here the distribution of the shear stress is assumed to be continuous along the interface between filament and matrix reaching its highest values near the ends.

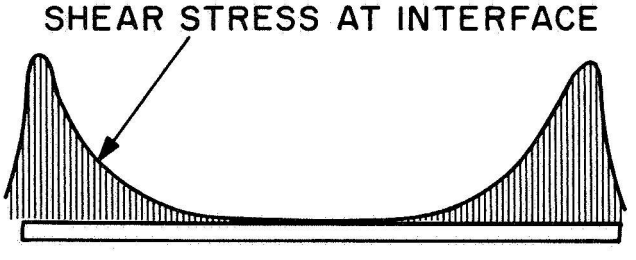

Figure 59. Distribution of shear stresses in a uniformly bonded filament

Actually, there are probably local variations in the shear stress distribution which result from surface imperfections and foreign materials ,such as minute dirt particles which are present on the surface. These can be considered of secondary importance however, compared to the case of the graphite coated filament where relatively large parts of the surface are prevented from bonding. In the simplest model of an intermittently bonded interface we can construct the condition shown in Figure 60. Here the shear loads are considered as a series of concentrated forces rather than the continuous distributed forces assumed previously. This has the effect of concentrating the stress trajectories in the regions of bonding and increasing the shear stress at these sites. As each bond area fails its effect on the adjacent areas is dampened to some extend by the unbounded region between them. This condition tends to inhibit a continuous and sudden crack growth mechanism both at the interface and in the matrix (included cracks).

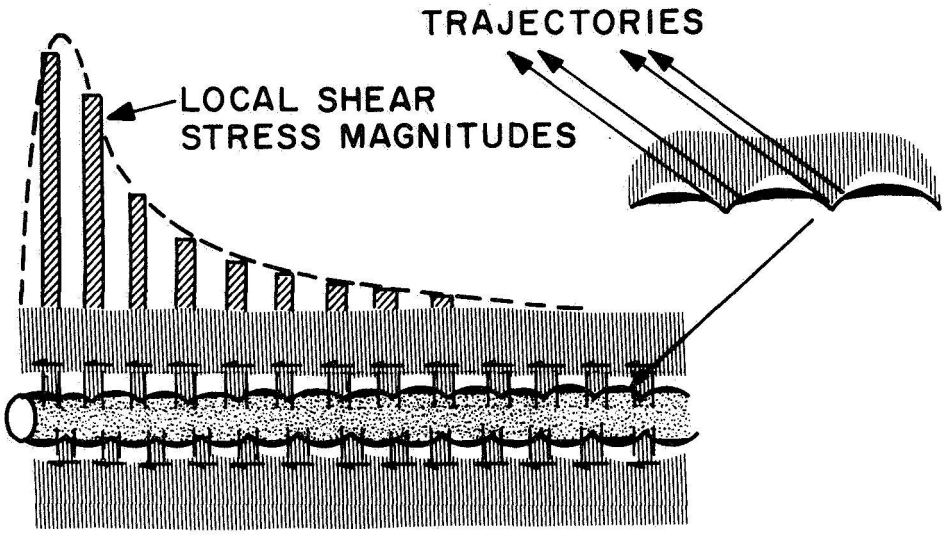

Figure 60. Model of intermittently bonded filament

Now consider what happens when the filament fractures. The fracture may occur at any point in the loaded region and the matrix being only partially bonded at the filament fracture site, is not as suddenly influenced by the fracture as in the continuously bonded condition. Consider Figure 61. At point A there is no bond to initiate the sudden crack,and at point B the matrix has no reentrant corner to make it crack sensitive.

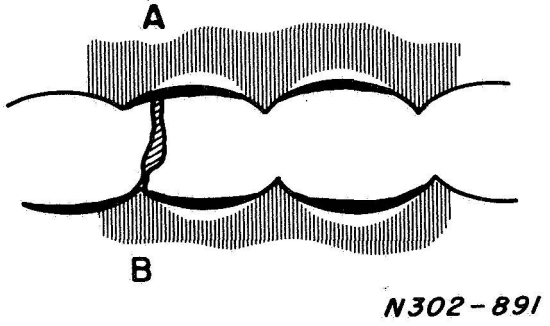

Figure 61. Details of intermittent bonding and its effect on matrix crack sensitivity (schematic)

Further, one can apply a stress concentration argument to the incidence of cracking in the matrix adjacent to a filament break. First consider what happens in the continuously bonded filament shown at the left of Figure 62. The immediate redistribution of load requires very high shears on each side of the break points A and B. These are very close to the crack and quite high, causing the matrix to experience very high stress concentrations at the point of the break. In the intermittent bond condition, shown at the right of Figure 62, the regions immediately adjacent to the fracture site are not bonded and therefore the new shears which are applied to the matrix at A and B are further away. Distribution of the new local matrix stress over a great length L in the matrix causes less stress concentration at the filament fracture site and therefore minimizes the possiblity of a matrix crack.

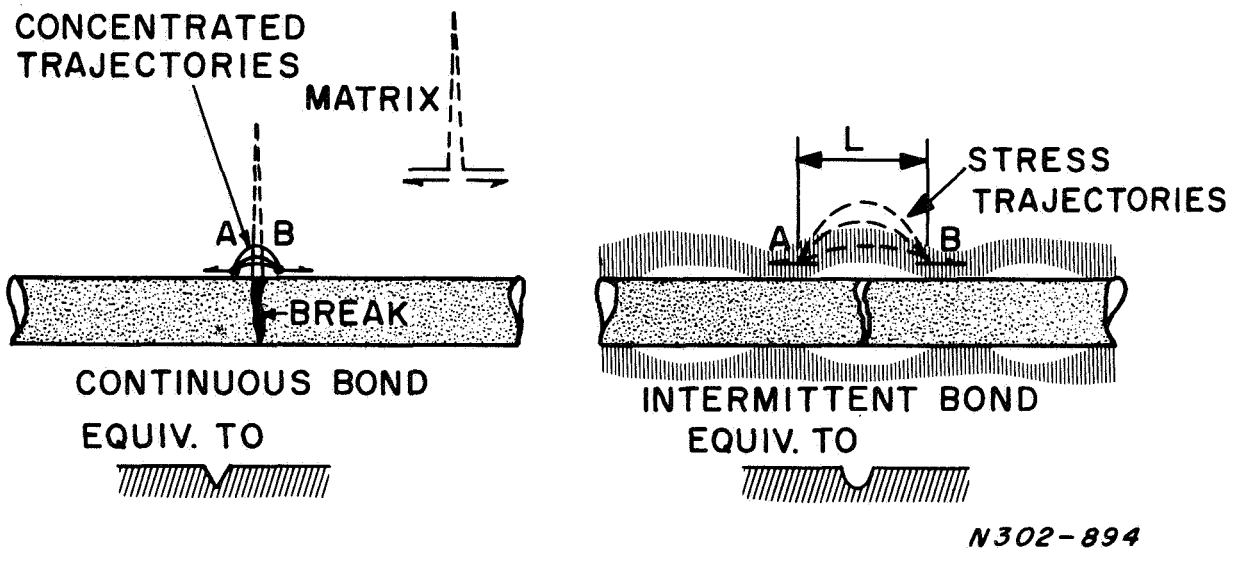

Figure 62. Distribution of stress trajectories as a function of bonding (schematic)

APPENDIX B

RELATION BETWEEN BOND STRENGTH AND COMPOSITE STRENGTH

This discussion by J. V. Mullen attempts to rationalize the fracture behavior observed in epoxy-boron composite materials which had been reported upon earlier. Underlying this treatment is the assumption that the cumulative damage mechanism of composite failure is valid. Present work with aluminum-B_4C/B/W composite materials has led to other models to explain their fracture behavior rather than the cumulative damage mechanism.

Assume that a certain number of filaments of given modulus and strength distribution and a matrix of specific strength, modulus, crack sensitivity, etc, is available. Assume further that the capability of varying the bond strength as defined by the shear stress τ at the interface exists. If it were possible to degrade the bond so much that $\tau = 0$, the filaments would not be loaded by the matrix at all and the volume the filaments occupy could be considered as voids in the matrix. All stress would be carried by the matrix material and since the voids (filaments) would reduce the strength of the matrix due to stress concentrations, the composite strength would be less than that of an equal volume of matrix with no filaments. This may be construed as a zero volume fraction condition. This is point A in Figure 63 where none of the filament strength is developed. As the bond strength is increased very gradually the matrix begins to transfer load across the interface to the filaments without any fracture of filaments,and the strength of the composite is increased by the contribution from the filaments. This process continues as the bond strength increases up to point B where the weakest filament fails. Because the total composite stress is still low the first weak filament fractures will be low energy breaks and will not throw out disk-shaped cracks [17] which could affect adjacent filaments. As these breaks occur at weak points in the filament, the bond strength will still be relatively low and considerable debonding will occur also. This debonding to some extent prevents the high energy breaks from occurring, until the bond strength is large enough to fracture filaments at the higher stress level corresponding to point C. At this point, high energy breaks begin to occur which throw out disk-shaped cracks affecting adjacent filaments. Each local fracture has a much more damaging effect than just the loss of one fiber and subsequent static redistribution of load, because this higher bond strength does not allow dissipation of energy through unbonding. For these reasons, the bond strength corresponding to point C is a critical bond strength τ_C for a given system, there is too much bond strength and fewer filament fractures can be sustained before the composite fails. Therefore, the overall composite strength is reduced as shown on CD. Now consider the implications of the bond strength variation in interpreting the rule of mixtures. In its ususal form, composite strength σ_C is expressed as

$$\sigma_C = \sigma_m (1 - V_f) + V_f \sigma_f \quad , \tag{f}$$

where

σ_m is matrix tensile stress

V_f is the volume fraction of filaments

σ_f is the average fiber strength .

In the case where the bond strength is zero, the effective volume fraction, V_f, equals zero, since the fibers, although present, are not reinforcing the matrix. Equation (f) then reduces to

$$\sigma_c = \sigma_m , \tag{g}$$

and the fibers reduce the strength of the matrix. For this reason, it is more realistic to use the form

$$\sigma_f = \sigma_m (1 - V_f) + eV_f\sigma_f , \tag{h}$$

where V_f is the volume occupied by filaments, and e is the mechanical compatibility of the fibers and matrix. The mechanical compatibility of fibers and matrix is a measure of how they complement one another, the filaments in reinforcing the matrix and the matrix in transferring load to and isolating the failures of filaments. There are several parameters which can influence the value of e, the most obvious being variation in bond strength. To illustrate, reconsider the variation in bond strength in the light of equation (h). First, consider what happens when the bond strength is zero. The matrix and filaments are acting separately with no coupling and the mechanical compatibility is therefore zero. Then

$$\sigma_f = \sigma_m (1 - V_f) + 0 ,$$

which is consistent with Figure 63 where composite strength is less than matrix strength because of the discontinuities introduced by the filaments. As the bond strength increases, the mechanical compatibility increases, because there is sufficient bond strength to load the filaments to fracture, but some unbonding occurs at the newly formed ends keeping the fracture isolated. The increase in e results in an increase in the "effective volume fraction" (eV_f). This concept of an "effective volume fraction" takes account of the fact that having a lot of filaments in the matrix does not guarantee high strength. Rather it is the volume of the filaments able to reinforce the matrix, thereby adding to the strength of the composite, which determines the overall strength. For this reason, the highest value of e is unity, that is, every filament placed in the composite is providing reinforcement for the matrix.

As the bond continues to increase above point B, filaments begin to fail, but energy is absorbed in unbonding too so that single-filament fractures are not catastrophic. Therefore, e continues to increase, since more filaments are being used efficiently; therefore, mechanical compatibility increases. Finally, the bond strength becomes so great that the filament fractures are not damped by

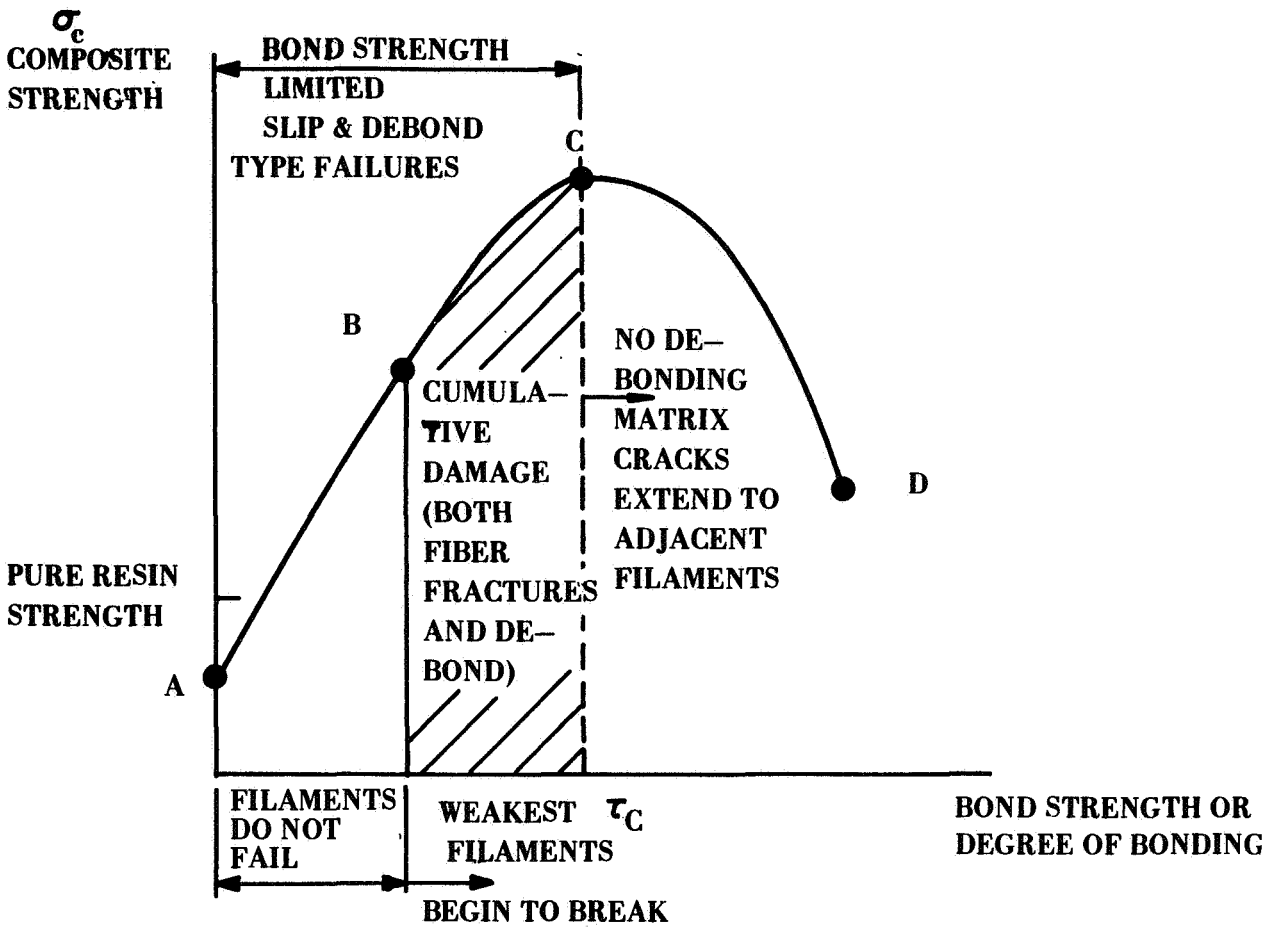

Figure 63. Proposed relationship between bond strength and composite strength for a resin–filament composite

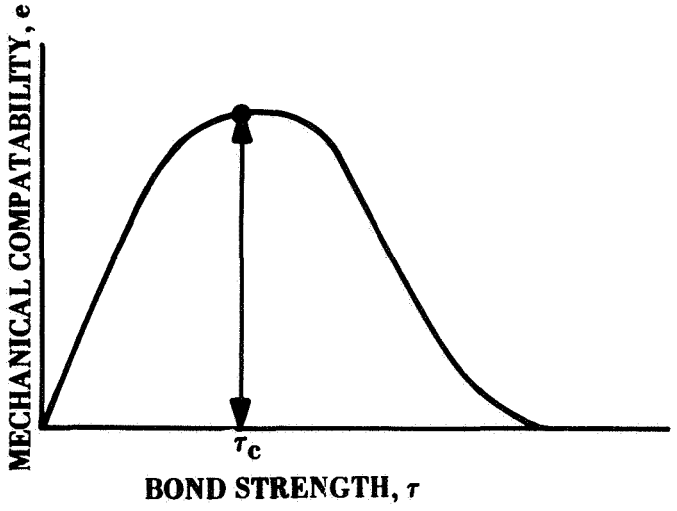

Figure 64. e vs. bond strength,τ

unbonding and each filament fracture influences adjacent filaments. Because each local failure results in considerable damage the effective volume fraction (eV_f) is greatly diminished, since premature failure will prevent the composite from developing its potential volume fraction V_f. Therefore, for bond strengths in excess of that defining point C in Figure 63, the value of e is decreasing and this means the strength of the composite must be diminished. The plot of mechanical compatibility versus bond strength would appear as shown in Figure 64. There is an optimum value of bond strength and therefore an optimum value of e, which determines the strength of the composite, all other things being equal .

Now consider the case where the only variable is the actual volume fraction of filaments, such parameters as crack sensitivity etc. remaining constant. Remembering that V_f is the actual volume fraction of fibers in the composite and (eV_f) is the "effective volume fraction", consider the case of zero volume fraction. When $V_f = 0$ there is no mechanical compatibility since there are no filaments, therefore $\sigma_c = \sigma_m$, the strength of the matrix alone. When very small numbers of filaments are added ($V_f \sim 10\%$) the presence of these filaments in remote locations causes stress concentrations and premature failure at stress levels slightly below the matrix strength σ_m. This means that the value of e may be either zero, such that

$$\sigma_c = (1 - V_f)\,\sigma_m = .9\sigma_m$$

or very slightly negative (e.g., e = -.1) in which case

$$\sigma_c = (1 - V_f)\sigma_m + (-.1)\,V_f\sigma_f \ .$$

Either case results in a composite strength less than that of the unreinforced matrix. As the volume fraction V_f is increased, the strength increases because the distribution of fibers becomes more uniform, yet the fibers are not so close that their local fractures influence one another. The compatibility e may be unity during this phase where the strength increase is due entirely to the increase in V_f,then

$$\sigma_c = (1 - V_f)\sigma_m + V_f\sigma^f \ ,$$

which is the standard expression for rule-of-mixtures behavior. Only when the value of V_f becomes large enough to cause critical spacing (that is, that spacing at which a single filament fracture begins to weaken those next to it) does the value of e begin to decrease. The greater the volume fraction V_f above the critical value (that causing critical spacing), the smaller the value of e. This is much more realistic than the usual form of the rule-of-mixture relation. A plot of the value of e against V_f, the actual volume of filaments, appears as shown in Figure 65. The corresponding strength is also given.

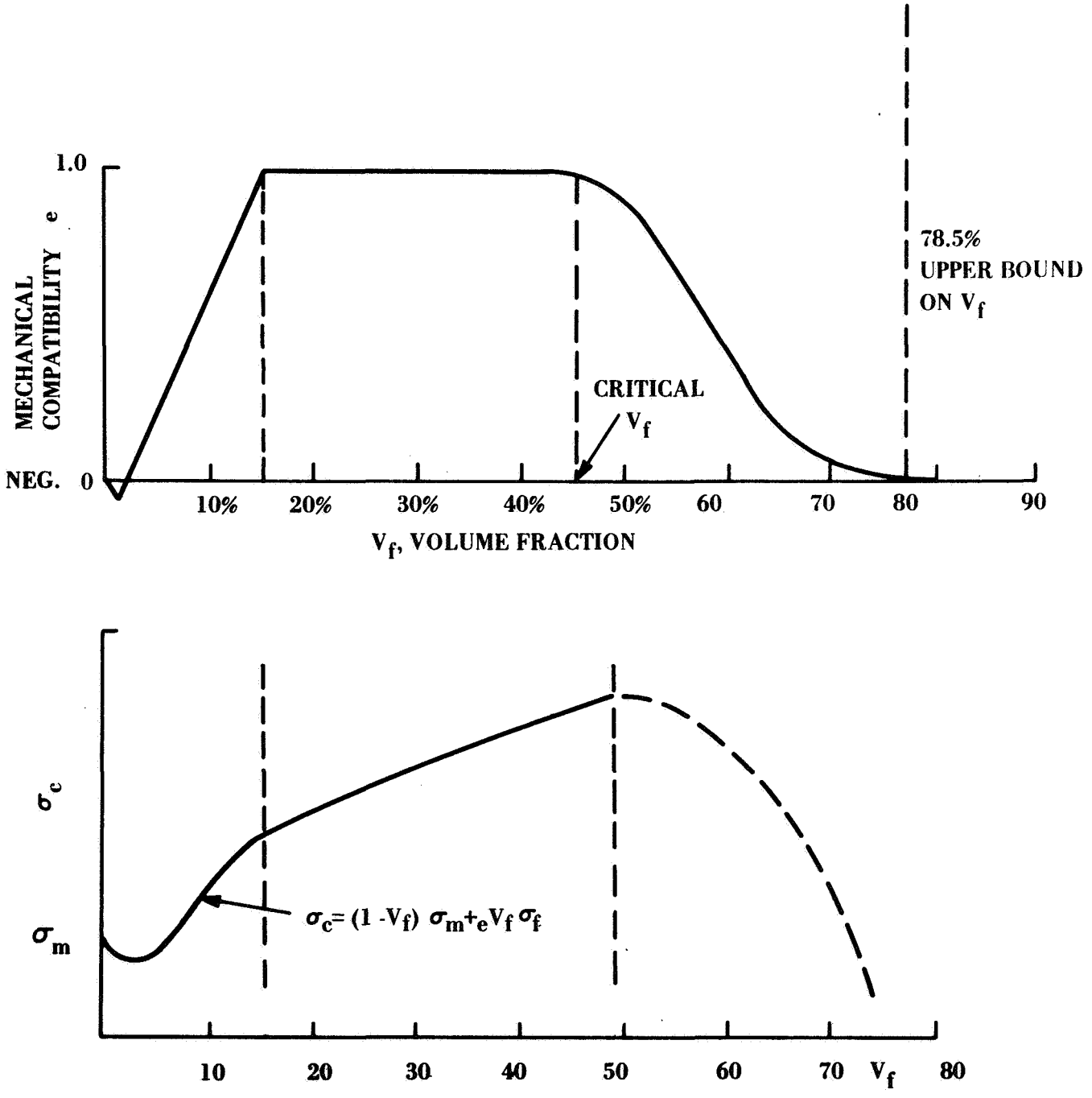

Figure 65. Variation in e and σ_c with V_f

APPENDIX C

THE ROLE OF MECHANICAL COMPATIBILITY IN ADVANCED FILAMENT COMPOSITES*

INTRODUCTION

This is a brief account of some experimental work done to develop and illustrate a model for rationalizing the varieties of mechanical behavior exhibited by filament reinforced composites in uniaxial tension. The mechanical response of an epoxy matrix to failure of an imbedded filament was measured and correlated with the phenomenology of fracture for single and for five-filament composites. The filaments were chosen to encompass a wide range of tensile strengths and elastic moduli. Epoxy was chosen as a matrix material because its transparency permitted microscopic examination of both failure surfaces and profiles with vertical, oblique, and transmitted illumination.

The first section of the paper summarizes the observed failure modes and some details of the epoxy formulation. The second section describes a model for behavior rationalization, which is also a convenient frame of reference for the subsequent discussion of experimental results.

From the experimental results it is inferred that composite performance depends upon the mechanical compatibility of a number of interrelated variables, including material properties, specimen geometry and test conditions.

FAILURE MODES IN FILAMENT EPOXY SPECIMENS

A previous study** established the fundamental fracture mechanism which occurs in filament reinforced composites. The three failure modes of primary concern are shown in Figure 66. The

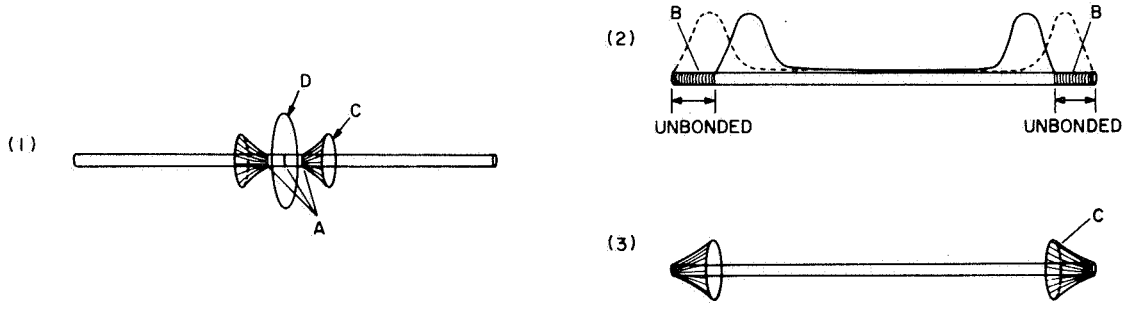

Figure 66. Three failure modes in a single filament

*Presented at the International Symposium on Macromolecular Chemistry, IUPAC, Toronto, 1968.

** Some Fundamental Fracture Mechanisms Applicable to Advanced Filament Reinforced Composites. *Journal of Composite Materials*, Vol. II, No. 1, 1968.

first involves a disk shaped crack (D) of the surrounding matrix initiated by the filament fracture. As the filament fracture occurs, new ends are formed which introduce a second fracture pattern (C) which will be discussed in the third mode. The second mode of failure is unbonding at the interface as shown in (2). The shear stress distribution is shown on the filament. Since this shear stress is highest near the ends, unbonding proceeds from that point and the actual length of fiber reinforcing the matrix is reduced. The shear stress distribution at the interface is shifted toward the center and the unbonding process continues. The third fracture mode is shown in (3) and represents a tensile failure of the matrix caused by the concentration of shear stress at the filament ends. The resolved shear stress results in a maximum tensile stress acting on all planes making an angle of 45 deg. with the fiber and therefore a conical crack is developed (C). This same mechanism occurs in (1) after the filament fractures because of the high shear stresses introduced at the newly formed ends. The conical or inclined cracks grow more slowly than the disk (D) because they are not induced by a sudden fracture but rather by a uniformly applied shear stress at the interface. These inclined cracks tend to become normal to the fiber as they grow out of the high shear stress region which extends a few diameters radially from the fiber. When the inclined crack turns normal to the fiber it is in growth competition with a non-catastrophic disk-shaped crack formed as shown in Figure (1). Since both the disk-shaped crack and the inclined crack extend radially to adjacent filaments they magnify the destructive effects of a single filament fracture. For this reason unbonding is the more desirable failure mode provided there is sufficient bond strength to develop the strength of the reinforcing fibers. By far the most damaging failure mode is the disk-shaped crack which occurs suddenly, generating a great deal of local strain energy and causing rapid and sometimes catastrophic growth normal to the fiber axis.

MODEL OF COMPOSITE BEHAVIOR

A simple qualitative rationalization of expected composite behavior (Fig. 67) has been developed and found to be a useful reference for: 1) rationalizing a wide variety of test results, 2) designing more clearly critical experiments. The ordinate on the diagram (Fig. 67) represents the normalized composite strength which would be expected from the rule of mixtures in its simplest form (non-catastrophic local redistribution by the matrix in a well bonded composite); the abscissa shows many of the strongly interrelated material, configural and test variables which determine the extent to which the rule of mixtures will be valid. Somewhat analagous to the concept of chemical compatiblity, the totality of these interelated variables may be regarded as the mechanical compatiblity of the system. It might, then, be said that mechanical compatibility is satisfactory when premature filament failures do not adversely affect the ability of the matrix to redistribute the load in the manner (tacitly) assumed by the rule of mixtures.

The three classes of composite behavior (Fig. 66) are categorized as 1) bond limited, 2) filament limited, and 3) matrix limited. A Bond Limited composite fails to utilize the average strength of the reinforcing element because, although the matrix is capable of redistributing the load, the bond is too weak to transmit the load to the matrix in the vicinity of prematurely broken filaments. Failure is characterized by only a relatively few breaks per filament and by extensive filament pull-out.

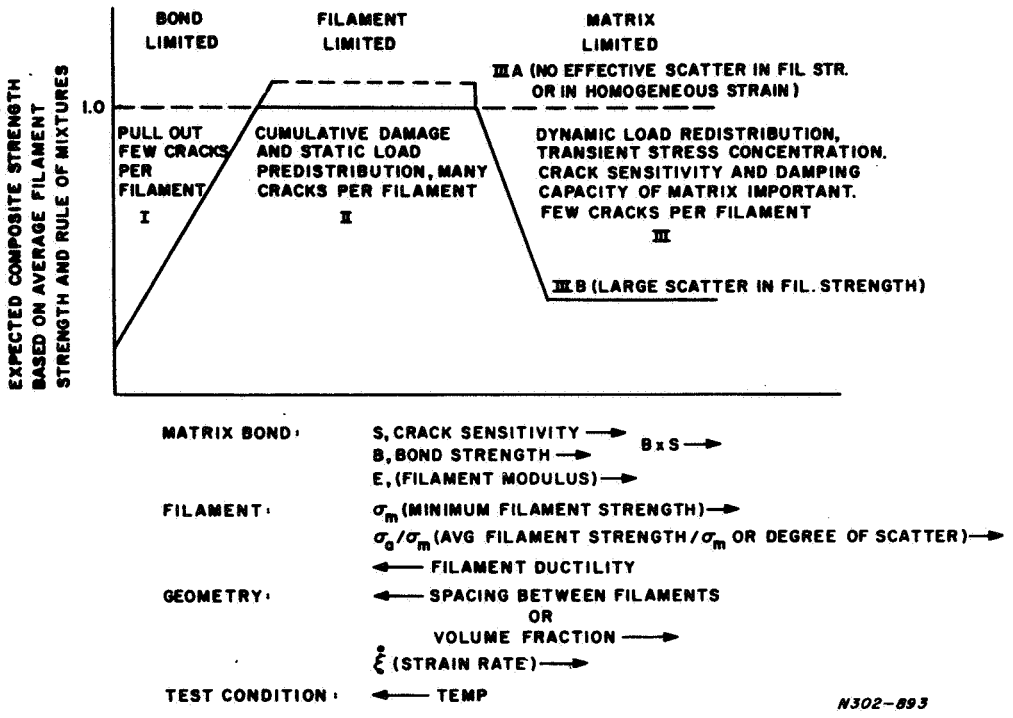

Figure 67. Schematic model for the graphic rationalization of the effect of materials properties, specimen configuration and test conditions on the performance of composites

Filament limited composites fail by cumulative damage (many breaks per filament show high strength utilization) and are free of substantial matrix contributions to premature failure. In Matrix Limited behavior, the matrix redistributes the load, associated with premature filament failure, in a manner (e.g., cracking) which adversely affects the strength of the composite. Composite failure is frequently brittle and characterized by relatively few breaks per filament. In contrast to Filament Limited behavior, the strength of Matrix Limited composites may be limited by "defects" rare enough to be regarded as statistically insignificant in the conventional characterization of separate composite components.

Although it was developed and tested in reference to the phenomenology of failure in filament epoxy systems, the model is believed to be more generally valid in the sense that composite performance will be governed by the marked degree of variable interdependence implied by the phrase, "mechanical compatibility".

EPOXY MATRIX

Epoxy Novalac was chosen as a matrix for this work. It is transparent, reasonably strong and its deformation behavior is easy to control. It was formulated to exhibit some inelastic deformation prior to maximum load over the test strain rates so that the embrittling effects of filament fracture could be demonstrated. The details of the formulates are shown in Table XXI

TABLE XXI. FORMULATION FOR EPOXY NOVALAC COMPOSITION

Material	Chemical Name	Symbol Used	Quantity Parts
Basic Epoxy	Epoxy Novolac	DEN 438	52
Plasticizer	Polypropylene Glycol	PPG 425	30
Curing Agent	Methyl Nadic Anhydride	MNA	36
Cure Promoter	Benzyledimethylamine	BDMA	1

THE EFFECT OF FILAMENT PROPERTIES ON THE MECHANICAL BEHAVIOR OF THE MATRIX

The effect of filament properties on the mechanical behavior of the epoxy matrix was determined in a series of uniaxial tension tests on single filament-epoxy specimens (~ 0.006 in^2 in cross section with a 1 inch gage length). The pertinent test results are shown in Table XXII. The four filament

TABLE XXII. TENSILE TEST RESULTS FOR CONTINUOUS SINGLE BRITTLE FILAMENTS IN AN EPOXY NOVALAC MATRIX (GAGE LENGTH ~ 1 INCH)

Spec. No.	Filament Material	Nominal Strain Rate (in./in/min.)	Strength, Max. Load/A_o (psi)	Total Elongation to Failure, (%)	No. of Non-Catastraphic Filament Breaks	REMARKS
529	E-Glass[1]	0.02	3010	> 16.5	35	Not failed - Test stopped
530	E-Glass[1]	2.0	4250	11.3[5]	38	
529 (reloaded)		0.02	3010	11.5	-	
449	Brittle Tungsten[2]	0.02	3900	14.7	6	No disk snaped cracks but observed on load defl. curves
450	" "	2.0	2460	1.3[5]	5	
521	B/W-Normal[3]	0.02	2920	3.7	6	1st Break at 2080 psi 6th Break at 2580 psi
522	" "	2.0	2620	1.4[5]	0	
518	B/W-Strong[4]	0.02	2340[6]	2.1	1	1st Break at 2300 psi
519	" "	2.0	2770	1.5[5]	0	
541A	Plain Epoxy	0.02	3030	17.8	-	Not failed - test stopped
541B	Plain Epoxy	2.0	4360	20.3[5]	-	Failure Origin at Surface

High, Low and Average Tensile Strength (5 Spec.) of (See Table V)	High	Low	Avg.
(1) E-Glass Filaments	48,000	22,400	30,500
(2) Brittle Tungsten Filament (WCA)	99,000	54,900	74,200
(3) Boron on Tungsten Filament-Normal	350,000	62,500	200,000
(4) Boron on Tungsten Filament-Strong	582,000	485,000	541,000

(5) Best Estimate-pen response precludes accuracy at small strains and high chart speeds

(6) Believed to be (ambiguously) low in view of filament tensile strength.

materials used cover, as a group, the strength range of less than 50,000 to more than 500,000 psi and the elastic modulus range 10 to 60 million psi. Specimens were made by casting and hand grinding and, therefore, exhibited some variation in gage length and thickness in each specimen and from specimen to specimen. The small errors in stress (area measured at specimen center) and gage length are of less significance than the qualitative differences in mechanical behavior and fracture mode.

An important result of these tests is the relationship of filament strength and modulus to the shape of the stress elongation curves (Fig. 68 & 69) as a function of strain-rate. All of the specimens

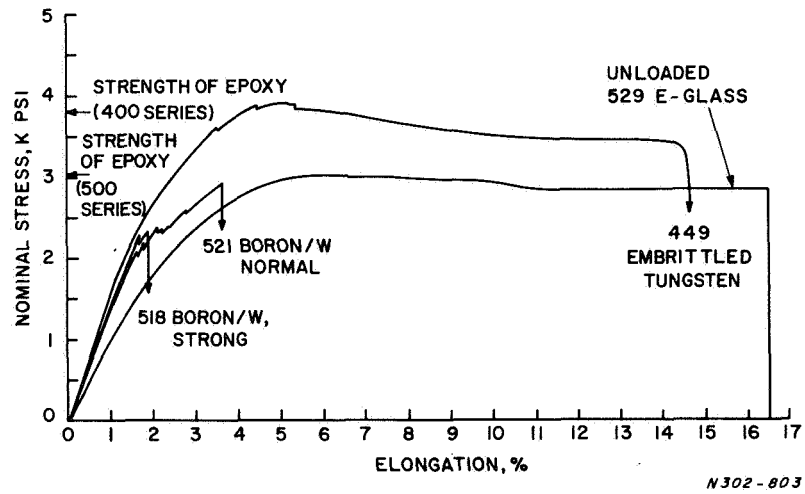

Figure 68. Stress-elongation curves for single-filament epoxy specimens tested in tension at 0.02 in/in/min

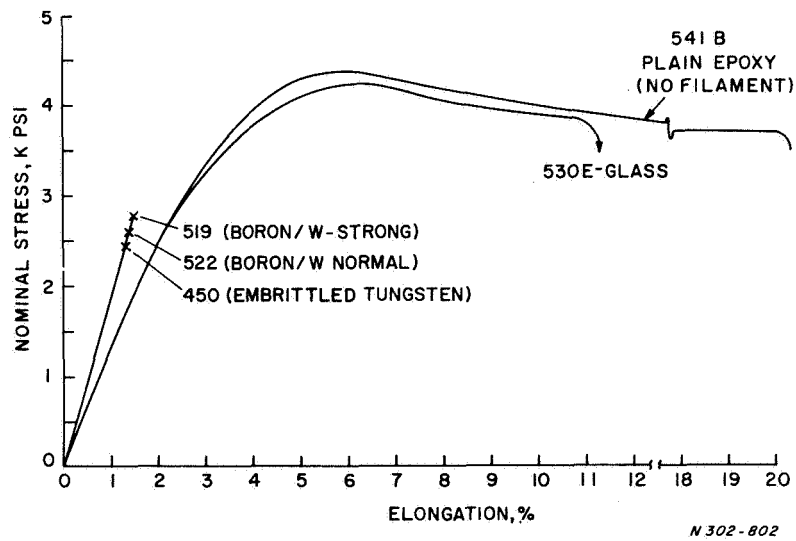

Figure 69. Stress elongation curves for single filament-epoxy tested in tension at 2 in/in/min

exhibit some non-linearity in the stress-elongation curves at the lower strain rate (0.02 in/in/min). On the other hand, at the higher strain rate (2.0 in/in/min), all curves are linear to failure except for E-glass-epoxy and plain epoxy specimens. An examination of the specimen fracture surfaces showed that the non-linear behavior is associated with a slowly propagating (radially marked) matrix tensile crack and that linear stress-elongation behavior is characterized by a rapidly propogating (nearly featureless) catastrophic matrix tensile crack. The tendency toward matrix embrittlement increases with increasing filament stength (and modulus) and increasing strain rate, which is evident in the measurements of the inelastic deformation occurring prior to maximum load (Fig. 70).

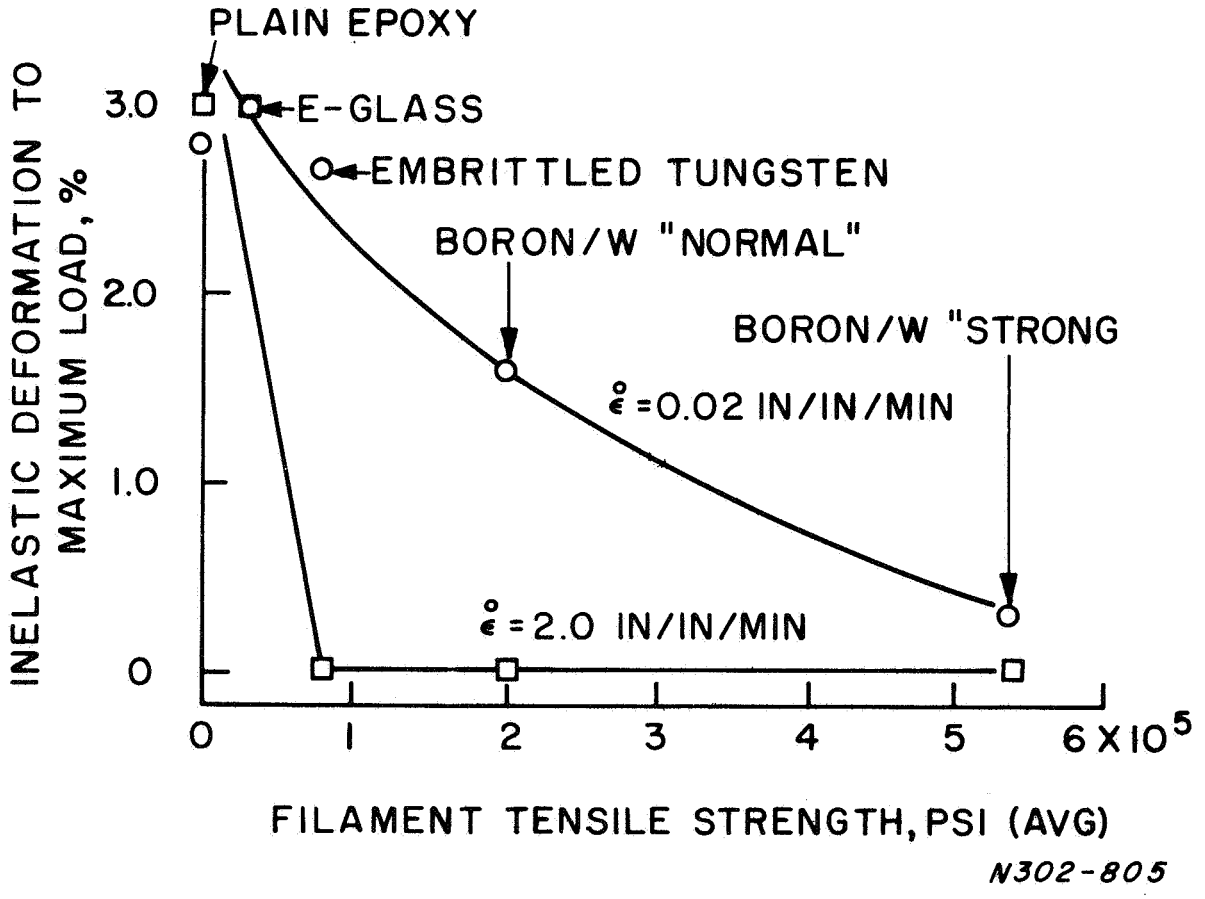

Figure 70. The inelastic elongation to maximum load as a function of filament tensile strength in single filament-epoxy novolac specimens

An important general question about reinforced composites is: "What is the effect on the mechanical response of a matrix of internal cracks created by the fracture of an embedded brittle filament?" The results of these tests on single filament-epoxy specimens provide the perspective which permits the answer: "Both test conditions and filament properties can have a profound effect on the mechanical behavior of the matrix. In consequence, predictions of composite performance based only on a knowledge of the conventional properties of individual components can be only fortuitously valid".

FILAMENT INTERACTIONS EFFECTS

In order to study filament interaction effects over a range of filament properties, a number of 5 filament-epoxy specimens were tested at two strain rates in unaxial tension. The specimen cross sections were ~0.009 in^2 and the gage length was 1 inch. Although the volume fraction was very small (~¼%), the interfilament spacing was approximately equal to that of a 2½% volume fraction. In addition to the filaments used in single filament-epoxy test specimens, two ductile filaments were also used (aluminum and tungsten). The tension test results are shown in Table XXIII. The inelastic elongations to maximum load and the specimen strengths, as a function of filament strength and test strain rate are shown in Figures 71 and 72, respectively.

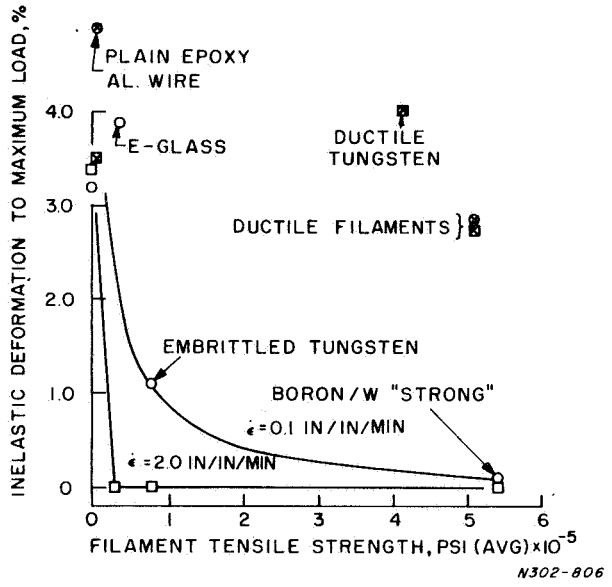

Figure 71. The inelastic elongation to maximum load as a function of filament tensile strength in 5 filament-epoxy novolac specimens

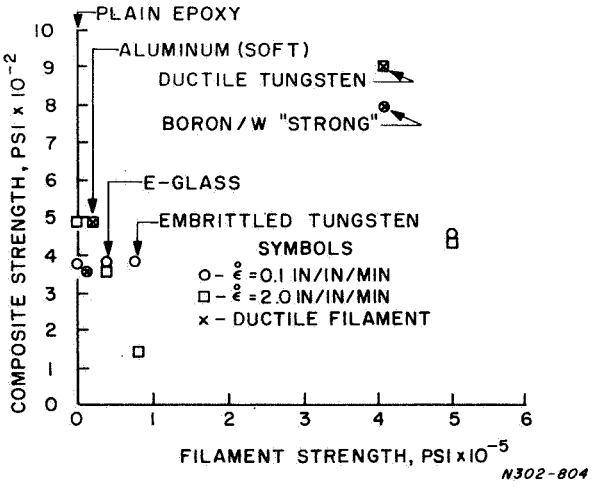

Figure 72. The tensile strength of 5 filament-epoxy novolac specimens as a function of filament tensile strength

TABLE XXIII TENSILE TEST RESULTS FOR 5-FILAMENT–EPOXY NOVALAC SPECIMENS (GAGE LENGTH ~1 IN).

Spec. No.	Filament Material	Nominal Strain Rate (in/in/min.)	Strength Max Load/A_o (psi)	Inelastic Elongation to Max. Load (%)	Number of Non-Catastrophic Cracks
410	E-Glass	0.1	3750	3.9	~165
411	E-Glass	2.0	3620	Nil	~100
404	Brittle Tungsten	0.1	3850	1.1	12 disk-shaped cracks
405	Brittle Tungsten	2.0	1480	Nil	4 disk-shaped cracks
406	B/W Strong	0.1	4630	0.1	1 disk-shaped crack
407	B/W Strong	2.0	4550	Nil	0
409	0.004" Aluminum	0.1	3590	4.7	Ductile extension of Al-No cracks
408	0.004" Aluminum	2.0	4900	3.5	Ductile extension of Al-No cracks
403	0.005" Ductile Tungsten	0.1	8000	4.0	No Disk-shaped cracks
402	0.005" Ductile Tungsten	2.0	9020	4.0	No Disk-shaped cracks
412	Plain Epoxy	0.1	3770	3.2	
441B	Plain Epoxy	2.0	4950	3.4	

In many respects, the results on 5-filament specimens were similar to those on single filament specimens. However, in addition, there was unambiguous evidence of filament interaction. All of the filament-epoxy specimens incorporating brittle filaments were strain-rate sensitive with regard to inelastic elongation and/or strength relative to plain epoxy (tested at the same strain-rate). The specimens incorporating the ductile filaments were at least as "ductile" as the plain epoxy. The weak ductile aluminum wire did not reinforce the epoxy at both strain rates. On the other hand, only the strongest brittle filament (boron) was capable of increasing the strength of the epoxy at the lower strain rate, and no brittle filament-epoxy specimen was stronger than the plain epoxy at the higher strain rate.

Perhaps the most striking evidence for the effect of filament interaction is contained in the results for specimens containing the low strength - low modulus E-glass at a test strain rate of 2.0 in/in/min. The single filament specimen (No. 530 Table XXII) exhibited the same inelastic deformation to maximum load (Fig. 70) and nearly the same strength as plain epoxy. The five-filament epoxy specimen was completely brittle and was not only weaker than the plain epoxy but also weaker than the single filament specimen. There were almost twice as many non-catastrophic breaks per filament in the single filament specimen. This shows that premature filament failure is likely to become increasingly catastrophic for the matrix as the filament spacing decreases even for low modulus, low strength brittle filament. The combination of low strength and high modulus was disasterous, and underlines the necessity for minimizing the scatter in the strength of high modulus brittle filaments.

The high modulus ductile tungsten reinforces because any premature filament failures are by necking and simultaneous debonding [1]. Therefore, even if the neck fractures, there is no bond to

provide a path into the matrix for the associated transient energy release.This suggests that the bond should be good enough to transmit the load in the vicinity of filament failure but that local unbonding is preferable to catastrophic matrix cracking.

THE EFFECT OF BOND STRENGTH ON MECHANICAL BEHAVIOR

The results of attempts to adjust the bond strength, by modifying the epoxy formation, were ambiguous because the matrix crack sensitivity was also affected. Conclusive results were obtained by testing coated single (B/W) filament epoxy specimens at a strain rate of 2.0 in/in/min. Fractures in a teflon coated filament did not damage the matrix, but the matrix was unable to redistribute the load owing to extensive unbonding and filament pull-out. The fracture origin (at the specimen surface) and the mechanical behavior was similar to that of plain epoxy. Five non-catastrophic fractures in a graphite coated filament did not seriously damage the matrix nor reduce its capacity for redistributing the load. This specimen was 10% stronger than plain epoxy and equally "ductile". All this was in marked contrast to the uncoated (B/W) filament specimen (No. 519 Table XXII) which failed brittlely at the first filament failure and at a strength only 2/3rds that of the plain epoxy. An examination of the failure locations in the graphite coated filament indicates that bonding was intermittant, on a fine scale, rather than weak, per se.

CONCLUDING REMARKS

Continuous filaments embedded in epoxy Novalac have been used to demonstrate the general effect of a number of variables which determine whether a composite will be bond limited, filament limited or matrix limited. A model, consistent with the results, has been developed to illustrate the strong degree of material and test variable interrelationship. It has been shown that in order to obtain filament limited composites (a basic "rule-of-mixture" assumption) it is necessary to have an appropriate match between bond strength and matrix crack sensitivity. Other critical variables have been shown to be filament strength (especially scatter), filament modulus, interfilament spacing and test conditions.